The application of surface plasmon resonance (SPR) immuno-biosensors for medical diagnosis

Dissertation

zur Erlangung des Grades

des Doktors der Naturwissenschaften

der Naturwissenschaftlich-Technischen Fakultät III

Chemie, Pharmazie, Bio- und Werkstoffwissenschaften

der Universität des Saarlandes

von

Jiwon CHUNG

Saarbrücken

2007

Tages des Kolloquiums: 23. 04. 2007

Dekan: Professor Dr. U. Müller

Berichterstatter:

        Vorsitzender: Professor Dr. M. Schmitt

        Gutachter: Professor Dr. Rita Bernhardt

                        Professor Dr. J. Jose

                        Professor Dr. J.-C. Pyun

        Akademische Mitarbeiter: Dr. A. Zöllner

Abbreviations:

Ab	Antibody
BSA	bovine serum albumin
CA 19-9	carbohydrate antigen 19-9
CEA	carcinoembryonic antigen
Con. (or C)	concentration of analyte in solution
C (in the additive assay)	Accumulated concentration
Da	Dalton
DMSO	Dimethyl sulfoxide
DNA	deoxyribonucleic acid
EDAC	1-ethyl-3-(3-dimethylaminopropyl) carbodiimide
EDTA	ethylenediaminetetraacetic acid
ELISA	enzyme-linked immunosorbent assay
FIA	flow injection analysis
hA	human albumin
hCG	human chorionic gonadotropin
hHBV	human hepatitis B virus
HRP	horse radish peroxidase
IA biosensor	immunoaffinity biosensor
IA layer	immunoaffinity layer
IgG	immunoglobulin
K (in the additive assay)	the accumulated concentration at the half of R_{max}
k_a	the association rate constant
K_A	the associatioin constant
K_D	the dissociatioin constant
LB	Langmuir-Blodgett
LLD	lower limit of detection
m	the mean signal
$milli^o$	milli degree
MEMS	micro electro mechanical system
min	minute
M.W.	molecular weight

N	number
Neu-ProA	NeutrAvidin-protein A comlex layer
NHS	N-hydroxysuccinimide
NSB	nonspecific binding
OD	optical density
PAP	peroxidase-anti-peroxidase
POC	point-of-care
r^2	the square of the correlation coefficient (r)
R	the sensor signal
R (in the additive assay)	the accumulated signal
R_t	the sensor response at time t
R_{max}	the maximal sensor response
R_{max} (in the additive assay)	the maximal accumulated signal
RI	refractive index
RIA	radioisotope immunoassay
RU	response unit (Biacore)
s	second
SAM	self assembled monolayer
S-Chimeric	NeutrAvidin-protein A chimeric complex immobilized on the biotinylated SAM layer
sd	the standard deviation of the signal
SIA	sequential injection analysis
S-Neu-ProA	NeutrAvidin-protein A complex layer on the biotinylated SAM layer
SPR	surface plasmon resonance
TMB	tetramethybenzidine
TSH	thyroid stimulating hormone

Abstract

(A) Zusammenfassung (German version)

Biosensoren werden häufig verwendet um bestimmte Analyten aus komplexen Gemischen mittels ihrer hohen Selektivität zu anderen Biomolekülen zu detektieren. Üblicherweise sind Biosensoren aus zwei verschiedenen Komponenten aufgebaut: erstens einer aus Biomaterialien bestehenden Oberfläche, die in der Lage ist, selektiv mit den Zielmolekülen in einer Testlösung zu reagieren und zweitens aus einer Signalverstärkungseinheit, die die beobachtete biologische Wechselwirkung in ein elektrisches Signal konvertiert.

Immunoaffinitäts (IA) Biosensoren machen sich die Eigenschaften von Antikörpern, hoch selektiv spezifische Antigene zu erkennen, zu Nutze. Eine solche IA-Oberfläche wurde in dieser Arbeit an einen Signalverstärker unter Verwendung von sich selbst generierenden Einzelschichten gekoppelt. Anschließend wurde ein Surface Plasmon Resonance (SPR) Sensorsystem (Spreeta^{TM}) zur Echtzeit-Detektion von Molekül-Molekül-Wechselwirkugen verwendet. Das Hauptziel der vorliegenden Arbeit war es, eine kostengünstiges SPR Biosensor Diagnostik-Verfahren zu entwickeln, das eine geringe Analysezeit in Anspruch nimmt, eine simultane Detektion verschiedener Interaktionen erlaubt und darüber hinaus über eine hohe Sensitivität aufweist.

1) Der erste Teil der Arbeit befasst sich mit der Entwicklung eines „Additiven Assays". Ziel dieses Tests ist es, Sensorchips mit IA-Oberflächen ohne ein Austauschen des Chips oder den Einsatz von Regnerierungs-Chemikalien wiederverwenden zu können. Üblicherweise werden IA-Oberflächen, die mehrfach verwendet werden sollen, unter Entfernung des bereits gebundenen Analyts regeneriert. Diese Methode ist sehr zeitaufwendig und kann darüber hinaus zur teilweise oder gar vollständigen Denaturierung der Antikörper und/oder Antigene auf der Sensorchip-Oberfläche führen. Beim „Additiven Assay" wird die Probe mehrfach über den Sensor gegeben, ohne dass bereits gebundene Analyten durch chemische Substanzen entfernt werden. Die Konzentration eines Analyts in der Probe wird ermittelt, indem das nach mehrmaliger Injektion der Probe aufgezeichnete akkumulierte SPR- Signal mit einer Eichkurve verglichen wird, die aus der Wechselwirkung zwischen immobilisierten BSA und Anti-BSA gewonnen wurde. Die Anwendbarkeit dieser Methode in der medizinischen Diagnostik wurde anhand der Detektion des Tumor-Markers CA 19-9

gezeigt. Die ermittelte Detektiongrenze für diesen Marker lag bei 410,9 U/ml. Dieser Wert liegt zwar über dem angestrebten Wert von 37 U/ml, ist jedoch ausreichend, um Proben von Patienten, die möglicherweise an Pankreas-Krebs erkrankt sind, zu analysieren (zwischen 400 – 192000 U/ml CA 19-9). Die Konzentrationsbestimmung von vier verschiedenen CA 19-9 Proben bekannter Konzentration unter Verwendung der Eichkurve lieferte eine geringe Standardabweichung von 5.3 %. Dieses Ergebnis zeigt eindeutig, dass der „Additive Assay" für die Analyse des Tumor-Markers CA 19-9 verwendet werden kann, ohne dass ein Chip-Austausch oder eine Regenerierung mit Chemikalien notwendig ist.

2) Der zweite Schwerpunkt dieser Arbeit bestand in der Entwicklung eines Biosensors, mit dem verschiedene Analyten simultan aus einer einzelnen Probe detektiert werden können. In der simultanen Detektionsmethode werden mehrere Analyten durch die jeweiligen spezifischen Antikörper, die auf derselben Sensor-Oberfläche immobilisiert sind, detektiert. Dabei werden zur Unterscheidung zwischen den jeweiligen spezifischen Antikörper-Antigen-Wechselwirkungen die Analyten nachträglich mit einem Massemarker versehen. Somit lassen sich ebenfalls spezifische Konzentrations-Eichkurven erzeugen, die anschließend unter Verwendung des ermittelten SPR-Signals zur Bestimmung der jeweiligen Analyt-Konzentration in den Proben verwendet werden können. In dieser Arbeit wurden zwei verschiedene Methoden zur simultanen Detektion angewendet. Modell 1: Verwendung einer Probe, die sowohl einen Analyt enthält, der aufgrund seiner Konzentration und Molekülgröße direkt mittels SPR detektiert werden kann als auch einen Analyt, der nachträglich mit einem Massemarker detektiert werden muss. Modell 2: beide Analyten müssen nachträglich und nacheinander mit verschiedenen Massemarkern detektiert werden. Die Anwendbarkeit dieser Modelle wurde anhand eines Testsystems bestehend aus einer IA-Oberfläche mit BSA und Anti-HRP sowie Proben, die Anti-BSA und HRP enthielten, untersucht. Die Ergebnisse zeigen, dass beide Modelle für die simultane Detektion von Analyten einsetzbar sind. Die klinische Relevanz von Modell 2 wurde für die Diagnose möglicher Frühgeburten von Diabetes-Patientinnen getestet, indem Urin-Proben auf das Vorhandensein von humanen Chorion-Gonadotropin (hCG) und humanen Albumin (hA) untersucht wurden. hCG ist ein Schwangerschaftsindikator, währenddessen hA für die Diagnose von Mikroalbuminurie (MA) verwendet wird. MA ist dabei ein Alarmsignal für schwangere Patientinnen mit Typ1 Diabetes, dass eine Frühgeburt bevorstehen könnte. Die hier ermittelten Detektionsgrenzen für hCG und hA betrugen 464 miU/ml bzw. 25 µg/ml mit einer Standardabweichung von 6,5% bzw. 5,9%. Diese Konzentrationen stellen die

minimale Detektionsgrenze da, um MA in der 4ten Schwangerschaftswoche zu bestimmen. Die gewonnenen Ergebnisse zeigen, dass Methode 2 für die simultane Detektion von verschiedenen Analyten erfolgreich eingesetzt worden ist.

3) Der dritte Teil der Arbeit hatte als Zielsetzung die Verbesserung der Sensitivität und der Detektionsgrenze des Biosensors. Dies sollte zum einen durch die Verwendung von bestimmten Massenmarkern und zum anderen durch das Generieren von orientierten IA-Oberflächen erreicht werden. Durch Massemarker wird die Molekülmasse des gebundenen Analyts vergrößert, was zu einer Verstärkung des SPR-Signals führt. Von den in dieser Arbeit getesteten Massemarkern gegen die jeweiligen Analyten wie z.B. sekundäre Antikörper, Avidin-biotinylierte-Antikörper und einen Peroxidase-anti-Peroxidase (PAP) Komplex war die Signalverstärkung durch den PAP-Komplex am effektivsten. Die Anwendbarkeit dieses Markers für diagnostische Verfahren wurde durch Analyse von humanen Antikörpern gegen Hepatitis B Viren (hHBV) getestet. Die Detektionsgrenzen für hHBV-Antikörper, die ohne Signalverstärker, unter Verwendung eines sekundären Antikörpers oder mittels des PAP-Komplexes ermittelt wurden, betrugen 9,2 nM, 4,39 nM bzw. 0,64 nM. Der mittels des PAP-Komplexes bestimmte Wert liegt nahe dem Detektionslimit des derzeit verwendeten kommerziell erhältlichen hHBV-Antikörper ELISA Tests (0,24 nM).

Es ist bekannt, dass die Sensitivität von Immunosensoren durch die Kontrolle der Orientierung und Dichte des Rezeptors auf der IA-Oberfläche erhöht werden kann. An eine gerichtete IA-Oberfläche können mehr Analyten binden, was zu einer Signalverstärkung verglichen mit anderen ungerichteten IAs führt. In dieser Arbeit wurde der Einfluss der Rezeptor-Molekül-Dichte auf die Detektionseffizienz unter Verwendung verschiedener Oberflächen getestet (anti-hIgG-Antikörper-, Avidin-, NeutrAvidin-, Protein A-, NeutrAvidin-Protein A-Komplex- und blanke Gold-Oberfläche). Die NeutrAvidin-Protein A-Komplex-Oberfläche wies dabei die höchste Rezeptor-Dichte sowie die höchste Menge an gebundenen Analyten verglichen mit der unbehandelten Gold-Oberfläche auf (1,9 bzw. 3,6 fach erhöht). Darüber hinaus führte die Generierung des NeutrAvidin-Protein A-Komplexes auf einer biotinylierten Oberfläche zu einer 1,3fach erhöhten Analyten-Bindungsrate verglichen mit der Bindungsrate an eine Oberfläche, an die der jeweilige Rezeptor direkt chemisch gekoppelt wurde. Die Anwendbarkeit des Systems auf medizinische Fragestellungen wurde untersucht, indem eine NeutrAvidin-Protein A-Komplex-IA für die Bindung von Carcinoembryonales Antigen (CEA) Antikörpern

verwendet wurde. Der diagnostisch relevante Detektionsbereich für dieses Antigen muss dabei zwischen 0-100 ng/ml liegen. Mit der hier getesteten NeutrAvidin-Protein A-Komplex-IA konnte die Bindungsrate verglichen mit der blanken Gold-Oberfläche 1,5fach erhöht werden. Die Detektionsgrenze lag bei 30 ng/ml CEA. Dieses Ergebnis zeigt, dass eine mittels des NeutrAvidin-Protein A-Komplex generierte gerichtete IA-Oberfläche zu einer Verbesserung der Sensitivität durch Erniedringung des Detektionslimits führt.

Zusammenfassend konnte in dieser Arbeit mit dem „Additiven Assay" ein kostengünstiger Biosensortest etabliert werden. Unter Verwendung einer simultanen Detektionsmethode wurde die Analysezeit für unterschiedliche Analyten entscheidend verringert und mit der angewendeten Signalamplifikationssmethode konnte die Sensitivität der Assays gesteigert werden. Die in dieser Arbeit gezeigten Methoden werden entscheidend zu der Entwicklung von SPR-basierten Biosensoren für medizinisch relevante Fragestellungen und Diagnosen beitragen.

(B) English version

A biosensor is an analytical device to detect target analyte in a complex mixture by using high selectivity of biomolecules as the molecular recognition tool. Usually, the biosensor consists of two major parts; 1) molecular recognition layer of biomaterials which reacts selectively with the target analyte from other substances in a sample, and 2) transducer which converts the biological event occurred in the molecular recognition layer into quantitative electrical signal. Especially, the immunoaffinity (IA) biosensor exploits the highly specific and selective interaction between antigen and antibody for the detection of a target analyte. Such an IA layer was connected to the transducer surface by using the self assembled monolayers (SAMs) as a linker layer. The surface plasmon resonance (SPR) sensor was used for label-free detection and real-time monitoring, and Spreeta^{TM} was used for this work. The major objective of this work is the development of SPR biosensor for medical diagnosis with the features of a cost-effective test by 'additive assay', short analysis time through 'simultaneous detection' and high sensitivity by 'signal amplification'.

[1] First topic is a reuse method of IA biosensor called 'additive assay' which enables the reuse of the IA layer without chip exchange and chemical treatment between measurements. For the reuse of IA biosensors, 'regeneration' method has been most frequently used for repeated measurements, which removes the already bound analyte from the IA layer. However, the regeneration method by chemical treatment usually requires additional analysis time and the regeneration procedures were reported to partially or completely denature the antigens or the antibodies on the IA layer. In the 'addtive assay' method, the sample is repeatedly injected to the IA layer without removing the already bound analytes by chemical treatment and then the concentration of sample is calculated from the actually measured signal by using previously prepared correlation curve between the accumulated concentration of additively injected sample and accumulated signal which represents the number of occupied binding sites. The application of additive assay for real medical diagnosis was demonstrated by using tumor marker (CA 19-9) as a target analyte. Though the detection limit by direct assay of SPR biosensor (410.9 U/ml) was higher than cut-off value (37 U/ml), however, it was enough for the general concentration range of CA 19-9 for most patient samples of pancreatic cancer (400 – 192,000 U/ml). When the concentrations of four samples were analyzed by using the correlation curve of CA 19-9, the average

deviation of the calculated concentrations from the real concentrations was estimated to be 5.3 %. This result shows that the additive assay can be applicated for the repeated measurement of CA 19-9 without chip exchange and chemical treatment.

[2] The second topic is the 'simultaneous detection' which enables the detection of multiple analytes on the single sensor element with single sample treatment. In the 'simultaneous detection', a sample with several analytes is treated to the single sensing region which has multiple receptors for each target analyte and then the concentrations of each analyte is analyzed sequentially with label antibodies by using the respective standard curves for the correlation between the concentration and signal. In this work, two simultaneous detection models (Model 1 and Model 2) were devised for the samples with the following composition: (1) one target analyte resulting in a sensor response without any label and the other analyte with only additional label (Model 1), (2) both target analytes requiring additional labels for detetion (Model 2). The feasibility of Model 1 and Model 2 was tested with two model antigen-antibody systems: IA layer with BSA and anti-HRP antibodies, Sample with anti-BSA antibodies and HRP. The result showed that the Model 1 and Model 2 were acceptable for application. The real medical diagnosis based simultaneous detection (Model 2) was demonstrated by analysis of human chorionic gonadotropin (hCG) and human albumin (hA) in human urine for the diagnosis of preterm delivery of patients with diabetes. The hCG has been used for the qualitative pregnancy test. The hA can be used for diagnosis of microalbuminurea and this diagnosis can be used as an alarm for women with type I diabetes, who have the steeply increased prevalence of preterm delivery. The detection limits for hCG and hA were estimated as 464 mIU/ml and 25 μg/ml, respectively, which were the minimum detection range for the diagnosis at the 4th week of pregnancy and microalbuminuria. The average errors of analysis based on Model 2 were 6.5 and 5.9 % for hCG and hA, respectively. This result shows that Model 2 was suitable for the simultaneous detection of both analytes.

[3] The third topic is the improvement of sensitivity and detection limit through two 'signal amplification' methods by using mass label (A) and by the orientation control of IA layer (B):
(A) The mass label attached to the already bound target analyte increases the total mass attached to the sensor surface and then it induces the increase of SPR signal. In this work, the efficiencies of several labels were compared with direct assay to select most efficient

label for signal amplification. Among several labels such as secondary antibodies, avidin-biotynylated antibodies and peroxidase-anti-peroxidase (PAP) complex, the amplification using the PAP complex was selected as the most efficient method. The feasibility of this signal amplification method was demonstrated by analysis of infectious disease marker, human hepatitis B virus (hHBV) antibody. The detection limits of SPR measurements by direct assay, sandwich assay and PAP complex method were calculated to be 9.20, 4.39 and 0.64 nM, respectively. This result from PAP method shows that the detection limit of SPR biosensor (0.64 nM) approached closely to cut-off value for medical diagnosis (0.24 nM) by using the commercial ELISA kit.

(B) The sensitivities of immunosensors are known to be improved by the control of IA layer (orientation & density). As more target analytes can be attached to this controlled IA layer, the signal at the same concentration of target analyte can be increased. In this work, among several controlled IA layers such as the layer of avidin, NeutrAvidin, protein A, NeutrAvidin-protein A complex, the NeutrAvidin-protein A complex on gold surface of SPR biosensor showed the highest surface density of receptor and ligand antibody, which were 1.9- and 3.6- fold higher than the bare gold surface, respectively. And the binding ratio of ligand per unit receptor antibody was also one of the highest values (1.9- fold higher than the bare gold surface). When the NeutrAvidin-protein A complex was prepared on biotin-labelled SAM, the binding ratio of ligand per unit receptor was found to be significantly improved (2.1- fold higher than the bare gold surface) in comparison to the IA layer prepared by chemical coupling of receptor antibody to the SAM layer (0.8- fold higher than the bare gold surface). For the feasibility test of orientation control, the NeutrAvidin-protein A complex was applied for the detection of a tumor marker, carcinoembryonic antigen (CEA), which has the detection range for diagnosis to be between 0 and 100 ng/ml. By using NeutrAvidin-protein A complex, sensitivity was improved to be 1.5-fold higher than bare gold surface and the detection limit of 30 ng/ml was achieved. This result shows that the control of IA layer (orientation & density) improved the sensitivity as well as the detection limit of IA biosensor.

These results demonstrated the 'additive assay' for cost-effective test, 'simultaneous detection' for short analysis time and 'signal amplification' for high sensitivity. The presented three methods in this study will be applied for the development of a practical SPR biosensor for the various medical diagnosis.

1. Introduction

A biosensor is an analytical device to detect a specific target analyte in a complex mixture by using the high selectivity of biomolecules for the molecular recognition. Usually, the biosensor consists of two major parts; 1) molecular recognition layer of biomaterials (e.q. enzyme, receptor-ligand, and antibody-antigen) which reacts selectively with the target analyte from other substances in a sample, and 2) transducer (e.q. optical, amperometic, potentiometric and acoustic) which converts the biological event occurring in the molecular recognition layer into quantitative electrical signal.

The immunoaffinity (IA) biosensor exploits the highly specific and selective interaction between antigen and antibody for the detection of the target analyte. The detection of the target analyte by the IA biosensor is based on the selective binding of the target analyte by the molecular recognition layer called immunoaffinity (IA) layer produced by immobilizing antigens or antibodies to the transducer surface. The IA biosensor has been applied for clinical diagnosis, microbiological and environmental applications. Despite the progress of the IA biosensor in recent years, further improvement in technical specifications is still required for the medical diagnosis, such as sensitivity, detection limit, analysis time and instrumentation (Ekin, 1999; Luppa et al., 2001).

1.1. Objective

This work aims to develop an IA biosensor based on an SPR-transducer for the practical application to medical diagnosis. Three technical topics were investigated for the realization of the aimed biosensor.

[1] The first topic is a reuse method of IA biosensor called 'additive assay' which enables the reuse of the IA layer without any chemical treatment. In this method, the sample is repeatedly injected to the IA layer without removing the already bound analytes by chemical treatment. The concentration of the sample is calculated from the actually measured signal by using the correlation curve between the accumulated concentration of additively injected sample and accumulated signal which represents the number of occupied binding sites (section 3.1).

[2] The second topic is the 'simultaneous detection method' which enables the detection of multiple analytes on the single sensor element with single sample treatment. In the 'simultaneous detection method', a sample with multiple analytes is injected to the IA layer which has multiple receptors for each target analyte. The concentrations of each analyte are then analyzed sequentially by using the respective standard curves for the correlation between the concentration and signal. Two simultaneous detection models were defined by the response ratio of the target analytes in a sample (section 3.2).

[3] The third topic is the improvement of sensitivity and detection limit through signal amplification by using mass label (A) and by the orientation control of the IA layer (B): A. The mass label was attached to the already bound target analyte and then the total mass attached to the sensor surface induced the increase of the SPR signal (section 3.3.1). B. The orientation of antibodies on the IA layer was controlled so that the surface density of receptor antibody and the binding amount of the ligand (analyte) to the IA layer could be increased (section 3.3.2).

1.2 State of the art of IA biosensor development

The IA biosensor uses immunoaffinity (IA) layer as the molecular recognition part for the selective binding of the target analyte, which is produced by immobilizing antigens or antibodies to the transducer surface. For the application of IA biosensor to the medical diagnosis, three core topics were selected: (1) reuse of IA biosensor, (2) simultaneous detection of more than two analytes in a sample, (3) signal amplification to improve the sensitivity of IA biosensors. In this section, the state of the art of the selected topics will be presented and the requirements for new technologies will be clearly specified.

1.2.1 Regeneration method for repeated measurements

The 'regeneration' method has been most frequently used for repeated measurements of IA biosensors, which removes the already bound analyte from the IA layer (see Figure 1-1). The interaction between antibody and antigen is known to be the combination of electrostatic force (E), polar force (L), van der Waals force and hydrogen bonding. Several reagents have been selected and optimized for rapid dissociation of antigen-antibody complexes as well as the stability of the IA layer with transducer. (Wijesuriya et al., 1994;

Anderson et al., 1999).
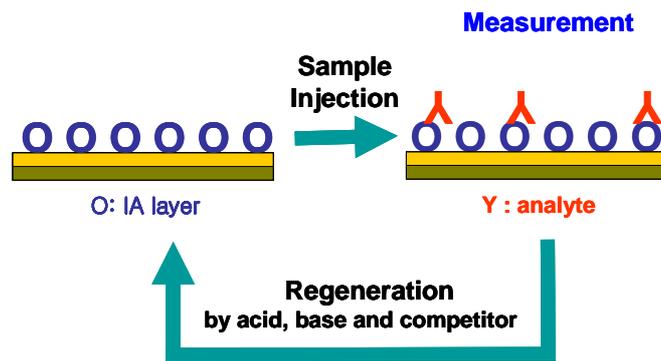
Figure 1-1: Conventional regeneration method for successive measurements using an IA biosensor. For the next measurement, the already bound analyte is removed by chemical reagents, such as acid, base and competitor.

(1) High or low pH

Acid (high pH) and base (low pH) solution can break the electrostatic bond between antibody and antigen. As a regeneration agent, the acidic solutions such as glycine-HCl (pH 1.7-2.2, 10-100 mM) and HCl (10-100 mM) and the basic solutions such as thriethanolamine (TEA) buffer (pH 11.0, 50 mM) and NaOH have been used for IA biosensors (Wijesuriya et al., 1994; Anderson et al., 1999). For example, a flow cell of a SPR biosensor (BIACORE 1000) was regenerated by glycine-HCl (pH 2.0) in the real-time immunoassay of ferritin, and the regeneration could be repeated more than 50 cycles (Cui et al., 2003). The SPR biosensor (BIACORE 3000) for the analysis of morphine-3-glucuronide was reported to be regenerated by base (10 mM NaOH) solution at least 30 cycles (Dillon et al., 2003). In the purification procedure of antibodies with the protein A column, IgG was eluted by using the glycine-HCl (50 mM, pH 2.5) as an elution buffer (Nakanishi et al., 1996).

(2) Ions at high concentration / Chaotropic agent

An ion is an atom or a group of atoms with a net electric charge by gaining or losing one or more electrons. The electrostatic interaction is mainly composed by charged groups of antigen and antibodies and the effect of charged groups can be dispersed by adding ions at high concentration. A highly concentrated salt solution such as 2-4 M $MgCl_2$ or 1M NaCl can decrease the electrostatic interaction between antigen and antibody through a high ionic strength. Therefore, such a salt solution has been used with chaotropic agents for regeneration of IA biosensors (Anderson et al., 1999).

Chaotropic agents such as urea or guanidine-HCl are denaturing salts which bind strongly to proteins and they decrease hydration. These agents can cause the disrupture of the molecular structure by weakening nonbonding forces such as hydrogen bonding, van der Waals interactions and the hydrophobic effect (Anderson et al., 1999). For example, trichloroacetic acid was reported to be very effective chaotropic agent in releasing cortisol from binding proteins in the use of a time-resolved fluoroimmunoassay (Eskola et al., 1985). The chaotropic agent can be used at acidic pH to improve the effect of regeneration. In the analysis of multiple mycotoxins such as DON, fumonisin B1, zearalenone and aflatoxin B1, chaotropic agent (6.0 M glycine chloride) at acidic pH (50 mM glycine, pH 2.0) was used to regenerate the SPR biosensor (BIACORE 2000) (van der Gaag et al., 2003).

(3) Detergent

Detergents have a general structure $R\text{-}SO_4^-Na^+$, where R is a long-chain alkyl group. Various detergents have been used for the regeneration of IA biosensors such as 0.3% Tween 20, 0.3% Tween 80, 0.3% Triton X-100 and 0.3% CHAPS (Anderson et al., 1999). Tween 20 and sodium dodecyl sulfate (SDS) have been reported to achieve rapid regeneration time and high numbers of reusable regenerations for the fiber-optic-based immunosensor (Betts et al., 1991).

Nonpolar solvents or chelating agents have been also reported for the application of regeneration. The nonpolar solvent is a solvent which has no positive or negative electric charge, such as dimethyl sulfoxide (DMSO), formamide, ethanol and acetonitrile. DMSO at high or low pH is reported to break the antibody-antigen bonds (Anderson et al., 1999).

Chelation is the process of reversible binding of a ligand to a metal ion, forming a metal complex. The capacitive biosensor based on synthetic proteins for sensitive detection of heavy metals such as Hg^{2+}, Cd^{2+}, Pb^{2+}, Cu^{2+}, and Zn^{2+} ions was regenerated with 10 mM ethylenediaminetetraacetic acid (EDTA) by removing the bound heavy metal ions (Bontidean et al., 2003). In the detection of herbicides with the SPR biosensor (BIACORE X), herbicides were injected onto the heavy-subunit-histidine-tagged Reaction Centers (HHisRCs)-immobilized chip. The HHisRCs were immobilized on the chip via nickel-histidine chelation chemistries and EDTA was used as regeneration buffer to remove the nickel ions (Nakamura et al., 2003).

As previously mentioned, several research groups have reported success in regenerating IA

layers for reuse in many cycles by treatment with acidic or basic solutions or competitor solutions.

As the regeneration efficiency depends mainly on the stability of antigen or antibody in the IA layer, however, the optimization process should be selected case by case. For example, in the competitive assay for the detection of the pesticide 2,4-dichlorophenoxyacetic (2,4-D) preincubated with antibody, the chip can not be regenerated by excess of 2,4-D and other attempts, e.g. using 0.1 M glycine of pH 2.5 were unsuccessful as well (Svitel et al., 2000). Even more drastic strategies recommended for Biacore chip regeneration, such as using pH less than 2 or pH greater than 10 cleaved the chip surface only partially. Furthermore, such procedures were reported to partially or completely denature the antigens or the antibodies on the IA layer (Bright et al., 1990; Betts et al., 1991). For each IA layer, between 60% and 90% of the antigen binding activity remained after 10 cycles of regenerations, and the activity continued to decrease in a nearly linear fashion (Betts et al., 1991). In most instances, after 10-20 regeneration cycles the sensor activity is significantly lowered. In the regeneration method, additional analysis time by the step of chemical treatment also make a disadvantage.

1.2.2 Detection of multiple analytes

To overcome the limitations of single analyte detection, simultaneous detection of multiple analytes have been reported, including flow injection analysis (FIA), sequential injection analysis (SIA), microsensor array and methods which uses different labels.

(1) Flow injection analysis (FIA) system

In the FIA type immunoassays, the sample passes through the sensing element by using a flowing carrier system. When several sensing elements are combined in the flow channel of the analysis system, multi-analyte detection can be done with one sample treatment. For example, glucose and L-lactic acid were simultaneously monitored during a fermentation process by on-line FIA with dual amperometric biosensors (Min et al., 1998). Four amperometric electrode biosensors were also simultaneously used to detect the insecticides paraoxon and carbofuran by using the FIA system (Bachmann et al., 1999).

(2) Sequential injection analysis (SIA) system

SIA is a variation of FIA. A selection valve is used to carry a stack of the sample to the

sensing zones sequentially and then to the detector. The SIA has enabled automated sample handling. When the sample is sequentially distributed to several sensing zones for different analytes, multi-analyte detection can be done. The SIA systems have been used for various analysis: the detection of 2,4,6-trinitrotoluene (TNT) and hexahydro-1,3,5-trinitro-1,3,5-triazine (RDX) by a capillary-based flow immunosensor (Narang et al., 1998), the determination of S- and R-captopril by amperometric biosensors (Stefan et al., 2000) and the continuous monitoring of glucose and lactate by a dual electrochemical assay system (Jones et al., 2002).

(3) Microsensor array

The microsensor arrays based on Micro-Electro-Mechanical System (MEMS) technique have been applied for multi-analyte detection by fabricating an array of sensing areas into a single chip.

A planar array immunosensor with a charge-coupled device (CCD) has been used for the simultaneous detection of several target analytes, such as 3 toxic analytes (staphylococcal enterotoxin B (SEB), ricin and *Yersinia pestis*) (Wadkins et al., 1998), six biohazardous agents (ricin, cholera toxin, *F.tularensis* LVS, *B.abortus* (killed), *B.anthracis* Sterne, SEB) (Rowe-Taitt et al., 2000) and both the tumor suppressor gene and protein (fragile histidine triad (FHIT) gene and protein) (Askari et al., 2002). The Bead Array Counter (BARC) biosensor containing a 64-element sensor array can be used to detect biological warfare agents such as *Bacillus anthracis, Yersinia pestis, Brucella suis, Francisella tularensis, Vibrio cholerae, Clostridium botulinum, Campylobacter jejuni* and Vaccinia virus by using DNA hybridization, magnetic microbeads and giant magnetroresistive (Edelstein et al., 2000). However, these array type methods require the same number of independent sensing areas as the target analytes.

(4) Different labels in the same assay zone

The multi-analytes analysis method using a single sensing element was first reported involving the use of radioisotopes such as ^{125}I and [131]I (Morgan, 1966). This radioisotope immunoassay (RIA) was applied for the diagnostics of insulin and growth hormone in human serum. The immunoassay for dual analytes was also reported, involving ^{125}I and [57]Co (Gutcho et al., 1977). However, the application of RIA is restricted by difficulties in handling and the waste treatment of radioisotopes.

ELISA kits for the detection of more than two target analytes at a single well of microplate

were also reported using different reporting enzymes and substrates (Blake et al., 1982). However, there are also several problems in multi-analytes detection by ELISA. In the case of sequential enzyme reaction for each analyte, the first color signal by one label can interfere with the second color signal by the other label, and the distinguishment of signals from different labels is often not clear.

Other types of assays have been also reported to use different fluorescent labels for the analysis of lutropin and follitropin in serum (Hemmilae et al., 1987), mixture of radioisotope labels and enzyme labels for the analysis of total and IgA-conjugated α_1-microglobulin (DeMars et al., 1989), different metal ion labels for the analysis of HSA and IgG (Hayes et al., 1994), particles of different sizes for the analysis of AFP and hCG (Frengen et al., 1995) and colored latex particles (Hadfield et al., 1987).

1.2.3 Signal amplification to improve sensitivity and detection limit

The SPR biosensor is reported to have a detection range affected by the detection method (for example, direct assay or sandwich assay) and molecular weight of the target analyte. In the case of single step assay, the detection ranges for the analytes at M.W. > 1000 Da are reported to be nM ~ µM (Lundstroem, 1994). In comparison to the conventional immunoassay such as ELISA, the sensitivity of the SPR biosensor should be improved for medical diagnosis. Signal amplifications by the attachment of mass label and the control of the IA layer (orientation & density) have been reported for the improvement of the sensitivity and detection limit.

1.2.3.1 Signal amplification by mass label

The multi-step (sandwich) assay, where various label proteins are added to the already bound analyte on the sensor surface for the signal amplification, has been applied for the signal amplification of IA biosensors. Especially in the SPR system, signal amplification by the following mass labels have improved the detection ranges of analytes to be pM ~ nM (Lundstroem, 1994; Mullett et al., 2000).

(1) Secondary antibody
The simplest label for the sandwich assay is an analyte-specific 'secondary antibody',

which is attached to the target analyte on the IA layer. However, the amplification effect is confined by molecular weight of antibodies (150 kDa) and usually the degree of amplification is not high. For example, the amplification ratio of ferritin detection was estimated to be only as much as 1.7-fold (Cui et al., 2003). Compared with the direct assay, the detection limit of thyroid stimulating hormone (TSH) detection in the sandwich assay was improved only from 12 ng/ml to 7 ng/ml (Kubitschko et al., 1997).

(2) Latex particle

Nanoparticles with heavy weight such as latex particle have been used for signal amplification of SPR IA biosensors. This latex particles can be coated with counterparts of the analyte by using EDAC/NHS technique (see Figure 1-6), and the effect of signal amplification is affected by the particle size, particle coating conditions and particle concentration. With hCG-coated latex (diameter 238 nm), the sensitivity for hCG detection was improved by a factor of 30 ~ 50 (Severs and Schasfoort, 1993). In the case of thyroid-stimulating hormone (TSH) detection, anti-TSH IgG-coated latex enhanced the detection limit from 12 ng/ml to 3 pg/ml (Kubitschko et al., 1997). Because of the large size of latex particles, the possible number of binding to the analyte on the IA layer is not so high and the enhancement effect is rapidly reduced at high analyte concentration.

(3) Gold colloid

Other nanoparticles with high refractive index such as colloidal gold can be used for sensitivity enhancement of SPR biosensors (Leung et al., 1994). Colloidal gold can be coated with various proteins by charge adsorption (Lyon et al., 1998). For the detection of human complement factor 4 (C4), the analyte was conjugated with colloidal gold conjugate and the detection limit could be improved to be 10-fold lower than the direct assay (Liu et al., 2004). Moreover, when the secondary antibody was conjugated with the colloidal gold, the detection limit was improved by 40-fold compared with the direct assay. However, the enhancement effect was also similar to be sandwich assay (1.25-fold) at high analyte concentration.

(4) Liposomes

Liposomes are an artificial microscopic vesicles consisting of an aqueous core enclosed by one or more phospholipid layers. The liposome immunosorbent assay (LISA) has been developed for improving the detection limit and sensitivity of SPR. In this assay, liposomes

and the secondary antibodies are biotinylated to be used as a label. After injection of the analyte, a biotinylated second antibody is added, and then avidin is used as the bridging molecule between the biotinylated antibody and the biotinylated liposome. The liposome strategy was used for the detection of interferon-γ (IFN- γ) and both sensitivity and detection limit were improved by ~ 10^4 times. However, because liposomes are very large vesicles (100~1000 nm) (Wink et al., 1998), the possible number of binding events to the analyte on the IA layer is also small and the enhancement effect is decreased at high analyte concentration.

1.2.3.2 Signal amplification by orientation & density control of IA layer

The orientation control and the density control of the antibody on the IA layer were conceived for the signal amplification of IA biosensors. As shown in the Figure 1-2A, the orientation control of IA layer means that variable regions of receptors in the IA layer are arranged to face the sample fluid. In this case, more target analytes can bind to the oriented IA layer (the orientation control) (Lu et al., 1996; Muramatsu et al., 1989). As shown in the Figure 1-2B, the density control of IA layer aims to bind as many receptors as possible to the IA layer. Hence, more target analytes can be attached to the IA layer and the sensitivity of the IA biosensor can be improved (the density control). Several techniques have been used to achieve the signal amplification by the control of those properties of the IA layer.

A
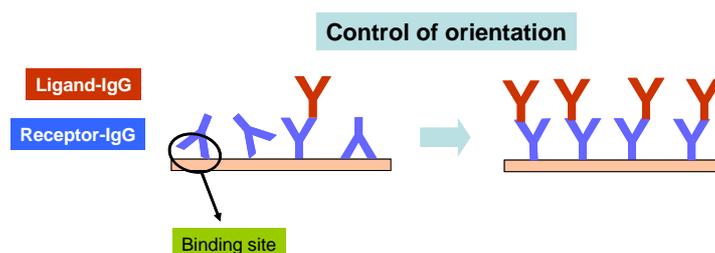
B
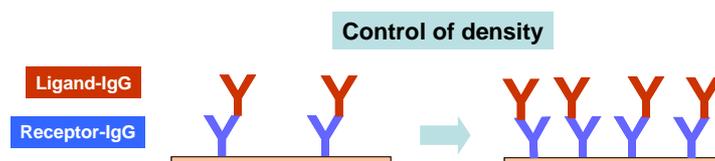
Figure 1-2: Signal amplification by the control of the IA layer. (A) Control of the orientation of receptor antibodies of the IA layer. **(B)** Control of the density of receptor antibodies on the IA layer.

(1) Protein A method

The most frequently used technique for the orientation control of the IA layer has been to apply protein A. Protein A is a cell wall protein deriving from *Staphylococcus aureus* which exhibits unique binding properties for IgG from a variety of mammalian species and for some IgM and IgA as well. As protein A binds to polysaccharides at the Fc region of the antibody, it has been applied to immunosensors for the orientation control of the antibody in the IA layer (Owaku and Goto, 1995; Kanno et al., 2000; Bae et al., 2005). For example, the effectiveness of protein A has been proved in the detection of *Yersinia pestis* Fraction 1 (F1) antigen by a fiber optic biosensor (Anderson et al., 1997) or red tide-causing plankton Chattonella marina by a piezoelectric immunosensor (Nakanishi et al., 1996).

(2) Avidin - biotinylated protein interaction

Avidin is a glycoprotein with a strong affinity for biotin (affinity constant $> 10^{15}$ M^{-1}). For the control of antibody orientation, the avidin is usually immobilized on the sensor surface, and then the biotin-labelled antibody against a target analyte is bound. As the biotin is known to be labelled at the Fc region of antibodies, the F(ab') region is exposed to the analyte after binding to the immobilized avidin. The avidin bridging method, however, proved relatively inefficient in the enzyme immunoassay (ELISA) of prolactin showing three fold improvement of the non-specific binding (Ahluwalia et al., 1991).

(3) The Langmuir-Blodgett (LB) film technique

The Langmuir-Blodgett (LB) film means a film of organic material (often surfactant molecules) assembled at the liquid-gas interface and it can be transferred onto a solid substrate. The LB technique has been used to make a closely packed and highly oriented protein layer and it was used for many commercial sensors for glucose detection (Davis and Higson, 2005). However, this protein layer produced by LB technique is not stable. As the protein layer immobilized using the LB technique is easily denatured and desorbed from the substrate, the fabrication of an immunosensor using this method seems to be impractical (Preininger et al., 2000; Bae et al., 2005).

(4) Self-assembly technique

Well-oriented immunosurfaces can be prepared by the direct immobilization of F(ab') fragments of IgG onto gold (Au) surfaces via the formation of a Au-thiolate bond (Brogan et al., 2003). The F(ab') fragment can be made by using pepsin and 2-mercaptoethylamine

(2-MEA) (see Figure 1-3). Enzymatic fragmentation of IgG produces F(ab')$_2$ fragment by pepsin and this fragment is further fragmented into two F(ab') by 2-MEA by reduction of S-S bonding. Each F(ab') has one binding site and one thiol (-SH) group. This F(ab') fragment can bind spontaneously to the gold surface of immunosensors through the specific interaction between thiol (-SH) group and the gold surface. Such a self-assembly technique was applied to detect insulin by using SPR sensor (Lee et al., 2005).
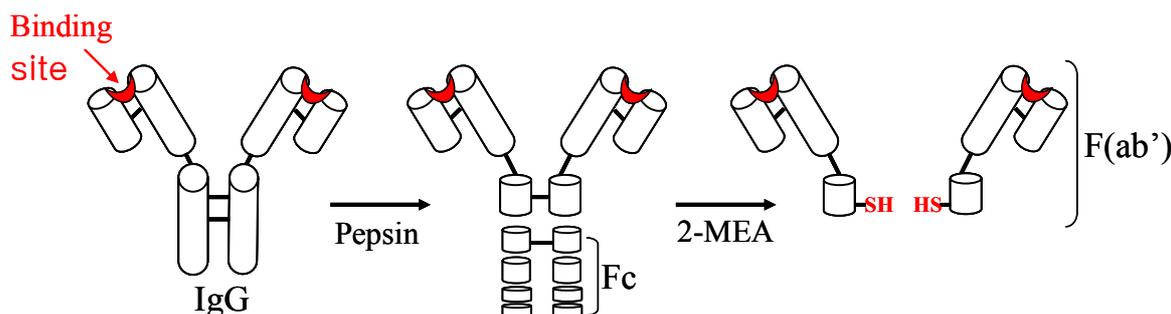
Figure 1-3: Scheme of the strategies used to prepare F(ab') of whole molecule IgG. Enzymatic fragmentation of IgG produces F(ab')$_2$ fragment by pepsin and this fragment is further cleaved into two F(ab') by 2-mercaptoethylamine (2-MEA).

(5) Charged substrate technique

Charged substrates have been used for the orientation control of IA layer on the self assembled monolayer (SAM). The orientation of anti-hCG antibody was found to be better oriented on the primary amine–terminated SAM (positively charged) than on the carbohydrate-terminated SAM (negatively charged) (Chen et al., 2003). Because the immobilization of an antibody on the negatively charged or positively charged surfaces is based on a physical adsorption, this strategy has a limitation in stability.

1.3 Principal elements for the construction of an immunoaffinity SPR biosensor

Usually an IA biosensor system (see Figure 1-4) is composed of four functional parts: (1) sampling, (2) molecular recognition, (3) transducer and (4) data processing.
(1) In the sampling part, a sample with the target analyte is prepared into a suitable format for the analysis by using the biosensor. For example, serum has many interrupting proteins for the specific detection of the target analyte and it is diluted for the effective detection. Sometimes, microfluidic sample handling system is used for the sample with restricted

volume, such as neonatal blood sample.

(2) The molecular recognition part of the IA biosensor detects the target analyte in the sample by the highly specific interactions between antibody and antigen. Such an interaction changes the physical properties of the molecular recognition part, such as refractive index, mass or density.

(3) The transducer converts these physical property changes into the electrical signal. For the detection of antigen-antibody interaction, several types of transducers have been applied for IA biosensors, such as electrochemical (potentiometric, amperometric or conductometric/capacitive), microgravimetric, optical, and thermometric. In this work, the surface plasmon resonance (SPR) sensor was used as transducer.

(4) The data processing part calculates the concentration of the target analyte from the electrical signal obtained from the transducer part.
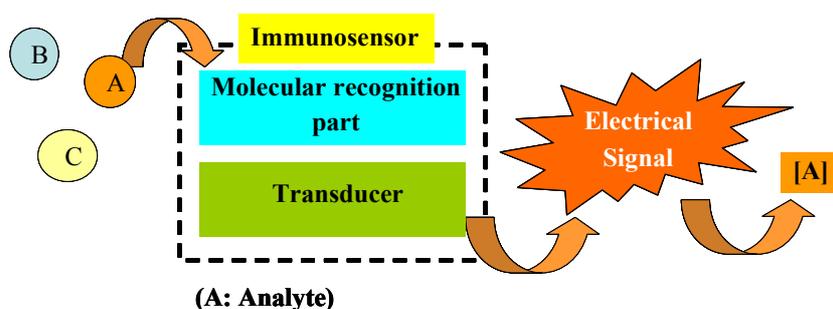
(A: Analyte)

Figure 1-4: General structure of an IA biosensor. The target analyte (A) in a mixture is selectively bound to the molecular recognition part and the quantitative electrical signal corresponding to the amount of bound analyte is generated by the transducer. The IA biosensor displays the concentration of the target analyte in the sample.

1.3.1 Properties of IA layer

When the sample is applied onto the IA biosensor, the sensor response is produced by the occupancy of the free binding site of the IA layer by the analyte. As correlation between the concentration and signal is used for the calculation of analyte concentration, the reproducible preparation of the IA layer is very important for the precise calculation of the analyte concentration.

Various techniques have been reported for the immobilization of antibodies (or antigens) to the metallic surface of the transducer. Such techniques can be classified into two categories: (1) physical adsorption to the metallic surface of the transducer, and (2) covalent coupling

of antibodies (or antigens) to the transducer, which is reported to have good reproducibility and coverage. Although the physical adsorption is simple to use, this technique is known to induce denaturation or conformational changes of the adsorption layer, poor reproducibility, elution by the detergent of the washing solution and so on (Bae et al., 2005).

Usually, the IA layer is composed of the adsorption layer and linker layer as shown in the Figure 1-5. The adsorption layer specifically binds the target analytes and the linker layer connects the adsorption layer to the surface of the transducer. The linker layer is prepared by modifying the surface of the transducer to bind the antibodies (or the antigens) of the adsorption layer and it also influences the orientation of the antibodies (or the antigens).
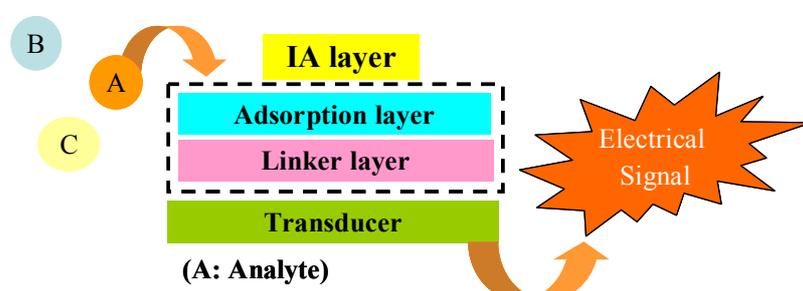
Figure 1-5: The functional structure of the IA layer. The layer is composed of an adsorption layer for the selective binding of target analyte and the linker layer for the stable binding of the adsorption layer to the transducer surface.

The self assembled monolayers (SAMs) have been frequently used as the linker layers. The strong adsorptions of thiol (R-SH), disulfide (R-S-S-R) and sulfides (R-S-R) to gold surface have been used to make well-ordered SAM on the SPR biosensor surface (Wink et al., 1997). The SAM can be easily prepared by immersion of the substrate into a solution containing an appropriate amphiphile (Ulman et al., 1996). The SAM has been reported to have many advantages for the application of IA biosensors. First of all, the non-specific binding can be reduced three to five times compared with conventional linker layers (Su et al., 1999). By using this well-ordered SAM, well-oriented immobilization of proteins could be prepared without altering the biological activities and the improvement of detection limits, reproducibility of the assay could be achieved.

In this work, 11-mercaptoundecanoic acid was used to prepare an SAM on the gold surface of the SPR transducer (see Figure 1-6A). The inside chemistry of SAM formation on the gold surface is known to be a two-step mechanism: (1) First step is the oxidative addition of

the S-H bond and reductive elimination of the hydrogen (chemisorb): R-S-H + Au → R-S-Au$^+$•Au + 1/2H$_2$. (2) After the fast formation of an S-Au bonding, the hydrocarbon chains are known to assemble together to form the well-ordered monolayer by Van-der-Waals forces between the hydrocarbon chains (Ulman et al., 1996; Davis and Higson, 2005). In the case of long alkyl chains such as 11-mercaptoundecanoic acid, strong intermolecular bonds can be formed to make well-ordered structures with amines, which are similar to the internal packing energies of crystalline hydrocarbon (Allara et al., 1995). After the preparation of SAM (linker layer) on the gold surface, the protein (adsorption layer) was covalently coupled to the SAM by the well-known chemistry, which uses 1-ethyl-3-(3-dimethylaminopropyl) carbodiimide (EDAC) and N-hydroxysuccinimide (NHS) as coupling reagents (see Figure 1-6B). In this reaction, the carboxylic groups of SAM are activated by a mixture of EDAC and NHS, and then amine groups of ligand are covalently bonded to the carboxylic groups of SAM. The remaining esters are deactivated by addition of ethanolamine (Johnsson et al., 1991).

A
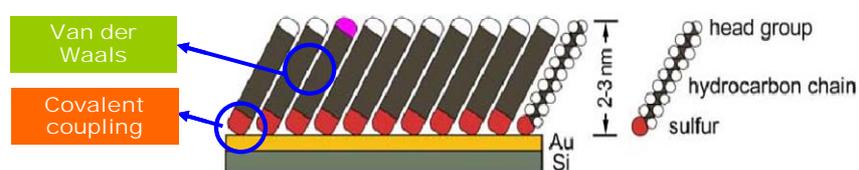
B
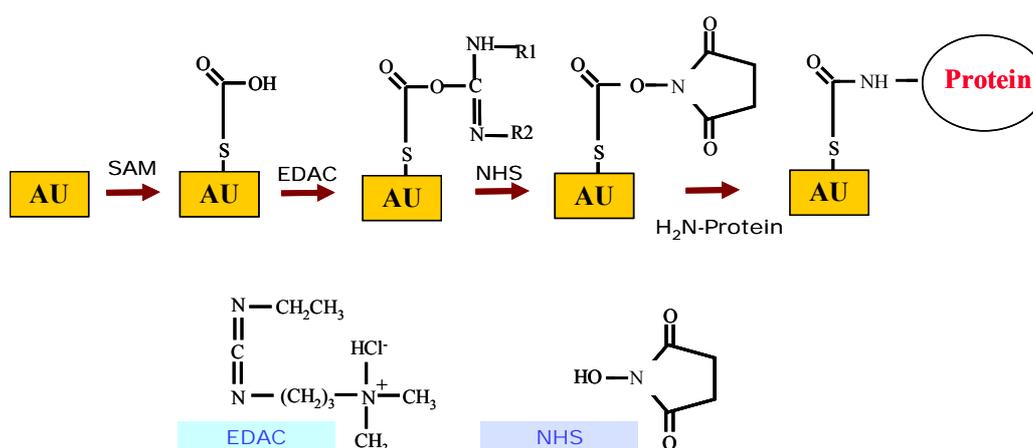
Figure 1-6: Self assembled monolayer (SAM) and it's coupling chemistry.

(A) Schematic view of the SAM on the gold surface. **(B)** The reaction of EDAC/NHS for coupling of protein to the carboxylate group of SAM.

1.3.2 Properties of SPR transducer

In principle, the SPR biosensor can detect all kinds of analyte binding to the IA layer without any additional labels such as fluorescent, radioactive or scattering labels (Homola, 2004). The surface plasmon resonance (SPR) effect occurs in the very close vicinity of a thin metal film surface at the interface of two transparent media of different refractive index (RI) (see Figure 1-7) (Kretschmann and Raether, 1968; Otto, 1968).

When incident light goes from optically dense media (higher RI) to less dense media (lower RI), it is partly reflected and partly refracted. Above a special angle of incident light, all light is reflected back into the dense media (total internal reflection) and a component of this light (the evanescent wave) can propagate into the less dense media to a distance of one wavelength (Faegerstam et al., 1992). If a thin metal film is positioned at the interface between two media, the evanescent wave of incident light is able to interact with free electrons (plasmons) in the metal film at a narrow angle range of incident light (SPR angle). When this surface plasmon is resonantly excited, a longitudinal charge density wave propagates along the interface between two different media. In this situation, light energy is lost to the metal film and the intensity of reflected light decreases. As the refractive index of the media changes, the SPR angle is also shifted. This shift of the SPR angle is a signal for the SPR sensor. This phenomenon is usually observed with noble metals such as gold and silver (De Bruijn et al., 1992).
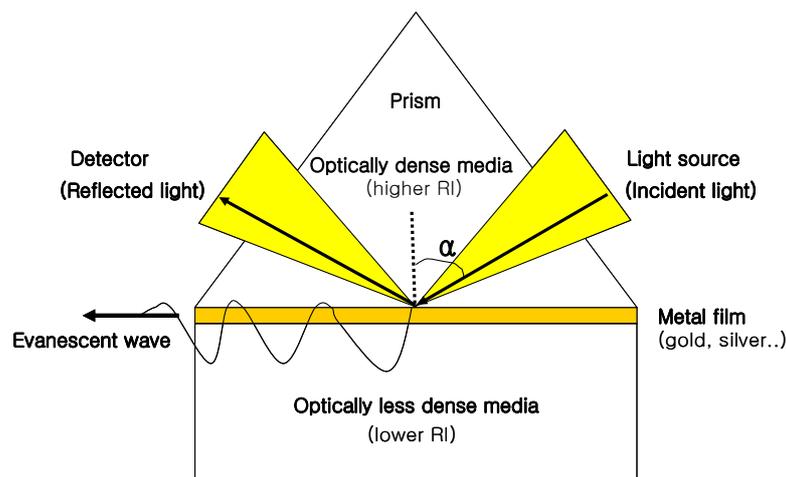
Figure 1-7: Structure of the surface plasmon resonance (SPR) transducer. A thin metal film is positioned at the interface between two media, and the evanescent wave of incident light is able to interact with free electrons (plasmons) in the metal film at a special angle (α) of incident light (SPR angle). As the binding of analyte to the sensor surface changes the SPR angle, the analyte concentration related to the amount of bound analyte can be measured by using the SPR transducer.

As the analyte binds to the the sensor surface, the refractive index and SPR angle changes according to the increase of the mass at the sensor surface (Sjoelander and Urbaniczky, 1991). When the interaction between analyte and the immobilized receptor occurs at the sensor surface, a sensorgram can be obtained in real time by plotting the signal against time, as shown in the Figure 1-8 (Liedberg et al., 1983; Lundstroem, 1994).
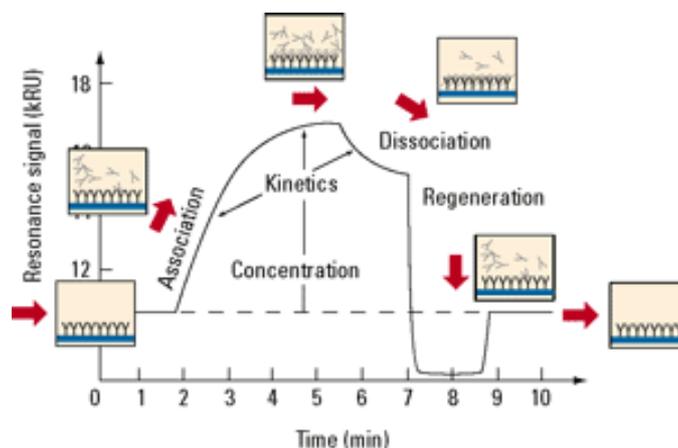
Figure 1-8: A typical sensorgram for the monitoring of analyte binding to the SPR biosensor. In the association step, analyte solution is injected to the biosensor for attachment. In the dissociation step, buffer solution replaces analyte solution and some analytes on the biosensor detached. For next experiment, all analytes on the biosensor are removed in the regeneration step.

In this work, the Spreeta^{TM} from Texas Instrument Inc. (TI) was used as a SPR transducer. Spreeta^{TM} sensor contains whole optical components necessary to implement SPR sensing, such as an infrared LED (830 nm peak wavelength), a 128-pixel linear diode array detector and a non-volatile memory chip for recording identification and calibration information (see Figure 1-9A). Spreeta^{TM} has the size of 4.1 cm x 2.9 cm x 1.3 cm and the active sensing region is located on the middle of the gold surface with the size of 0.45 mm x 0.1 mm (see Figure 1-9B). The sensor surface is prepared on a glass chip by sputtering a 50 nm gold layer and it was fastend to the plastic prism with epoxy. The SPR effect occurs on the thin gold layer: at a certain angles of incidence, part of the energy of the transverse-magnetic polarized incident light will be coupled into a surface plasmon wave traveling along the interface between the gold layer and the analyte. This device has the limit of detection of 1 pg/mm^2. As the evanescent field decays exponentially from the surface, SPR technique is sensitive to refractive index variation within 300 nm from the surface (Chinowsky et al., 2003).
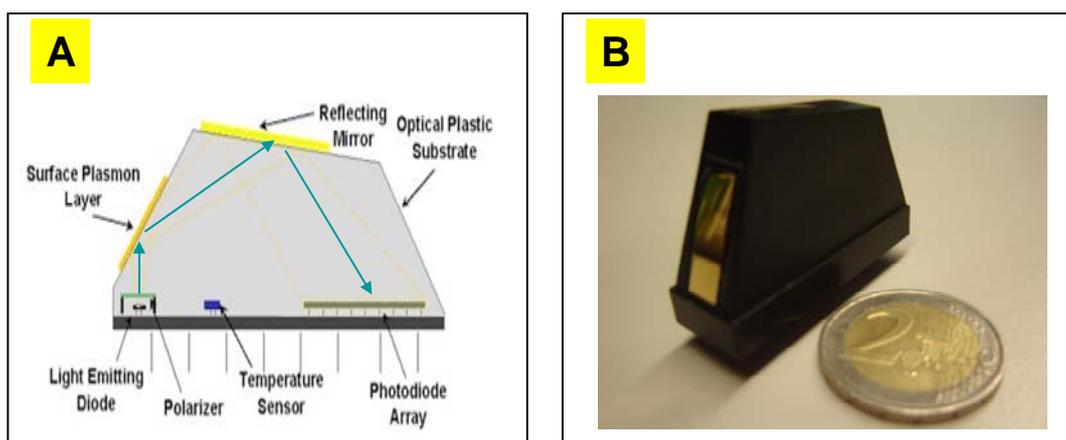
Figure 1-9: The Spreeta™ SPR sensor from Texas instrument Co. LTD. (A) Inside structure of the Spreeta™. The light from the LED is reflected at the surface plasmon layer, and then it reflected to the photodiode array. **(B)** The Spreeta™ chip with the size of 4.1 x 2.9 x 1.3 (cm).

In a view of medical diagnosis, the SPR sensor has several advantages, such as label-free detection, real-time monitoring and one-shot analysis. Especially, Spreeta™ requires relatively small instrumentation and it is suitable for point-of-care testing (POCT) (Homola, 2004). As the POCT can supply laboratory test result without central laboratory, POC system has been developed for medical diagnosis in a small clinics as well as home-health care (Soper et al., 2006). Such a POCT have been used to detect several analytes such as glucose, hemoglobin, urine dipsticks, pregnancy and drug testing (Nichols, 2001). The development of POC technologies will be used for better screening of at-risk patients, tighter surveillance of disease recurrence and better monitoring of treatment.

1.4 Biomarkers for medical diagnosis

The biomarker is defined as a change in biological response ranging from molecular through cellular and physiological responses to behavioural changes (Allan et al., 2006), which includes several indicators of a biologic state, such as nucleic acids, proteins and low-molecular-weight metabolites. Especially, a biomarker can be used to examine organ function or other aspects of health in medicine. In the medical point of view, this biomarker must not only signal the presence of a disease such as cancer, but should also predict the state of disease such as the stage of tumorigenesis (Soper et al., 2006). However, this disease-indicating analyte is mixed with a lot of other materials in serum or urine. The

biosensor can selectively detect biomarker as a target analyte to inform the presence of a disease and quantify the amount of biomarker to know the state of disease through the high "selectivity" and "sensitivity" of biosensor.

In this work, the application of the SPR biosensor technology for medical diagnosis was demonstrated by using several biomarkers for medical diagnosis, such as tumor markers (CA 19-9, CEA), an infectious disease marker (hHBV Ab), a hormone (hCG) and a plasma protein (hA).

(1) Tumor markers (CA 19-9, CEA)

Tumor markers are substances developed in tumor cells and secreted into body fluids. As the concentration and the kind of tumor markers are related with the active tumor mass and site, the tumor markers can be used for the medical diagnosis of cancer.

Carbohydrate antigen 19-9 (CA 19-9) used in the additive assay is one of the most widely used carbohydrate tumor markers for gastrointestinal malignancies. CA 19-9 has a subunit of 210 kDa glycoprotein and it's aggregate has a molecular weight between 600 and 2,000 kDa. Especially, it is reported to be found in patients of pancreatic cancer with a high score of over 79 % (Del Villano et al., 1983; Suresh, 2001). Conventionally, various kinds of immunoassays such as enzyme immunosorbent assay (Ohkura et al., 1985), Chemiluminescence immunoassay (Nishizono et al., 1991; Lin et al., 2004), electrochemical immunoassay (Du et al., 2003) and fluorescence immunoassay (Song et al., 2004) have been applied for the medical diagnosis of CA 19-9.

Carcinoembryonic antigen (CEA) is another widely used tumor marker in oncology, which is a glycoprotein with the molecular weight of 180 kDa. CEA is considered to be a broad spectrum cancer marker because various malignancies at the colorectal, lung, breast, stomach, ovary, pancreas and other organs can cause the elevated CEA concentrations. CEA assay is mainly used for the monitoring of the recurrence of cancer and it is most frequently used for recurrence tests of colorectal cancer (Suresh, 2001). Conventionally, various kinds of immunoassays such as enzyme immunoassay (Hurley et al., 1986), Chemiluminescence immunoassay (Nishizono et al., 1991) and so on have been applied for the medical diagnosis of CEA.

(2) Infectious disease marker (hHBV Ab)

Human hepatitis B virus (hHBV) is a widespread cause of liver disease. There are several markers for this disease and the appearance of each marker has a characteristic sequence. As hHBV antibody appears several months after the disappearance of hHBV antigen, hHBV antibody tests can be used to confirm recovery and immunity in patients with acute hepatitis. And it is also used to check that vaccination has been effective (Mushahwar, 2001). The conventional method of hHBV diagnosis has been ELISA. Several kinds of biosensors were reported using electrochemical (Erden et al., 1999), piezoelectric (Zhou et al., 2002) and optical (Ivanov et al., 2003) principles.

(3) Hormone (hCG) and plasma protein (hA)

The human chorionic gonadotropin (hCG) and plasma protein (hA) can be used for preliminary diagnosis for the abortion and the preterm delivery during early pregnancy.

The concentration of human chorionic gonadotropin (hCG) in urine has been measured for the qualitative pregnancy determination (Wehmann et al., 1981). Usually, the doubling time of hCG in early pregnancy has been reported to be two days and the failure to increase over a period of four days or more is an unfavourable sign to threaten abortion (Chard, 2001). Thesedays, lateral-flow immunoassay called rapid test is widely used for the pregnancy test to measure the concentration of hCG (Wheeler, 2001). Several kinds of biosensors were also reported using electrochemical immunoassay (Lu et al., 2005), fluoroimmunometric assay (Neto et al., 2005) and radioimmunoassay (Vaitukaitis et al., 1972).

In diabetes mellitus, the concentration of glucose in the blood is abnormally high. There are two main types of diabetes mellitus. Type I diabetes patients have a significantly reduced secretion of insulin and type II diabetes is associated with insulin resistance and obesity. The 'microalbuminuria' means the presence of low concentration of human albumin (hA) in urine and it is known to be related with the diabetes (Clark, 2001). Especially for women with type I diabetes, the prevalence of preterm delivery has been reported to increase steeply for those with microalbuminuria and diabetic nephropathy (Ekbom et al., 2001). To detect albumin concentration of microalbuminuria, sensitive immunoassay methods have been developed including RIA, immunoturbidometric assay, nephelometric assay and ELISA (Clark, 2001).

1.5 Concept for the development of an improved biosensor

The overall goal of this work is the application of the SPR immuno-biosensor for medical diagnosis. Because the SPR biosensor still needs improvement in technical specifications for the medical diagnosis (such as sensitivity, detection limit, analysis time and instrumentation), three topics have been targeted to improve this type of biosensor.

[1] The first topic is a reuse method for the IA biosensor called 'additive assay' which enables the reuse of the IA layer without chip exchange and chemical treatment between measurements. In this work, the binding of anti-BSA antibodies to the BSA layer will be used as a model of immunoaffinity interaction to prepare a correlation curve and demonstrate the additive assay. Before making the correlation curve, three requirements for the realization of the additive assay should be satisfied: (1) Reproducible preparation of IA layers to use the same correlation curve. (2) Stable IA layer. (3) Stable antigen-antibody interaction. The correlation curve will be made by relation between the accumulated concentration of additively injected sample and accumulated signal which represents the number of occupied binding sites. After making the correlation curve, the feasibility of additive assay will be tested by injection of samples at mixed concentrations. After defining the valid uncertainty of accumulated concentration as the detection limit, the valid range of accumulated concentration will be determined. In this valid range, several analytes with different concentration will be injected in arbitary sequence and the respective concentrations will be calculated from each signal by using the correlation curve. After comparing the calculated concentrations with those of real values, the average error of the additive assay will be evaluated to determine whether the additive assay is feasible for the immunosensors. The additive assay will be also demonstrated by using another SPR biosensor called Biacore 3000, which will be performed by cooperation with the group of Prof. Bernhardt at Saarland University (Germany). And then the result will be compared with that of Spreeta^{TM}. The application of the additive assay for real medical diagnosis will be demonstrated by using the tumor marker (CA 19-9) as a target analyte.

[2] The second topic is the 'simultaneous detection' which enables the detection of multiple analytes on a single sensor element with single sample treatment. In this work, two simultaneous detection models (Model 1 and Model 2) will be devised for the sample with the following composition: (1) one target analyte resulting in a sensor response without any label and the other analyte with additional label (Model 1), (2) both target analytes requiring additional labels for detetion (Model 2). The IA layer was prepared by

immobilizing BSA and anti-HRP antibodies together. And the sample was composed of anti-BSA antibodies and HRP. After making the respective standard curves for the correlation between the concentration and signal, the average errors of simultaneous detection based on Model 1 and Model 2 will be calculated for anti-BSA antibodies and HRP to determine whether each Model is acceptable for application. As requirements for the realization of the simultaneous detection, (1) cross-reaction arising from non-specific binding among the participating antigens and antibodies will be tested and (2) the binding capacity of the IA layer for each target analyte will be optimized by adjusting of the concentration ratio of the molecular recognition element at the immobilization step. The real medical diagnosis based simultaneous detection will be demonstrated by analysis of human chorionic gonadotropin (hCG) and human albumin (hA) in human urine for the diagnosis of preterm delivery of patients with diabetes.

[3] The third topic is the improvement of the sensitivity and detection limit through two 'signal amplification' methods by using mass label (A) and by the orientation control of the IA layer (B): (A) In comparison with the direct assay, the amplification ratio by using secondary antibodies, avidin-biotynylated antibodies and peroxidase-anti-peroxidase (PAP) complex will be estimated to select the most efficient label for signal amplification by considering the non-specific binding of label protein. The feasibility of this signal amplification method will be demonstrated by analysis of an infectious disease marker, human hepatitis B virus (hHBV) antibody. The detection limit of the SPR biosensor by using the selected method will be compared with the cut-off value for medical diagnosis (0.24 nM) by using the commercial ELISA kit. (B) In this work, the surface density of receptor antibody (anti-hIgG) will be compared by attachment of receptor antibody to the layer of avidin, NeutrAvidin, protein A, NeutrAvidin-protein A complex and bare gold surface of SPR biosensor. The ligand antibody (hIgG) will be injected to each IA layer and the binding ratio of ligand antibody per unit receptor will be estimated as a parameter of orientation control. By considering the surface density of (1) receptor and (2) ligand antibody and (3) the binding ratio of ligand per receptor antibody, the most efficient layer will be selected. With the selected layer, test will be also done on biotin-labelled SAM in comparison to the IA layer prepared by chemical coupling of receptor antibody to the SAM layer. For the feasibility test of orientation control, the selected layer will be applied to detect a cancer marker, carcinoembryonic antigen (CEA).

2. Materials and Methods

2.1 Materials

- Chemicals

11-mercaptoundecanoic acid, N-(3-dimethylamino-propyl)-N'-ethylcarbodiimide (EDAC), N-hydrosuccinimide (NHS), p-nitrophenyl phosphate, tetramethylbenzidine were purchased from Sigma-Aldrich Chemical Co. (Deisenhofen, Germany). All reagents for the Biacore 3000 instrument such as amine coupling kit and HBS running buffer were purchased from Biacore International SA (Freiburg, Germany). EZ-Link^{TM} Biotin Hydrazide was bought from Pierce Biotechnology, Inc. (Rockford, IL, USA).

- Antigen - Antibodies

Bovine serum albumin (BSA), rabbit anti-BSA antibody (polyclonal), human Chorionic Gonadotropin (hCG), human albumin (hA) and goat anti-human albumin antibody (polyclonal) were purchased from Sigma-Aldrich Chemical Co. (Deisenhofen, Germany). Carbohydrate antigen 19-9 (CA 19-9), mouse anti-CA 19-9 (monoclonal), rabbit anti-hHBV (polyclonal), carcinoembryonic antigen (CEA), mouse anti-CEA antibody (monoclonal) and goat anti-CEA antibody (polyclonal) were purchased from Fitzgerald Inc. (Concord MA, USA). Human hepatitis B virus (hHBV) antigen was purchased from Yashraj Biotechnology, Ltd. (Mumbai, India). Goat anti-hCG antibody (polyclonal) was obtained from Affinity BioReagent, Inc. (Hamburg, Germany). Goat anti-horseradish peroxidase, donkey anti-rabbit IgG, donkey alkaline phosphatase conjugated anti-rabbit IgG, human IgG, (hIgG) donkey anti-hIgG, rabbit Peroxidase-Anti-Peroxidase (PAP), and donkey biotin conjugated anti-rabbit IgG were purchased from Jackson immunochemical research laboratories, Inc. (West Grove, PA, USA).

- Others

Newborn calf serum was bought from Biochrom AG (Berlin, Germany). The commercial ELISA kit for the diagnosis of hHBV (Monorisa$^{®}$ Anti-HBs 3.0, Ver. 3.0) and non-fat milk were purchased from BioRad Laboratories GmbH (Muenchen, Germany). Biotin labeled protein A, protein A and avidin were purchased from Calbiochem-Novabiochem GmbH (Schwalbach, Germany). NeutrAvidin^{TM} was bought from Pierce Biotechnology, Inc.

(Rockford, IL, USA). Casein was bought from Merck, Inc. (Darmstadt, Germany). Water was purified by Milli-Q system (Millipore Co., MA, USA).

2.2 Methods

2.2.1 Preparation of IA layer

The IA layer was prepared on the gold surface of the Spreeta™ chip at 37°C. First, the self-assembled monolayer (SAM) was prepared on the gold surface by incubating 5 mM 11-mercaptoundecanoic acid in ethanol for 2 hrs. For the coupling of biomolecules, the sensor surface was rinsed with ethanol and then with 10 mM PBS buffer (pH 4.5). The PBS buffer was prepared by mixing 10 mM di-sodium hydrogen phosphate (Na_2HPO_4) with 0.15 M KCl and 10 mM sodium dihydrogen phosphate (NaH_2PO_4) with 0.15 M KCl. Biomolecules were coupled to SAM by using the coupling reagents of EDAC (50mM) and NHS (50 mM) in 10 mM PBS (pH 4.5). The SAM was first treated with EDAC and NHS for 10 min and then the solution of biomolecules in 10 mM PBS (pH 4.5) was incubated. The concentration of the biomolecules and incubation time are summarized in Table 2-1. After immobilizing recognition parts, the other reactive sites of SAM were blocked by 1 M ethanolamine (Naimushin et al., 2002; Kim et al., 2005; Lee et al., 2005).

Table 2-1. The concentration of biomolecule and incubation time for making IA layer.

	The concentration of biomolecules	Incubation time
Additive assay (section 3.1)	BSA (10 mg/ml)	10 min
	CA 19-9 (500 μg/ml)	1 hr
Simultaneous detection (section 3.2)	BSA (0.1 mg/ml) and anti-HRP (2mg/ml)	1 hr
	Anti-hCG (500 μg/ml) and anti-hA (100 μg/ml)	1 hr
Signal amplification by using mass label (section 3.3.1)	hHBV antigen (75 μg/ml)	2 hr
Signal amplification by the orientation control of IA layer (section 3.3.2)	Anti-CEA (0.5 mg/ml)	1.5 hr

In the signal amplification with the control of IA layer, several modified surfaces were prepared on the bare gold surface or the SAM surface. After modification of sensor surface, the anti-hIgG solution at the concentration of 1 mg/ml in the 10 mM PBS (pH 7.4) was incubated as a receptor protein for 90 min. In order to prevent the non-specific binding, the protein bound sensor surface was treated with highly concentrated BSA solution (10 mg/ml).

For the preparation of modified surfaces on the bare gold surface, several proteins such as avidin, protein A and NeutrAvidin were prepared on the bare gold surface by incubating the protein solution for 90 min. The concentration of protein was adjusted to be 1 mg/ml in 10 mM PBS (pH 7.4).

The NeutrAvidin-protein A complex layer on the bare gold surface was prepared by sequential treatment of NeutrAvidin (1 mg/ml) and biotin-labelled protein A (1 mg/ml) for 90 min, respectively (see Figure 2-1A).

For the preparation of NeutrAvidin-protein A complex layer on the SAM surface, NeutrAvidin (1 mg/ml for 90 min) was attached to the SAM surface by using EDAC/NHS and then biotin-labelled protein A (1 mg/ml for 90 min) was attached to the NeutrAvidin layer (see Figure 2-1B).

For the preparation of NeutrAvidin-protein A complex layer on the biotin-labelled SAM surface, biotin hydrazide at the concentration of 1 mg/ml was attached to the SAM surface by using EDAC/NHS for 60 min, and then NeutrAvidin (1 mg/ml for 90 min) and biotin-labelled protein A (1 mg/ml for 90 min) were also sequentially treated to prepare NeutrAvidin-protein A complex layer (see Figure 2-1C).

The chimeric complex which was made by mixing equimolar biotin-labelled protein A and NeutrAvidin was incubated for 60 min after treatment of biotin hydrazide at 1 mg/ml on the SAM layer for 60 min (see Figure 2-1D).
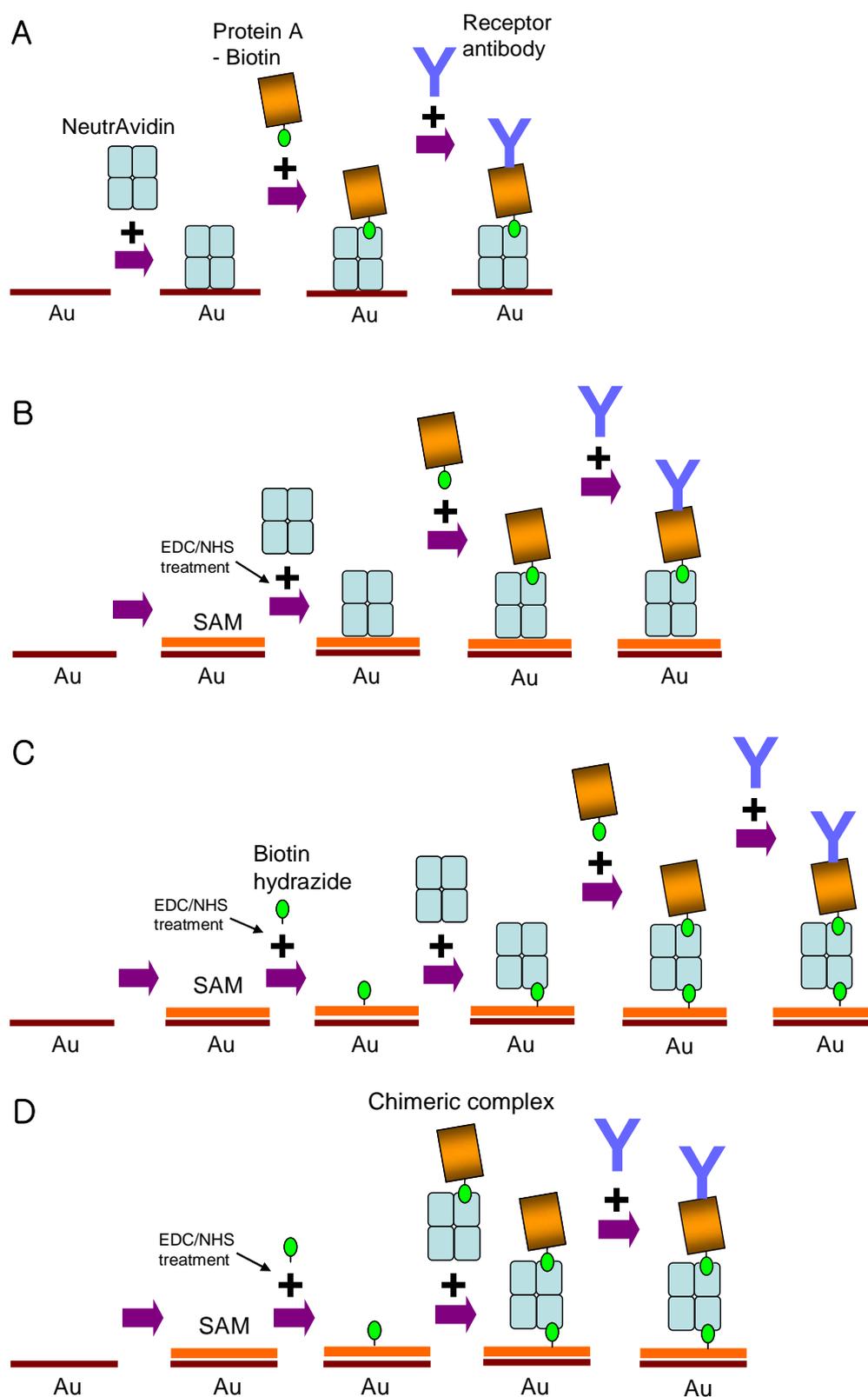
Figure 2-1: Schematic of description for the preparation of modified surfaces. (A) NeutrAvidin-protein A complex layer on the bare gold surface. **(B)** NeutrAvidin-protein A complex layer on the SAM surface. **(C)** NeutrAvidin-protein A complex layer on the biotin-SAM surface. **(D)** Chimeric complex layer on the biotin-SAM surface.

2.2.2 Signal measurement of SPR biosensor.

The typical sensorgram by SPR biosensor is shown in Figure 2-2. The signal detection was composed of three steps; washing step before sample injection, sample incubation step, washing step after sample injection. For the washing step, 0.5 % Tween 20 was flowed at the point of '1' and incubated for 4 min at washing step, and then 20 µl of sample was flowed at the point of '2' and incubated for 10 min in the sample injection step. In this work, we used stopped-flow measurement system which is similar to the cuvette based SPR systems. The measurement was performed at the stopped-flow condition after washing step to avoid wrong measurement of refractive index by the sample with high protein concentration, such as serum. As shown in Figure 2-2, the 'Signal' is calculated to be the difference between SPR angles at the washing step before sample injection and after sample injection.
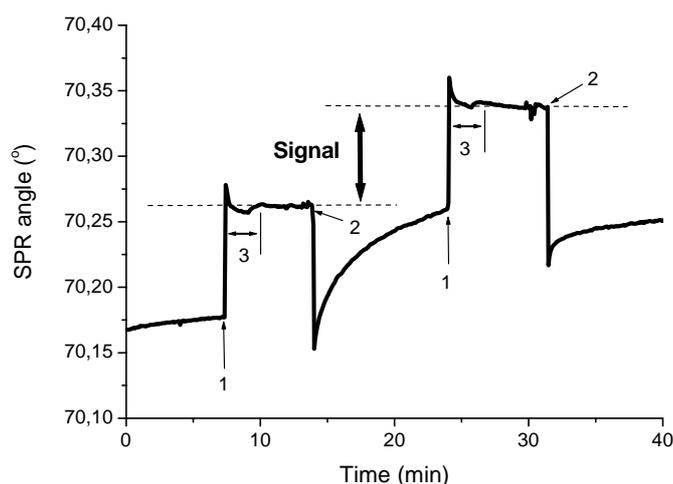
Figure 2-2: A typical sensorgram of the SPR biosensor.

The point '1' indicates injection of washing buffer which flows for 2 min as indicated by '3'. The point '2' indicates the sample injection. The 'Signal' is calculated to be the difference between SPR angles at the washing step before sample injection and after sample injection.

(1) Sensor response at the equilibrium

The sensor response of analyte binding was calculated by the following equation based on the binding kinetics of one-to-one interaction (O'Shannessy et al., 1993):

$$R_t = \left[\frac{C \cdot R_{\max}}{(C + K_D)} \right] \cdot \left[1 - e^{-t(C + K_D)k_a} \right]$$ where R_t is the sensor response at time t, C is the

concentration of analyte in solution, $R_{\max}$ is the maximal sensor response, K_D is the

dissociation constant, k_a is the association rate constant. The response of SPR sensor

reaches a signal plateau after a certain incubation time. The equation can be simplified as

follows: $R_t = M \cdot \left[1 - e^{-t \cdot K} \right]$ where M and K are independent parameters to the sample

concentration. For the calculation of parameters of M and K, the sample at the

concentration C was injected and the sensor response had been recorded for enough

incubation time (2 hour). The obtained sensorgram was fitted by using the non-linear fitting

of Origin software (Microcal Software, MA) based on the above equation (see Figure 2-3A).

A   **B**
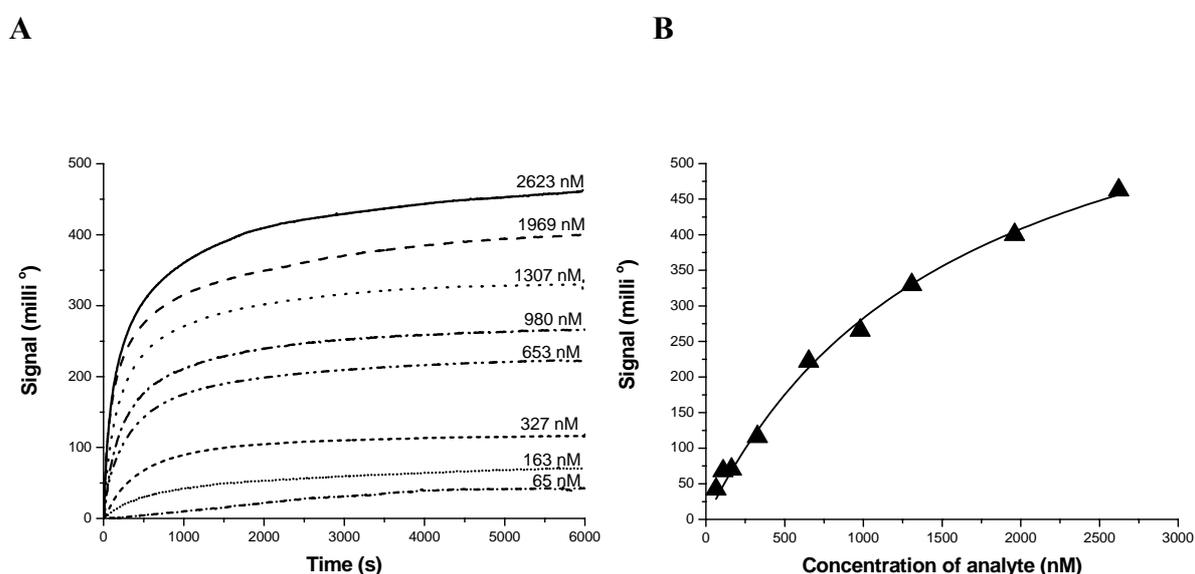
Figure 2-3: The sensor response at the equilibrium.

The SPR sensor response of the reaction between anti-BSA antibody (analyte) and BSA (IA layer).
(A) The SPR sensorgrams with several concentrations of analyte (anti-BSA antibody). After proper
incubation time, the maximum signal value for each concentration (M) can be calculated as the
signal at the equilibrium by using the non-linear fitting: $R_t = M \cdot \left[1 - e^{-t \cdot K} \right]$ where M and K are
independent parameters to the sample concentration. **(B)** The does-response curve at the equilibrium.
To make does-response curve, the concentration and the signal at the equilibrium (M) for each
concentration were plotted as X-axis and Y axis and the maximum signal value for all concentration

($R_{\max}$) and K_D were calculated by using the non-linear fitting of $M = \left[\frac{C \cdot R_{\max}}{(C + K_D)} \right]$.

The calculated M value was the maximum signal value for each concentration such as the signal at the equilibrium. When the calculated M values were plotted to the respective concentration, the maximum M value (R_{max}) and K_D were calculated by using the non-linear fitting of $M = \left[\dfrac{C \cdot R_{max}}{(C + K_D)} \right]$ (the Langmuir isotherm model), and then this equation could be used for the sensor response at the equilibrium (see Figure 2-3B). For this calculation, more than five concentrations were selected for each analyte within the concentration range used in this work.

(2) Optimization of incubation time.

Generally, the sensor response reaches the equilibrium after a long incubation time and it is not efficient for real application. For more efficient application, the incubation time should be shortened. In this case, the standard curve which is obtained by short incubation time has less similar physical meaning with Langmuir isotherm model. In this work, the optimum incubation time was selected to get a high enough fitting result (r^2) to the fitting model, where "r^2" is the the square of the correlation coefficient (r). Compared with the does-response curve at the equilibrium of Figure 2-3B (r^2=0.995), the "r^2" value after the incubation time of 10 min was slightly changed from 0.995 to 0.993 (see Figure 2-4). From this result, the incubation for 10 min could be applied in this experiment.
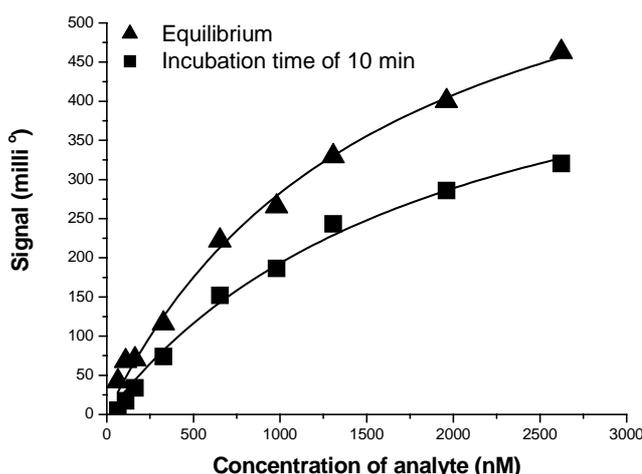
Figure 2-4: The sensor responses with different incubation times. Compared with the does-response curve at the equilibrium of Figure 2-3B (r^2=0.995), the "r^2" value with the incubation time of 10 min was slightly changed from 0.995 (▲) to 0.993 (■). From this result, the standard curve following incubation for 10 min was also observed to fit well to the same model.

The other factors were also considered for the selection of an optimum incubation time. For example, the incubation time is related to the sensitivity of the measurement, the baseline drift and the detection limit. For suitable measurements in this work, the optimum incubation time should be determined by considering these parameters along with the square of the correlation coefficient (r^2).

(3) Calculation of lower limit of detection (LLD) by using baseline drift.

The sensitivity of an assay has been defined as the lower limit of detection (LLD), and it has been estimated from the slope of the dose-response curve. The LLD is the lowest analyte concentration that makes a positive signal significantly different from the negative signal in the absence of antigen. In a noncompetitive assay, the LLD is usually defined as three standard deviations from the mean of the zero analyte control. Accordingly, signal for LLD is m + 3sd, where "m" is the mean signal obtained in absence of antigen, "sd" is the standard deviation of the signal in absence of antigen. LLD is the concentration where signal of m + 3sd is positioned in the dose-response curve (Ezan and Grassi, 2000). The baseline drift was measured in absence of antigen by repeated injection of 10 mM PBS (pH 7.4) which is used as a sample buffer and 0.5 % Tween 20 (see Figure 2-5).
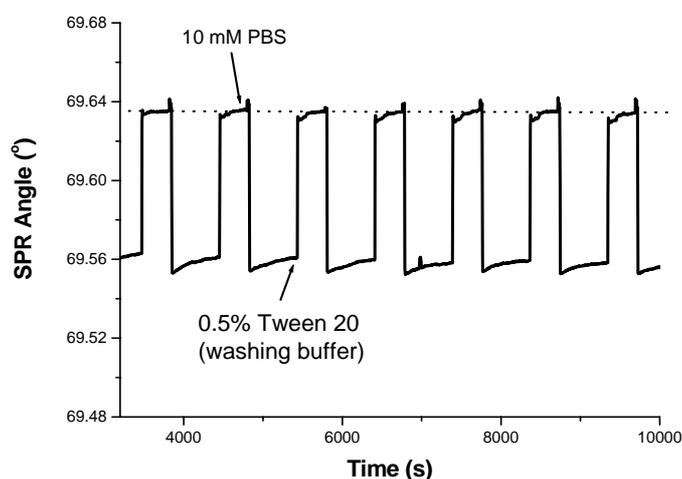
Figure 2-5: SPR sensorgram by repeated injections of 0.5% Tween 20 and PBS by turns. The baseline drift was calculated by the repeated injection of 10 mM PBS (pH 7.4). The baseline drift was estimated to be 0.9 (m) ± 0.4 (sd) milli° (n = 50) and signal for LLD (m + 3sd) was calculated to be 2.1 milli° in this system.

The baseline drift was calculated by the difference of SPR angles by 0.5 % Tween 20 solution measured before and after the injection of 10 mM PBS. The baseline drift was estimated to be 0.9 (m) ± 0.4 (sd) milli° (n = 50). From this result, signal for LLD (m + 3sd) was calculated to be 2.1 milli° in this system.

As the baseline drift decreased to be stabilized, signal was kept less than ± 1 milli° for 30 min and then the concentration of LLD was also decreased. As the refractive index is sensitive to temperature, the change of temperature is related to the baseline drift (Roos et al., 1998). The influence of the temperature on the responses of the transducer was investigated by variation of the temperature of the water bath, which was slowly cooled down in the ice box from 42 ^{o}C to 22 ^{o}C. As the temperature change of 1 ^{o}C caused a baseline drift of 8.7 milli ^{o} (see Figure 2-6), the temperature of SPR sensor system should be set to be ±0.5 ^{o}C for the drift of less than 5 milli ^{o}.
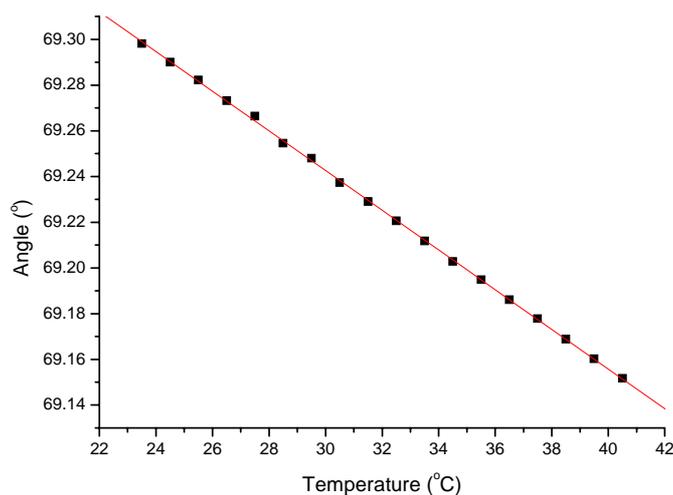
Figure 2.6: Influence of the temperature on the SPR signal.

2.2.3 Instruments

(1) Spreeta^{TM} system

The Spreeta^{TM} chip from Texas Instrument Co. (Dallas, TX, USA) was used for SPR measurement. The response of SPR chip was transferred on-line to a PC by a 12-bit analog-to-digital converter. Before the preparation of an IA layer, the SPR chip was first calibrated with the air and then with deionized water of refractive index (RI) of 1.33. The SPR chip

was equipped with an integrated flow cell with a capacity of 5 µl. The sample and the washing solution were injected to the flow cell of the SPR chip using an autosampler and an integrated peristaltic pump from EKF diagnostik GmbH (Magdeburg, Germany) (see Figure 2-7). The pumping rate was set to be 1.0 ml/min. The peristaltic pump and the autosampler were controlled using a programmable microprocessor board. The flow of solution was programmed to stop during the incubation step and the measurement step. In the preparation of IA layer, the injection of reagents was performed by a peristaltic pump from Amersham-Pharmacia Biotech AB (Uppsala, Sweden). The whole instrument was kept in an incubator and the temperature was set to be 37 °C.
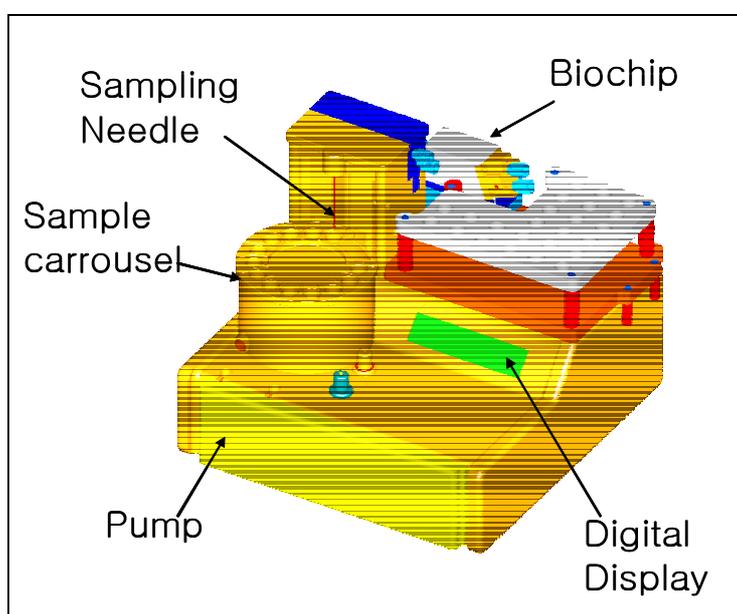
Figure 2-7: SPR system in KIST-Europe.

The SPR chip was equipped with an integrated flow cell with a capacity of 5 µl. The sample and the washing solution were injected to the flow cell of the SPR chip using an autosampler and an integrated peristaltic pump which were controlled using a programmable microprocessor board. The whole instrument was kept in an incubator and the temperature was set to be 37 °C.

(2) Biacore^{TM} system

The additive assay was also demonstrated using another SPR biosensor called Biacore 3000. In previous work, the IA layer was prepared by immobilization of BSA to the SAM layer of Spreeta^{TM} chip. In the Biacore system, modified cellulose layer (CM5 chip) was used for the preparation of the IA layer. Therefore, the number of binding sites on the CM5 chip was

expected to be different from Spreeta^{TM} chip. The gold surface of the CM5 chip is covalently covered with a matrix of carboxymethylated dextran, a flexible unbranched carbohydrate polymer forming a thin surface layer approximately 100 nm thick. Coupling of protein to the CM5 chip was performed by activating the carboxyl groups on the chip with a solution containing 50 mM EDAC and 50 mM NHS. The pumping rate was set to be 5 μl/min. After coupling of protein, remaining free ester groups were blocked by 1 M ethanolamine. All protein-containing solutions were prepared in Biacore HBS-EP buffer (0.01 M HEPES buffer pH 7.4, 0.15 M NaCl, 3 mM EDTA and 0.005% Surfactant P20). Analysis of the data was accomplished by using the Biacore evaluation software 3.1.

(3) ELISA

Enzyme-linked immunosorbent assay (ELISA) is widely used for a selective and sensitive analysis of biological samples. Typically, horseradish peroxidase (HRP) with high turnover rate is most commonly utilized in an ELISA protocol (Vo-Dinh et al., 2004). The immobilization of receptor antibody was performed in a 96-well microplate for 2 hr at 37 °C, and then it was blocked by using 10 mg/ml BSA. After washing with 0.5 % Tween 20, test sample (100 μl) was incubated for 1 hr. For the measurement of target analyte, HRP conjugated label was treated and the colorimetry was performed by treating tetramethybenzidine (TMB) (0.02 mg/ml in 0.2 M citrate buffer) with hydrogen peroxide. The concentration of the test sample was calculated using a standard curve for each analyte. The optical density was measured at 450 nm using a SPECTRA Rainbow Thermo (TECAN DEUTSCHLAND GmbH).

3. Results

The major objective of this work is the development of a SPR biosensor for medical diagnosis with the features of a cost-effective test by 'additive assay', short analysis time through 'simultaneous detection' and high sensitivity by 'signal amplification'. For the realization of this major objective, the three topics were investigated as follows:

- Additive assay for the repeated measurements without regeneration step

'Additive assay' enables reuse of the IA layer without chip exchange and chemical treatment between measurements. The concentration of each measurement is calculated by using a previously prepared correlation curve. This method was demonstrated to be feasible by measuring a cancer marker (CA 19-9). The result showed that the 'additive assay' could be applied for the repeated measurement of CA 19-9 without chip exchange and chemical treatment (see Section 3.1).

- The simultaneous detection of multiple analytes

'Simultaneous detection' enables the analysis of multiple analytes in the same sample. The molecular recognition part of SPR IA-biosensor was prepared by immobilizing two kinds of receptor antibodies. Each concentration of analyte was measured by treatment of labelled antibodies and by using standard curves. The feasibility of this method was demonstrated by the analysis of hCG and hA in urine for the diagnosis of preterm delivery. The result showed that 'simultaneous detectioin' of both analytes with single sample treatment could be applied for the short analysis time (see Section 3.2).

- Signal amplification of SPR biosensor

Two 'Signal amplification' methods were developed to improve the sensitivity and detection limit of SPR IA-biosensor.

(1) The mass label attached to the already bound target analyte increases the total mass attached to the sensor surface and then it induces the increase of SPR signal. Among several kinds of mass labels, PAP method was selected for the efficient signal amplification. With this mass label, the feasibility of this signal amplification method was demonstrated by the detection of hHBV antibody. The result showed that the detection limit of SPR biosensor approached closely to cut-off value for medical diagnosis by using the commercial ELISA

kit (see Section 3.3.1).

(2) The control of IA layer (orientation & density) could improve the sensitivity and detection limit of IA biosensor. For this work, several kinds of proteins were tested. As an efficient controlled IA layer, NeutrAvidin-protein A complex layer was selected. With this layer, the feasibility of this signal amplification method was demonstrated by analysis of a cancer marker (CEA). The result showed that control of IA layer (orientation & density) improved the sensitivity and detection limit of IA biosensor (see Section 3.3.2).

These results demonstrated the 'additive assay' for cost-effective test, 'simultaneous detection' for short analysis time and 'signal amplification' for high sensitivity. The presented three methods in this study will be applied to develop a practical SPR biosensor for the various medical diagnoses.

3.1 Additive assay for the repeated measurements without regeneration step

The 'additive assay' aims to use SPR immunosensor for repeated analysis without chemical treatment between measurements. In the additive assay, the concentration of sample is calculated from the actually measured signal by using a correlation curve. In this work, the accumulated concentration of additively injected sample was correlated to the accumulated signal. By using a this way prepared correlation curve, the feasibility of the additive assay was tested by injection of samples at mixed concentrations and the real medical diagnosis was demonstrated by using the tumor marker (CA 19-9) as a target analyte.

3.1.1 The comparison of the conventional methods

The 'regeneration' method has been conventionally used for the repeated measurements by immunosensors. In this method, the already bound analytes are removed from the IA layer by chemical treatment such as high or low pH agents for each measurement. As shown in Figure 3.1, the IA layer is regenerated by removing the already bound analytes before each measurement. In this case, the signal (S_1) is expected to have constant relation to the concentration (C_1) of the analyte. After several times of regeneration steps, the damage of the IA layer is known to occurr so that the relation between signal and concentration is changed. In this case, new calibration of the IA biosensor is required. For example, when the anti-BSA antibody (327 nM) was injected to the BSA layer on the CM5 chip and NaOH

was repeatedly treated for regeneration, the SPR signal at 1st injection was measured to be 794 RU and the SPR signal at 7th injection was changed to be 619.6 RU. This result shows that there was a 22 % reduction of binding activity after only six regeneration treatments. As the regeneration is repeated, the signal to the same concentration is expected to be decreased gradually. In the additive assay, measurements are performed without the regeneration step. The analytes are additively injected to the IA layer without removing the already bound analytes as shown in Figure 3-1. As the number of binding sites is confined in the IA layer, the number of free binding sites is reduced as the analytes are additively bound to the IA layer. After a certain amount of binding sites are occupied by repeated treatment of samples, the IA layer becomes saturated and the sensor no longer responds to the injection of sample.
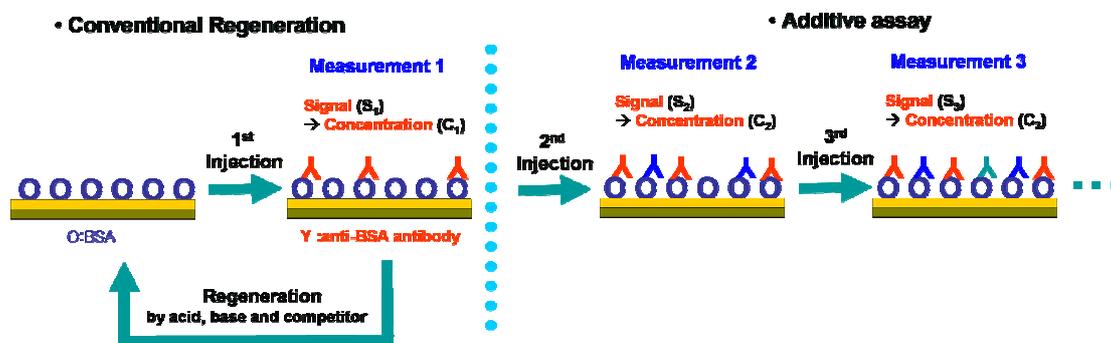
Figure 3-1: The schematic diagram of the additive assay in comparison to the conventional regeneration method.

3.1.2 Requirements for additive assay

The additive assay is based on the correlation between the accumulated concentration of additively injected sample and accumulated signal. For the realization of the additive assay, the following requirements should be satisfied: (1) The layer-to-layer homogeneity should be achieved to use the same correlation curve. (2) The IA layer on the sensor surface should be stable enough during the whole measurement steps. (3) The binding of analytes should be maintained during the whole measurement steps.

(1) Reproducible preparation of IA layers

The IA layer of a SPR biosensor has a constant number of binding sites for analytes. Usually, the signal of the IA biosensor is generated by the occupancy of the free binding sites of the IA layer. If the number of the free binding sites is different, the biosensor signals from the sample at the same concentration are also different. Therefore, the IA layer to IA layer homogeneity should be achieved for the realization of an additive assay to use the same correlation curve. The reproducibility of IA layers can be investigated by comparing the number of free binding sites. Four IA layers were prepared and each IA layer was treated with a standard sample (108.7 nM) and then five samples were sequentially injected (54.7 → 65.3 → 108.7 → 163.3 → 326.7 nM) (see Table 3.1). As the biosensor signal is proportional to the number of free binding sites in each IA layer, the signal from standard sample and the accumulated signal by sequentially injected samples can be used to compare the number of free binding sites of different IA layers. The standard signal and accumulated signal from four IA layers was estimated to be 28.9 ± 0.5 milli° and 215.9 ± 6.2 milli°, respectively. The deviation was calculated to be 1.7 % and 2.9 %, respectively. These deviations were used for the calculation of measurement errors and the limit of detection.

Table 3.1: Reproducibility of the response of IA layers (chip-to-chip difference)

No. of Chips	Standard Signal[2] (milli°)	Accumulated Signal[3] (milli°)
1	29.5	212.6
2	28.4	221.7
3	29.1	220.5
4	28.8	208.8
Mean ± sd	28.9 ± 0.5 (1.7%)[1]	215.9 ± 6.2 (2.9%)[1]

1: Deviation is defined as (100 x standard deviation (sd) / mean).

2: A standard signal was measured by injecting standard sample at the concentration of 108.7 nM.

3: Accumulated signal is the sum of signals which were made by five sequentially injected samples.

(2) Stability of the IA layer

The IA layer should be stable enough to be maintained during the whole additive assay steps. If the IA layer is not stable, a part of IA layer can be detached from the sensor surface during washing steps required for signal measusrement. In this case, the total number of free binding sites is changed and the standard correlation curve can not be used for the additive assay as mentioned previously.

The stability of the IA layer was estimated by measuring the baseline drift by repeated injection of blank sample (10mM PBS) as shown in Figure 3-2. The sensor signal from the BSA binding to SAM layer was 151 ± 11.1 milli°. If this BSA-layer (IA layer) is detached from the sensor surface, the signal would be decreased from this value after blank sample treatment. Baseline drift after repeated blank sample injection was estimated to be -0.1 ± 0.9 milli° (n = 16). This value is also similar to the baseline drift on the bare gold sensor surface without IA layer (0.9 ± 0.4 mili°). This result indicates that there was no significant detach of the IA layer and the IA layer can be maintained stable for long enough time required for additive assay.
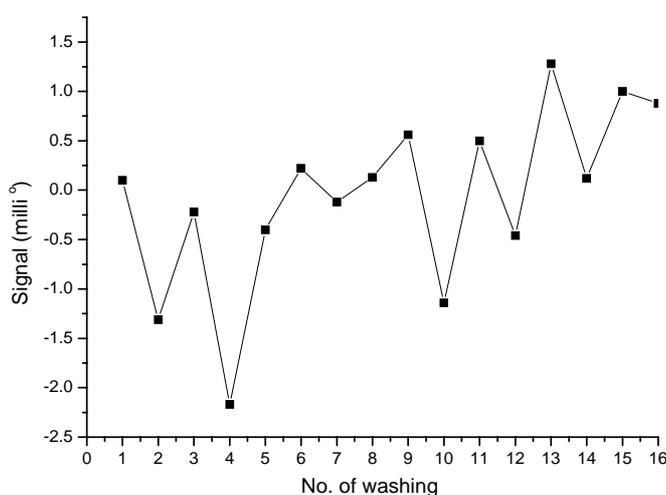
Figure 3-2: Baseline drift at the injection of blank samples (10 mM PBS) to the BSA layer (n=16). The stability of the IA layer (BSA layer) was estimated by measuring the baseline drift by repeated injection of blank sample (10mM PBS). Baseline drift after repeated blank sample injection was estimated to be -0.1 ± 0.9 milli° (n = 16). This value is also similar to the baseline drift on the bare gold sensor surface without IA layer (0.9 ± 0.4 mili°).

(3) Stability of antigen-antibody interaction.

As previously mentioned, the additive assay is based on the correlation between the accumulated signal and the accumulated concentration. This means that the analytes bound to the IA layer should be maintained during additive assay. If analytes are dissociated from IA layer, the accumulated signal is decreased. In this case, the correlation between the accumulated concentration of additively injected sample and accumulated signal will be changed and the correlation curve can not be used for measurement. The stability between

the IA layer and analytes is in proportion to the value of affinity constant (K_A) representing the final ratio between bound and unbound analytes to the IA layer. Therefore, the valid range of K_A can be used to select a suitable pair of IA layer and analytes. In this experiment, BSA (IA layer) and anti-BSA antibodies (analytes) were estimated to be a suitable antigen-antibody pair for the additive assay. By using several sensorgrams of different concentrations, K_D can be calculated (see section 2.2.2(1)) and K_A is an inverse number of K_D. From the four sensorgrams (54.8, 65.4, 109 and 326 nM of anti-BSA antibodies), the K_A value for BSA and anti-BSA antibodies was calculated to be 1.17 $\times$ 10^6 [1/M] by using the Biacore evaluation software 3.1 with a 1:1 binding model (see Figure 3-3). Therefore, the additive assay can be applied for a pair of antigen and antibody which has higher K_A value than 10^6 [1/M].
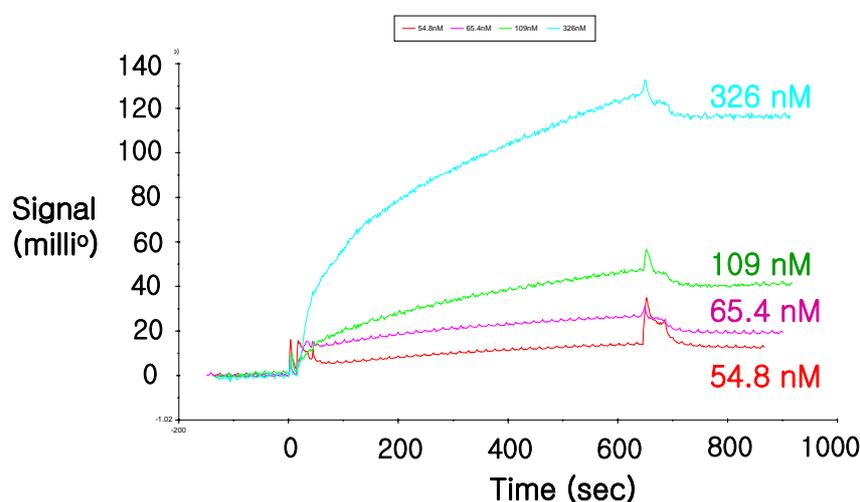
Figure 3-3: The sensorgram for calculation of affinity constant (K_A). BSA and anti-BSA antibodies were used as IA layer and analytes, respectively. From the four sensorgrams (54.8, 65.4, 109 and 326 nM of anti-BSA antibodies), the K_A value for BSA and anti-BSA antibodies was calculated to be 1.17 $\times$ 10^6 [1/M] by using the Biacore evaluation software 3.1 with a 1:1 binding model.

3.1.3 Correlation curve for the additive assay

In the additive assay, measurements are performed without regeneration step to remove the already bound analytes. As the number of free binding sites is reduced by the binding of analytes to the IA layer, the sensor response of next measurement is different from that of a freshly prepared sensor. Even if the sample at the same concentration is injected repeatedly,

the number of free binding sites decreases and the corresponding sensor response also decreases as shown in Figure 3-4. To indicate accumulation of analyte by repeated injection, the X-axis was represented to be the addition of concentrations of injected samples from the first injection (accumulated concentration) and signal responses for each measurement were plotted as Y-axis. When the first sample at the concentration of x nM obtains the sensor signal of y_1 milli° and the second sample at the same concentration obtains the sensor signal of y_2 milli°, the first sample and the second sample are plotted to be (x, y_1) and $(2x, y_2)$, respectively. The physical meaning of accumulated concentration is directly related to the amount of adsorbed analyte to the IA layer.
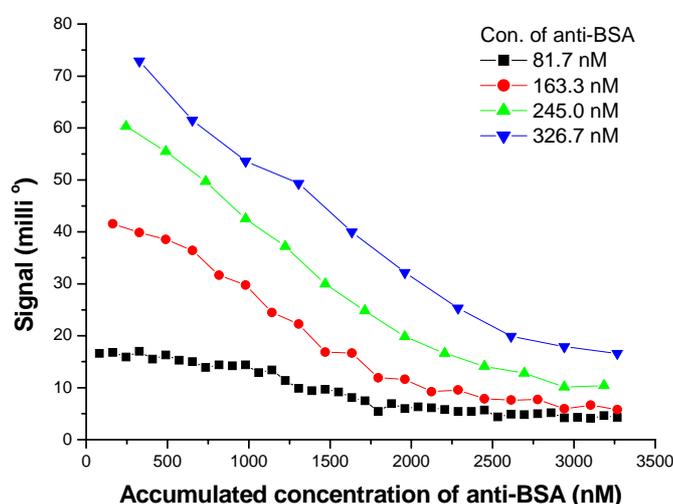
Figure 3-4: Signal decrease by additive injection of samples at the same concentration. For each curve, the samples at the same concentration were repeatedly injected to one sensor chip and these experiments were carried out with several concentrations of anti-BSA antibodies (81.7, 163.3, 245, 326.7 nM). The X-axis was calculated by simply adding the concentrations of injected samples from the first injection (accumulated concentration) and signal responses for each measurement were plotted as Y-axis. When the first sample at the concentration of x nM obtains the sensor signal of y_1 milli° and the second sample at the same concentration obtains the sensor signal of y_2 milli°, the first sample and the second sample are plotted to be (x, y_1) and $(2x, y_2)$, respectively. Even if the samples at the same concentration are repeatedly injected, the number of free binding sites decreases and the corresponding sensor response also decreases.

For the calculation of sample concentration from the actually measured sensor response by using the correlation curve, the accumulated signal is required, which is recorded from the

first sample measurement. As the history of measurement indicates the number of occupied binding sites on the IA layer, the accumulated signal can be used to correlate the actual signal to the actual concentration. If the Y-axis is assigned to be the accumulated signal, the curves approach into a single curve, even if each curve was obtained by the repeated injections of respective concentrations (see Figure 3-5A). Each point of Figure 3-5A was obtained by accumulated addition of injected concentration and measured signal. When the first sample at the concentration of x_1 nM obtains the sensor signal of y_1 milli° and the second sample at the concentration of x_2 nM obtains the sensor signal of y_2 milli°, the positions of the first sample and the second sample are (x_1, y_1) and $(x_1 + x_2, y_1 + y_2)$, respectively.

A   **B**
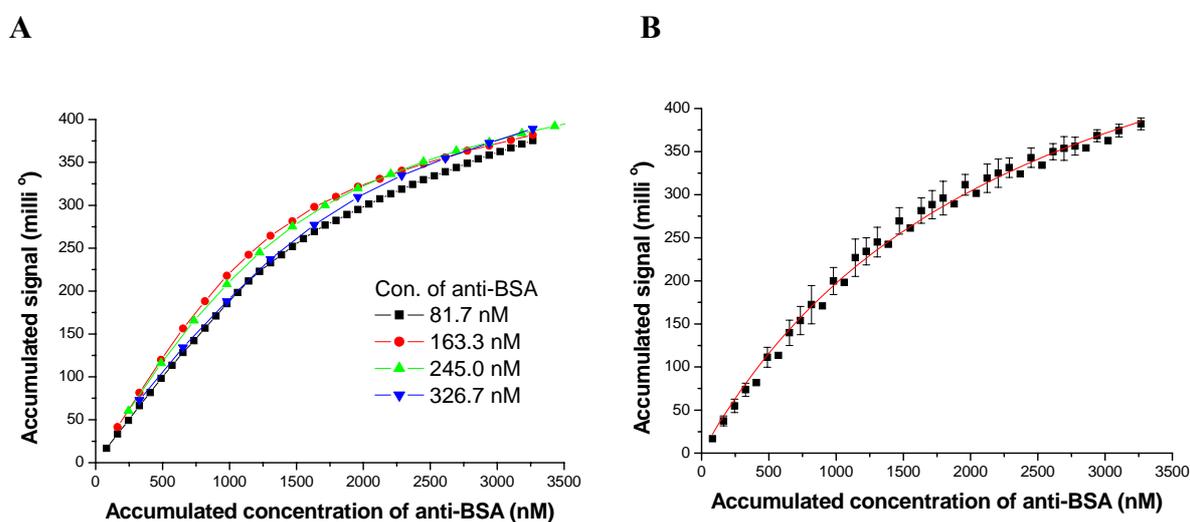
Figure 3-5: Correlation curve for the additive assay. For the calculation of sample concentration from the actually measured sensor response, the calculation curve is required. For preparion of the correlation curve, the accumulated signal (Y-axis) and the accumulated concentration (X-axis) were calculated by simply adding the measured signals and the concentrations of injected analytes from the first injection. **(A)** Repeated injections of samples at the same concentration. From the data of Figure 3-4, signals of each plot were changed as accumulated signals (Y-axis). **(B)** Non-linear curve fit of the plot of repeated injections. After calculating mean values of accumulated signals from all points in Figure 3-5A, non-linear curve fit of the plot was applied with a binding model: $R = [R_{max} \cdot C / (K + C)]$ ($r^2=0.995$). In our model, "R" and "R_{max}" (664.3 milli°) represent accumulated signal and maximum accumulated signal, respectively. "C" represents accumulated concentration and "K" (2369.1 nM) represents the accumulated concentration at the half of R_{max}.

For the non-linear curve fitting of the repeated injection of Figure 3-5B, the equation of Langmuir isotherm (O'Shannessy et al., 1993; Morton et al., 1995; Karlsson and Faelt, 1997) was applied as a binding model: $R = [R_{max} \cdot C / (K + C)]$. In our model, "R" and "R_{max}" (664.3 milli°) represent accumulated signal and maximum accumulated signal, respectively. "C" represents accumulated concentration and "K" (2369.1 nM) represents the accumulated concentration at the half of R_{max}. Although the result of repeated injection has no concrete relation to the model of Langmuir isotherm, the plot of accumulated concentration and the accumulated signal of Figure 3-5A closely fits to the calculated curve (r^2=0.995) as shown in Figure 3-5B.

The availability of this correlation curve was tested by the injection of samples at mixed concentrations. When the several analytes with different concentrations were injected in arbitary sequence, the respective concentrations were calculated from each signal by using the obtained correlation curve and compared with those of real values to evaluate the average error of the additive assay (see Figure 3-6).

As shown in Figure 3-6, the signals by samples at mixed concentration were found to be plotted closely on the correlation curve. Twelve samples of anti-BSA antibodies were injected according to the following sequence: 163.3 → 65.3 → 98.0 → 130.7 → 130.7 → 98.0 → 65.3 → 163.3 → 65.3 → 98.0 → 130.7 → 165.3 nM. When the accumulated signals and the accumulated concentrations for each sample were plotted together with the correlation curve, each point closely plotted to the correlation curve. The deviation of each point from the correlation curve was calculated to be 2.6 % (n=12). This means that the correlation curve by repeated injection of sample at the same concentration can be used to calculate the concentration of an unknown sample.
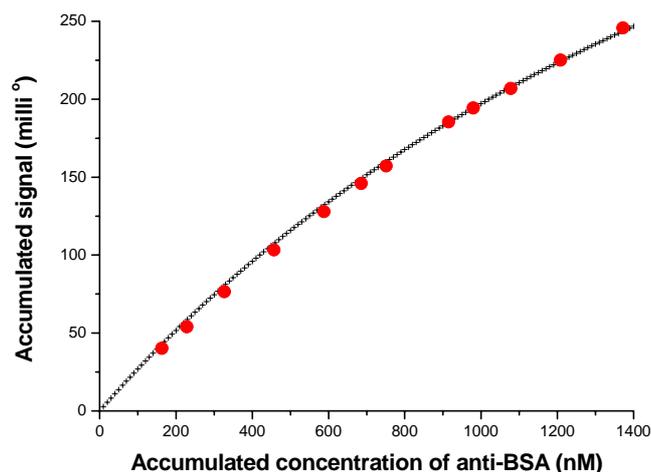
Figure 3-6: The signals by injection of samples at mixed concentrations plotted on the correlation curve. For the availability test of the correlation curve from Figure 3-5B, several analytes with different concentrations were injected in arbitary sequence. The respective concentrations were calculated from each signal by using the correlation curve and compared with those of real values to evaluate the average error of the additive assay. The signals by samples at mixed concentration were found to be plotted closely on the correlation curve. Twelve samples of anti-BSA antibodies were injected according to the following sequence: 163.3 → 65.3 → 98.0 → 130.7 → 130.7 → 98.0 → 65.3 → 163.3 → 65.3 → 98.0 → 130.7 → 165.3 nM. The deviation of each point from the correlation curve was calculated to be 2.6 % (n=12). This low value of deviation means the correlation curve made by repeated injection of sample at the same concentration can be used to calculate the concentration of an unknown sample.

Calculation of analyte concentration by using correlation curve

When several samples at different concentrations were additively injected to the IA layer, the concentration of each sample can be calculated from the actually measured sensor response by using the correlation curve. In details, if the sensor response from the first injection is S_1, the concentration of the first sample is estimated to be C_1 which matches to the sensor signal of S_1 on the correlation curve. And the accumulated signal is recorded to be S_1 as shown in Figure 3-7. If the second sample produces the sensor response of S_2, the accumulated concentration is estimated on the correlation curve, which matches to the accumulated signal of $S_1 + S_2$. As this accumulated sensor signal corresponds to the accumulation concentration of $C_1 + C_2$ on the correlation curve, the concentration of second sample was calculated as C_2 by subtracting the concentration of C_1 which actually

corresponds to the accumulated concentration before second sample injection. For the next measurement, the accumulated signal is updated to be $S_1 + S_2$.
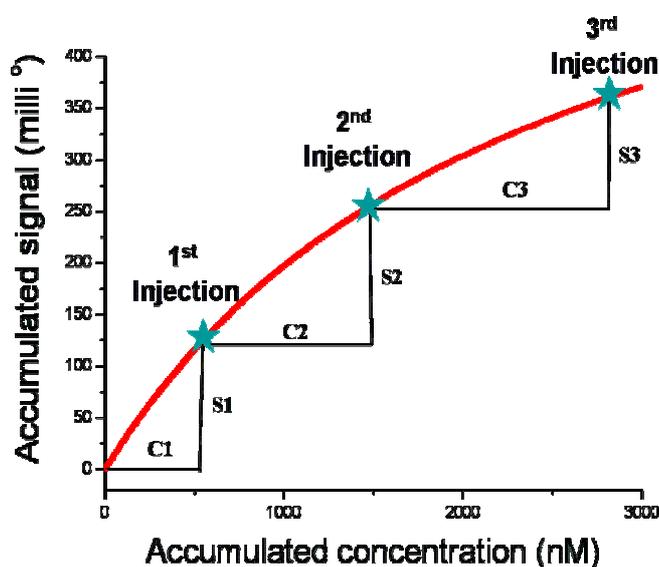
Figure 3-7: Calculation of sample concentration by using the correlation curve. If the sensor response from the first injection is S_1, the concentration of the first sample is estimated to be C_1 and the accumulated signal is recorded to be S_1. If the second sample produces the sensor response of S_2, the accumulated concentration is estimated on the correlation curve, which matches to the accumulated signal of $S_1 + S_2$. As this accumulated sensor signal corresponds to the accumulation concentration of $C_1 + C_2$ on the correlation curve, the concentration of second sample was calculated as C_2 by subtracting the concentration of C_1 which actually corresponds to the accumulated concentration before second sample injection.

Feasibility test of additive assay

The applicable range of accumulated concentration of the correlation curve was determined by using the uncertainty of signal measurement as a boundary condition. The data at the valid range of accumulated concentration was selected by considering the restrictions of correlation curve. The deviation (sd) of baseline stability was calculated to be ± 0.6 milli°. According to the accumulated signal point (R, Y-axis), this baseline uncertainty (α) of ± 0.6 milli° makes a different uncertainty of concentration ($\Delta C_1 < \Delta C_2$) at the accumulated concentration (C, X-axis) (see Figure 3-8). After the preparation of BSA layer, the lower limit of detection (LLD) was calculated to be 2.3 milli° by using m + 3sd of baseline stability, where "m" is mean signal (0.5 milli°) and "sd" is standard deviation (± 0.6 milli°)

in absensce of anti-BSA. The detection limit of concentration corresponding to the signal (2.3 milli°) was 8.3 nM in the correlation curve. Generally, the uncertainty of measurement is specified to be the gray zone of measurement. If the valid uncertainty of accumulated concentration is defined to be the detection limit (8.3 nM), the applicable range of accumulated concentration is determined by solving the following equations:

$$\Delta C = C_2 - C_1 \leq 8.3 \text{ nM}$$

$$R - \alpha = R_{max} \quad x \quad C_1 / (K + C_1)$$

$$R + \alpha = R_{max} \quad x \quad C_2 / (K + C_2)$$

$$R = R_{max} \quad x \quad C / (K + C)$$

With the R_{max} and K in Figure 3-5B, the accumulated concentration (C) was determined to be lower than 930.2 nM by solving the above equations, so the valid range of accumulated concentration was determined to be 8.3 – 930.2 nM by considering the detection limit.
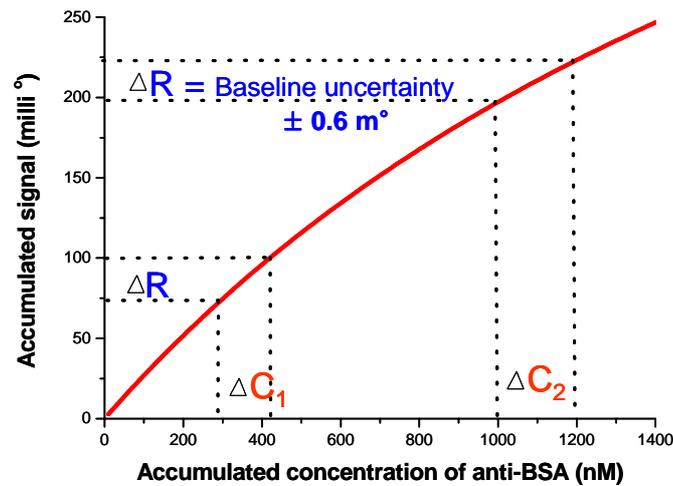
Figure 3-8: The uncertainty of the calculated concentration by using the correlation curve. According to the level of accumulated signal, the baseline uncertainty (α) of signal ($\pm$ 0.6 m°) makes a different uncertainty of concentration ($\Delta C_1 < \Delta C_2$) at the accumulated concentration.

In the valid range of accumulated concentration (8.3 – 930.2 nM), the calculated analyte concentrations ([αBSA] ^{M}) in Figure 3-6 were compared with those of real values ([αBSA]^R) and the average error of additive assay was determined to be 5.4 % (n = 8) (see Table 3-2). This result shows that the additive assay is feasible for the immunosensors.

Table 3-2: Deviation of the analyte concentration from the additive assay method.

Nr.	Signal^A (milli°)	Signal^M (milli°)	[αBSA]^A (nM)	[αBSA]^M (nM)	[αBSA]^R (nM)	Error (%)
1	40.2	40.2	152.6	152.6	163.3	-6.6
2	54	13.8	209.6	57	65.3	-12.7
3	76.5	22.5	308.3	98.7	98.0	0.7
4	103.3	26.8	436.2	127.9	130.7	-2.1
5	127.9	24.6	564.9	128.7	130.7	-1.5
6	145.9	18	666.8	101.9	98.0	4.0
7	157.2	11.3	734.5	67.7	65.3	3.5
8	185.4	28.2	917.2	182.7	163.4	11.8
					The average error (%) = 5.4	

* Abbreviations: 'Signal^A'and 'Signal^M' mean accumulated signal and signal from measured data, respectively. '[αBSA]^A' and '[αBSA]^M' represent the accumulated concentration and concentration from measured data, respectively. '[αBSA]^R' is a real concentration of anti-BSA antibodies. Error (%) was calculated by ([αBSA]^M - [αBSA]^R)·100/ [αBSA]^R. The average error is calculated from the absolute errors.

Additive assay by using Biacore^{TM} system

The additive assay was also evaluated by using another SPR biosensor called Biacore 3000. In previous work, the IA layer was prepared by immobilization of BSA to the SAM layer of Spreeta^{TM} chip. In the case of Biacore, the modified cellulose layer of CM5 chip was used for the preparation of the IA layer. As shown in Figure 3-9, the correlation curve of the Biacore shows a different correlation curve with different fitting parameters of R$_{max}$ (177.7 milli°) and K (543.8 nM) compared with the additive assay by Spreeta^{TM} system. The accuracy of the additive assay using Biacore was also calculated with the detection limit of 0.3 nM, which was calculated by using m+3sd of baseline uncertainty (0.1 milli°) according to the former procedure. If valid uncertainty of measurement is set to be 8.3 nM (detection limit of spreeta^{TM}), the valid range of accumulated concentration was calculated to be 0.3 – 1156 nM. In this concentration range, the average error was calculated to be far more than 5 %. With the detection limit of 0.3 nM, the valid range of accumulated concentration was calculated to be less than zero. When the uncertainty is set to be 1 nM, the valid range was

calculated to be 0.3 – 435.5 nM and the average error was calculated to be 4.4 %. This result shows that the additive assay is feasible for Biacore as well as Spreeta[TM] with the average of error less than 5 %. Although the valid range of accumulation concentration was narrower than that of Spreeta[TM], the Biacore was determined to achieve a far higher accuracy of measurement than that of Spreeta[TM].
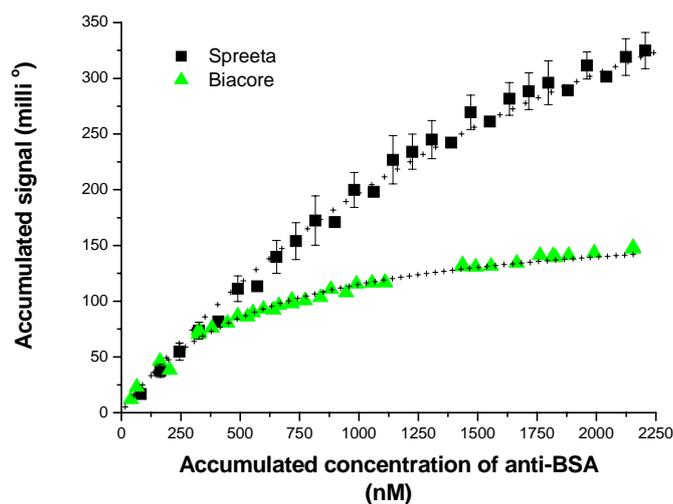
Figure 3-9: Correlation curve for additive assay by using Biacore[TM] (▲) and Spreeta[TM] (■). Although the valid range of accumulation concentration was narrower than that of Spreeta[TM], the Biacore was determined to achieve a far higher accuracy of measurement than that of Spreeta[TM].

3.1.4 The medical application of additive assay with the serum sample.

The serum samples in the medical diagnosis include the target analytes as well as other components which can interrupt effective detection of the target analyte by non-specific binding or interference to decrease analyte binding. Such non-specific binding makes some deviation in correlation curve by changing the signal to concentration ratio. For the feasibility test of the additive assay with the serum sample, HRP and anti-HRP antibodies were used as a model Ag-Ab pair and the concentration of total protein was set to be upto ~ 50 mg/ml by mixing calf serum. When the relation between accumulated concentration and accumulated signal were plotted with three concentrations (28.96, 14.48 and 7.24 μg/ml), the sample with 50 % serum showed larger deviation among the other correlation curves than the sample without serum (see Figure 3-10). At the serum concentration of 50 %,

standard correlation curve with small deviation could not be calculated from several concentrations of samples and the additive assay was not suitable for medical diagnosis. The non-specific binding of serum was regarded to be the major reason.

A   **B**
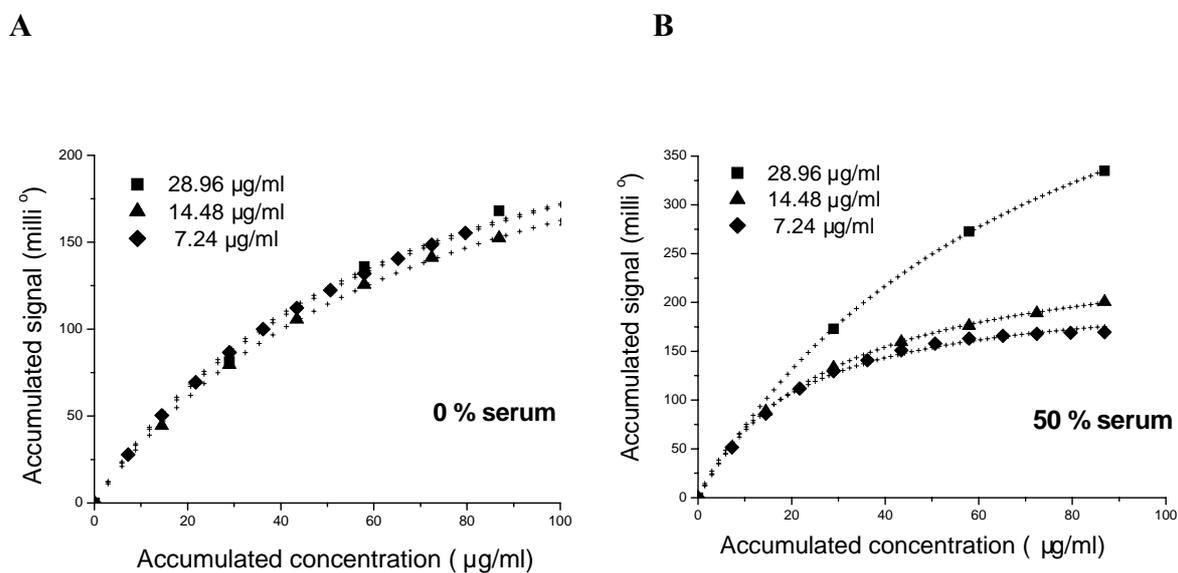
Figure 3-10: Deviation among each correlation curve from several concentrations with the sample in the 0 % and 50 % serum. The IA layer was made by HRP and target analytes were anti-HRP antibodies (■: 28.96 μg/ml, ▲: 14.48 μg/ml, ◆: 7.24 μg/ml). **(A)** Sample in the 0 % serum. **(B)** Sample in the 50 % serum. The sample with 50 % serum showed larger deviation among individual correlation curves than the sample with no serum. With the 50 % serum concentration, the additive assay was not suitable for medical diagnosis and the non-specific binding of serum was regarded to be the major reason.

The effect of non-specific binding by serum is shown in Table 3.3. The absolute signal of the sample in 50 % serum was higher than the signal of the sample without serum (sample in PBS). Furthermore, the signal to concentration ratio calculated according to the formula: (signal of high concentration) / (signal of low concentration) was not uniform for different analyte concentration. This increase seemed to be made from non-specific binding of the proteins in the serum. As the changes of absolute signal value and signal ratio were major reasons for dispersion of individual correlation curves, the minimization of non-specific binding was required for the realization of the additive assay.

Table 3.3: The effect of serum concentration to the SPR signal.

Analyte (μg/ml)	with 0% serum		with 50% serum	
	Signal (milli°)	Signal ratio	Signal (milli°)	Signal ratio
7.24	27.8	1	51.5	1
14.48	44.4	1.6	88.5	1.7
28.96	81.2	2.9	173	3.4

For the application of additive assay, all individual correlation curves from several concentrations should be fit into a single standard correlation curve. Without decreasing non-specific binding, the 'gray zone' of correlation curve was too broad to ensure the acceptable error range (below 5%) for medical diagnosis. This minimization of deviation can be realized by the minimization of non-specific binding of serum to the IA layer. The dilution of sample can be one solution to decrease the non-specific binding for the medical application of additive assay with the serum sample.

The additive assay was tested by using serum samples at several dilution factors. The accuracy of the additive assay was influenced by the dilution factor of the serum. With the three concentrations of 7.24, 14.48, 28.96 μg/ml, samples at the same concentration were repeatedly injected to a SPR biosensor and all points of individual response curves of respective concentrations were summated statistically with mean value of signal to obtain a standard correlation curve as shown in Figure 3-11. The fitting result for correlation coefficient (r^2) of 0 %, 5 %, 10 % and 50 % serum were calculated to be 0.999, 0.996, 0.971 and 0.945, respectively. As the concentration of serum was increased, the square of the correlation coefficient (r^2) was decreased. Moreover, the standard deviation of each point in the correlation curve was also increased according to the increase of serum concentration, which made large error in the real application of additive assay.
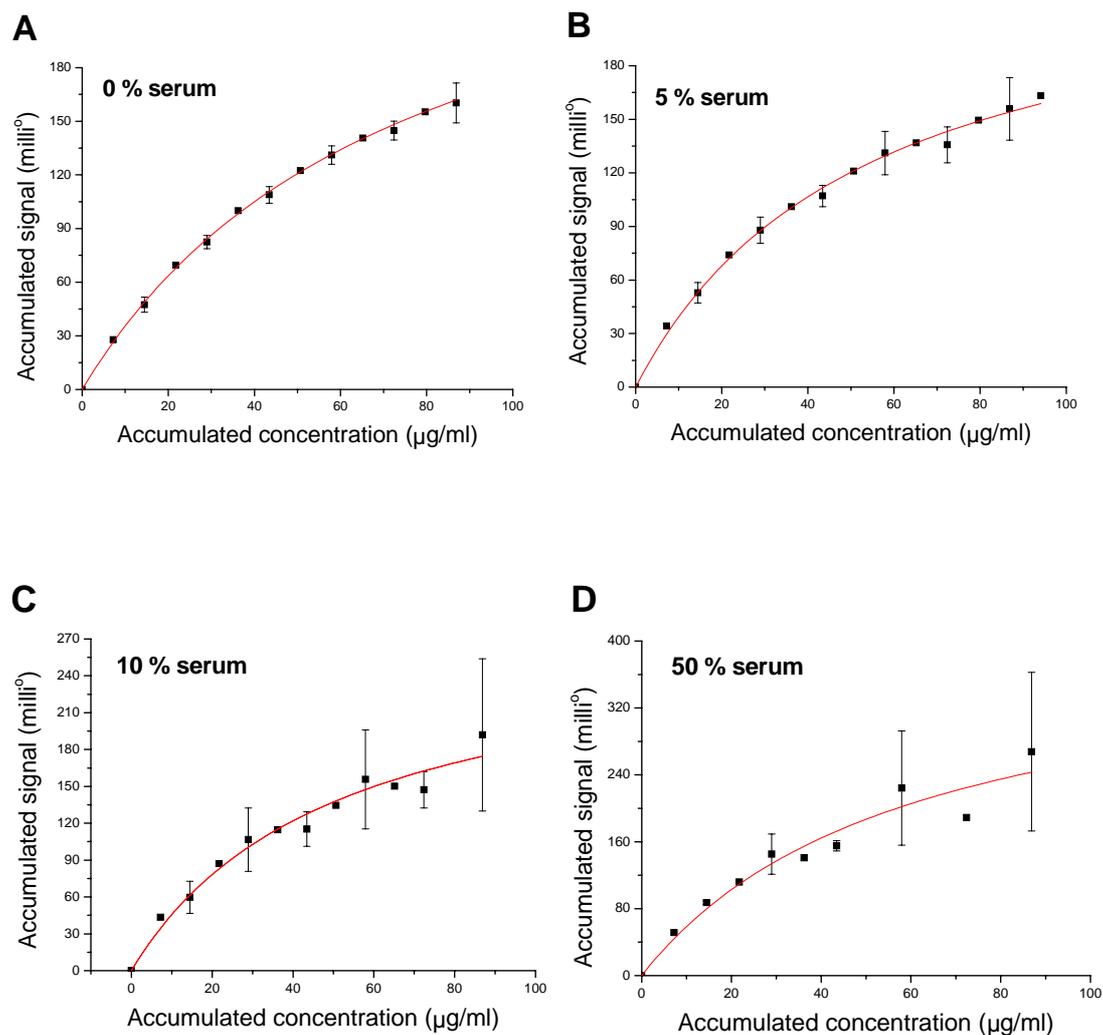
Figure 3-11: The correlation curve of additive assay according to the dilution factor of serum sample. (A) 0 % serum (r^2 = 0.999). **(B)** 5 % serum (r^2 = 0.996). **(C)** 10 % serum (r^2 = 0.971). **(D)** 50 % serum (r^2 = 0.945).

The feasibilities of each correlation curve were tested by repeated injections of target analyte (14.48 μg/ml, n=4), which compared the calculated concentrations with the real values to calculate the error values (see Table 3.4). The mean error values of 0 %, 5 %, 10 % and 50 % serum were calculated to be 6.4, 9.9, 29.4 and 29.3 %, respectively. In the high concentration of serum (10 % and 50 % serum), the mean error values were calculated to be as high as 30 % and the additive assay could not be performed with these error values by using the correlation curve. The result showed that the serum content of less than 5 % is adequate for the additive assay to have a mean error value less than 10 %. However, the blocking method of IA layer instead of dilution should be improved to minimize the non-

specific binding because dilution of sample also decreases the positive signal of sample.

Table 3.4: The feasibility of correlation curve according to the dilution factor of serum sample.

No. of injection	0 % serum		5 % serum		10 % serum		50 % serum	
	*$[C]^{cal}$ (μg/ml)	**Error (%)	$[C]^{cal}$ (μg/ml)	Error (%)	$[C]^{cal}$ (μg/ml)	Error (%)	$[C]^{cal}$ (μg/ml)	Error (%)
1	13.6	-6.1	13.3	-8.1	11.3	-22.0	16.5	14.0
2	13.9	-4.0	13.5	-6.8	10.6	-26.8	12.3	-15.1
3	13.6	-6.1	12.8	-11.6	9.3	-35.8	9.3	-35.8
4	13.1	-9.5	12.6	-13.0	9.7	-33.0	6.9	-52.3
Mean		6.4		9.9		29.4		29.3

*$[C]^{cal}$ is a calculated concentration.

**Error is a deviation between real concentration and calculated concentration.

3.1.5 Additive assay of a tumor marker, carbohydrate antigen 19-9 (CA 19-9)

The application of the additive assay was demonstrated by the detection of a cancer marker called CA 19-9. The CA 19-9 is a tumor marker from patients with gastrointestinal malignancies and it is reported to be frequently found in the patients with pancreatic cancer with a high score of over 79 % (see section 1.4). In this work, the SPR biochip of Texas Instrument (TI, Dallas, USA) was used for the detection of CA 19-9 by using an IA layer prepared on the gold surface of the SPR biochip. For the improvement of detection limit, a signal amplification method was also tested by additional treatment of anti-CA 19-9 antibodies after the sample injection.

Detection time for the CA 19-9

For the detection of CA 19-9, the IA layer of anti-CA 19-9 antibodies was prepared on the SPR biosensor. The SPR sensor responses in Figure 3.12 were obtained by the injection of CA 19-9 samples in 10 mM PBS (pH 7.4) to a freshly prepared IA layer. As shown in Figure 3-12A, the SPR sensor response reaches a signal plateau after a certain incubation time and the signal at 30 min was estimated to be over 85 % of the value at signal plateau. From this result, the incubation time was determined to be 30 min. Figure 3-12B shows the

response curve prepared by injection of CA 19-9 samples at different concentrations when the incubation time was set to be 30 min. The response curve was fit well (r^2=0.993) to the model response curve based on the simple binding model: $R = [R_{max} \cdot C / (K_D+C)]$. Here, 'R' and 'C' represent the sensor response and concentration of CA 19-9, respectively. K_D is the dissociation constant and R_{max} is the maximal sensor response. The detection limit was calculated to be 410.9 U/ml at the baseline drift of ± 0.8 milli° according to the conventional calculation method for immunoassay (Ezan and Grassi, 2000).

A
B
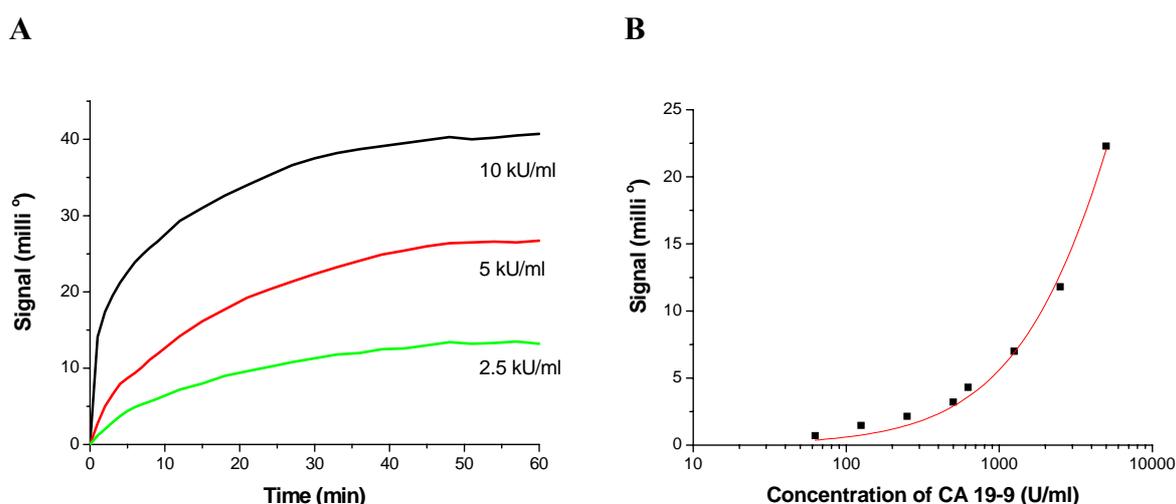
Figure 3-12. SPR sensor response by the injection of CA 19-9 sample. The SPR sensor responses were obtained by the injection of CA 19-9 samples in 10 mM PBS (pH 7.4) to a freshly prepared IA layer. **(A)** Dependence of SPR sensor response on the incubation time. The SPR sensor response reaches a signal plateau after a certain incubation time (~60 min). The signal at 30 min was estimated to be over 85 % of the value at signal plateau. From this result, the incubation time was determined to be 30 min. **(B)** Does-response curve for CA 19-9. The response curve was prepared by injection of CA 19-9 samples at different concentrations when the incubation time was set to be 30 min. The detection limit was calculated to be 410.9 U/ml at the baseline drift of ± 0.8 milli°.

Feasibility test of additive assay for the CA 19-9

The correlation curve for the detection of CA 19-9 was prepared according to the previously discribed method (section 3.1.3). As shown in Figure 3-13A, several samples of different concentrations at the target analysis range were prepared, and then the sample at each concentration was repeatedly injected. The sensor responses were plotted on the graph with the X axis of accumulated concentration and the Y axis of accumulated signal. As shown in

Figure 3-13B, the correlation curve could be obtained by averaging the responses in Figure 3-13A and it was fit by using simple binding model: $R = [R_{max} \cdot C / (K+C)]$. Here, 'R' and '$R_{max}$' (92.7 milli°) represent 'accumulated signal' and 'maximal accumulated signal', respectively. 'C' and 'K' (14.3 kU/ml) represent 'accumulated concentration' and 'accumulated concentration at the half of R_{max}', respectively. Although any concrete physical relation was not in this fitting model, the obtained correlation curve was apparently fit well to the simple binding model (r^2=0.993).
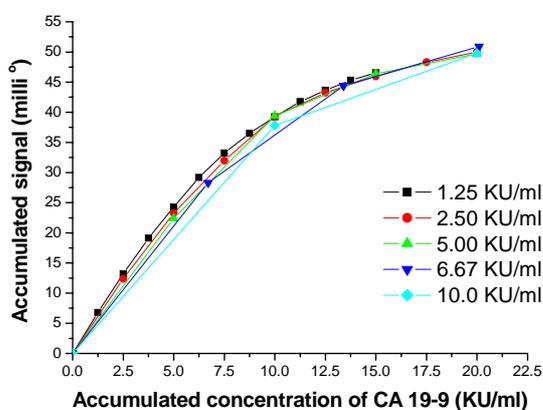
A   **B**
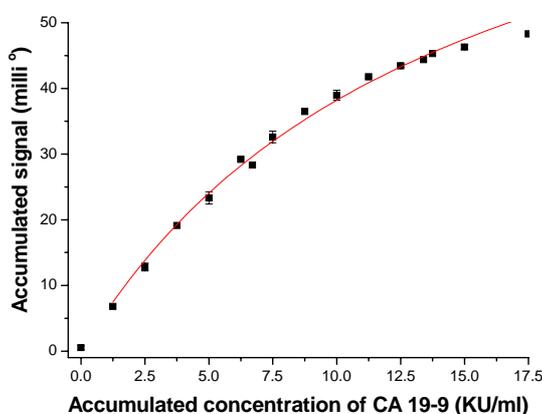
Figure 3-13: Correlation curve for the dectection of CA 19-9. (A) The accumulated sensor response by repeated injection of CA 19-9. The accumulated signal (Y-axis) and the accumulated concentration (X-axis) were calculated by simply adding the measured signals and the concentrations of injected analytes from the first injection. **(B)** Correlation curve for the additive assay of CA 19-9. After getting mean values of accumulated signals from all points in Figure 3.13A, non-linear curve fit of the plot was applied with a binding model: $R = [R_{max} \cdot C / (K + C)]$. In our model, the obtained correlation curve was apparently fit well to the simple binding model (r^2=0.993).

To demonstrate the feasibility of the correlation curve for the additive assay of CA 19-9, four CA 19-9 samples in PBS at different concentrations were sequentially injected as follows: 1.3 → 2.5 → 5.0 → 6.7 kU/ml. Then, the concentration of each sample was calculated from the measured sensor response by using the correlation curve of Figure 3-13. When the measured accumulated signals and the real accumulated concentrations of four samples were plotted together with the correlation curve of CA19-9, each point closely matched to the correlation curve as shown in Figure 3-14.
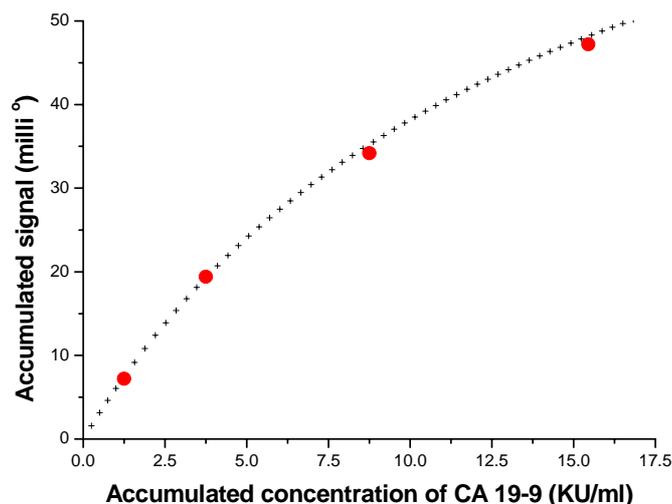
Figure 3-14: The SPR signals of four samples at the mixed concentration plotted on the correlation curve. Four CA 19-9 samples in PBS at different concentrations were sequentially injected as follows: 1.3 → 2.5 → 5.0 → 6.7 kU/ml. When the measured accumulated signals and the real accumulated concentrations of four samples were plotted together with the correlation curve of CA 19-9, each point closely matched to the correlation curve.

When the concentrations of the four samples were analyzed by using the correlation curve of CA 19-9, the average deviation of the calculated concentrations from the real concentrations was estimated to be 5.3 % as summarized in Table 3-5.

Table 3-5: The deviation of additive assay for the analysis of CA 19-9.

No.	Signal^M (milli°)	[CA19-9]^C (kU/ml)	[CA19-9]^R (kU/ml)	Error (%)
1	7.2	1.2	1.3	-3.9
2	12.2	2.6	2.5	3.0
3	14.8	4.6	5.0	-8.6
4	13.1	6.5	6.7	-3.5
				The average error (%) = 5.3

*Abbreviations: 'Signal^M' represents the measured signal. '[CA 19-9]^R' and '[CA 19-9]^C' represent the real and the calculated concentration, respectively. Error (%) was calculated by ([CA 19-9]^C − [CA 19-9]^R)·100/[CA 19-9]^R.

Signal amplification by sandwich assay

Usually in medical diagnosis of CA 19-9 based on the immunoassay, the positiveness of sample is determined by establishing the cut-off value which is reported to be 37 U/ml for CA 19-9. The concentration range of CA 19-9 is known to be in the range of 400 – 192,000 U/ml for most patient samples with pancreatic cancer (Del Villano et al., 1983). As the detection limit of CA 19-9 was estimated to be 410.9 U/ml, further improvement of sensitivity is required for the medical diagnosis of CA 19-9.

Usually for the amplification of SPR response, the formation of complex is performed by using antibodies (Goh et al., 2003), latex particle (Severs and Schasfoort, 1993), gold colloid (Leung et al, 1994), liposome (Wink et al, 1998), peroxidase-anti-peroxidase (PAP) complex (Chung et al., 2005) and so on which produce an increased refractive index change by binding to the already bound analytes to the IA layer.

In this work, the additional injection of antibodies against CA 19-9 was tested to achieve the signal amplification through the sandwich formation to the already bound CA 19-9 of IA layer. As shown in Figure 3-15, the sensor responses were amplified as much as six-fold in the range of 600-2500 U/ml and the detection limit by the sandwich assay was calculated to be 66.7 U/ml with the baseline drift of 1.3 ± 0.3 milli°. This value is quite close to the cut-off value for positive determination of CA 19-9 in medical diagnosis.
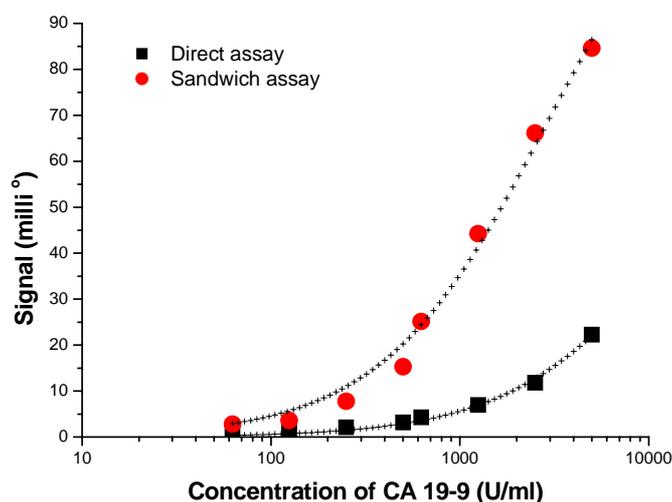
Figure 3-15: Signal amplification by sandwich assay. The sandwich labels of anti-CA 19-9 antibodies were treated to the already bound CA 19-9 for signal amplification. The sensor responses were amplified as much as six-fold in the range of 600-2500 U/ml and the detection limit by the sandwich assay was calculated to be 66.7 U/ml with the baseline drift of 1.3 ± 0.3 milli°. This value is quite close to the cut-off value for positive determination of CA 19-9 in medical diagnosis.

In the case of sandwich assay, analytes on the IA layer were not totally saturated by one treatment of sandwich labels, and it caused relatively higher error for additive assay. Moreover, many interrupting materials in blood usually make a non-specific binding to increase detection limit in the real medical application. For the real medical application of additive assay to medical diagnosis of CA19-9, the selection of an effective amplification method as well as the studies to prevent the non-specific binding are required.

3.2 The simultaneous detection of multiple analytes in a single sensing element

'Simultaneous detection' aims to the analysis of multiple analytes by using a single sensor element. In the 'simultaneous detection', the sample with several analytes is injected to a single sensing region which has multiple receptors for each target analyte. By using the respective standard curves correlating the signal to concentration, the feasibility of 'simultaneous detection' was tested by using two model antigen-antibody pairs. The real medical diagnosis of simultaneous detection was demonstrated by analysis of human chorionic gonadotropin (hCG) and human albumin (hA) in human urine, which is known to be related to the abortion and the preterm delivery of patients with diabetes.

In this work, two simultaneous detection models were suggested according to the responding signal ratio of the target analytes in a sample.

Model 1 is applicable for the sample with two analytes at the far different signal range. In this case, analyte 1 produces a detectable signal and analyte 2 makes no signal to be detected without the treatment of additional label. As shown in Figure 3-16A, the sample with two analytes was injected and the signal was measured. As analyte 2 in sample does not make a detectable signal, the first measured signal (Signal 1) is correlated to the concentration of analyte 1. Then, a label for analyte 2 is injected and the measured signal is correlated to the concentration of analyte 2.

Model 2 can be applied for the sample with two analytes which produce signals only with additional labels. Therefore, the signal of each analyte is measured separately by injection of corresponding labels as shown in Figure 3-16B. After the sample injection, the label for analyte 1 makes a signal (Signal 1) which is correlated to the concentration of analyte 1. Then, additional label for the analyte 2 is injected to make a signal (Signal 2) which is correlated to the concentration of analyte 2.

A
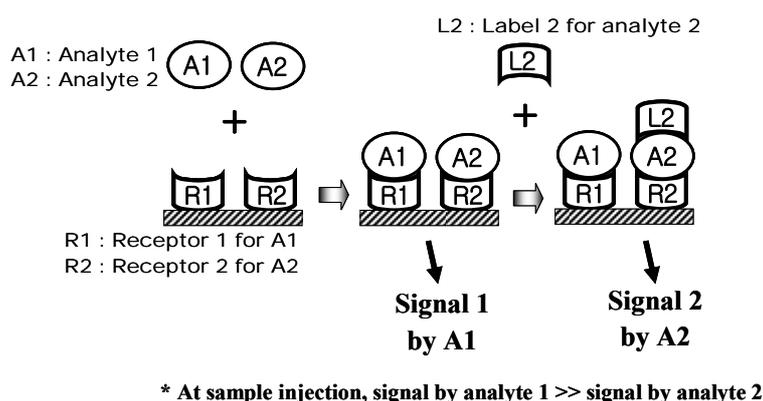
B
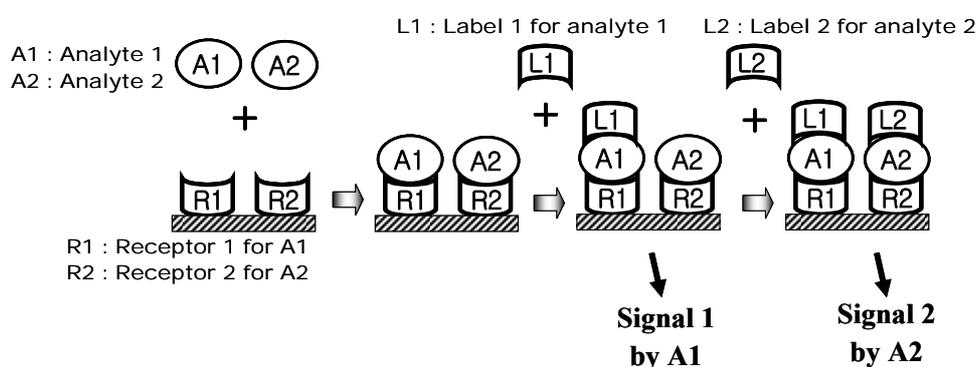
Figure 3-16: Schematic diagram of simultaneous detection models. **(A)** Model 1. The sample with two analytes was injected and the signal was measured. As analyte 2 in sample does not make a detectable signal, the first measured signal (Signal 1) is correlated to the concentration of analyte 1. Then, a label for analyte 2 is injected and the measured signal is correlated to the concentration of analyte 2. **(B)** Model 2. After the sample injection, the label for analyte 1 makes a signal (Signal 1) which is correlated to the concentration of analyte 1. Then, additional label for the analyte 2 is injected to make a signal (Signal 2) which is correlated to the concentration of analyte 2.

3.2.1 Standard curves for simultaneous detection using Model 1 and Model 2

The standard curves for analysis were prepared for Model 1 and 2 by using two antigen-antibody pairs: (1) BSA and anti-BSA antibodies, (2) HRP and anti-HRP antibodies. The IA layer for each model was prepared by immobilization of anti-HRP antibodies and BSA together. The samples were prepared by mixing HRP (42 kDa) and anti-BSA antibodies (150 kDa) at appropriate concentrations in 10 mM PBS (pH 7.0). The measurements for standard curves were made by injection of each analyte at the known concentration, which was adjusted for the application of Model 1 and Model 2.

The standard curve for Model 1

The sample concentration for Model 1 was adjusted for one analyte (anti-BSA antibodies) to make detectible signals without additional label and for the other analyte (HRP) to make detectible signal only with additional label (anti-HRP). Schematic diagram of Model 1 is shown in Figure 3-17A and the standard curve for Model 1 is shown in Figure 3-17B where two analytes have significantly different concentration ranges.

The standard curves for anti-BSA antibodies and HRP were separatetly made by the injection of single analyte. Each curve was made with several concentrations and the signal value for one concentarion was calculated from the mean value (n=3). The curve fit was performed by using the Langmuir isotherm as a fitting model: $R = [C \cdot R_{max} / (C+K)]$, where R is the sensor response, C is the concentration of analyte in solution, R_{max} and K are constants which mean the maximal sensor response and the concentration which make a half size of R_{max}, respectively (Faegerstam et al., 1992; O'Shannessy et al., 1993). In this work, the sensor response (R) was measured at the incubation time of 10 min. For the concentration range used in this work, this signal value was estimated to be 80 % of the signal at equilibrium. Although K is related to the dissociation constant, it does not exactly mean the dissociation constant. The simple binding model was used only to get an empirical curve which apparently fits well to the experimental data. The standard curves for anti-BSA antibodies and HRP have the parameters of R_{max}=455.8 (milli°), K=5365.9 (nM) and R_{max}=176.3 (milli°), K=107.7 (nM), respectively. The non-linear fitting based on the simple binding model was performed using Origin™ software (Microcal Software, Inc., MA, USA). From the baseline drift by blank samples, the limit of detections for anti-BSA antibodies and HRP were determined to be 21.3 and 1.1 nM (n=8), respectively (Ezan and Grassi, 2000). The standard curves of anti-BSA antibodies (r^2=0.997) and HRP (r^2=0.991) fit well to the fitting model. This result shows that two curves by Model 1 could be used as standard curves of correlation between the signal and the concentration.

A
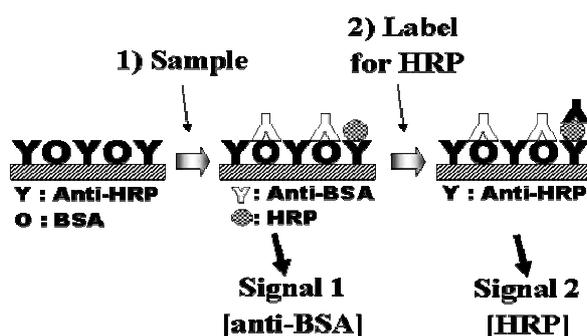
B
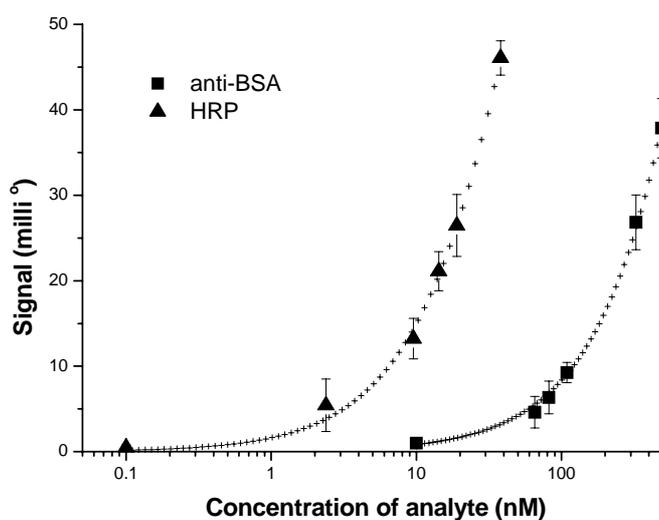
Figure 3-17: Standard curve for Model 1. **(A)** Schematic diagram of simultaneous detection Model 1. The sample concentration for Model 1 was adjusted for one analyte (anti-BSA antibodies) to make detectible signals without additional label and for the other analyte (HRP) to make detectible signal only with additional label (anti-HRP antibodies). **(B)** Standard curve for Model 1. The standard curves for anti-BSA antibodies and HRP were separatetly made by the injection of single analyte. Each curve was made with several concentrations and the signal value for one concentarion was calculated from the mean value (n=3). As the curve fits were performed by using the Langmuir isotherm as a fitting model, the does-response curves of anti-BSA antibodies (r^2=0.997) and HRP (r^2=0.991) fit well to the fitting model. This result shows that two curves by Model 1 could be used as standard curves of correlation between the signal and the concentration.

The standard curve for Model 2

The same IA layer of Model 1 was used for the preparation of the standard curve of Model 2. A schematic diagram of Model 2 is shown in Figure 3-18A. Each analyte was injected and the signal was measured after the injection of additional label. As the label for analytes (anti-BSA antibodies and HRP), anti-rabbit IgG and anti-HRP antibodies were used at the concentrations of 173 and 320 nM, respectively. The standard curve for Model 2 was prepared for the analytes at similar concentration ranges as shown in Figure 3-18B.

The standard curves for anti-BSA antibodies and HRP were separatetly made by the injection of single analyte. Each curve was made with several concentrations and the signal value for one concentarion was calculated from the mean value (n=3). The curve fit was performed by using the Langmuir isotherm as a fitting model: $R = [C \cdot R_{max} / (C+K)]$. The fitting parameters of the standard curve for anti-BSA antibodies was calculated to be R_{max}= 106.8 (milli^{o}), K=152.2 (nM), and the standard curve for HRP has the parameters of R_{max}=84.6 (milli^{o}), K=21.0 (nM). The limit of detections for anti-BSA antibodies and HRP were determined to be 2.6 and 0.5 nM (n=8), respectively. The does-response curves of anti-BSA antibodies (r^2=0.993) and HRP (r^2=0.997) fit well to the fitting model. This result shows that two curves by Model 2 could be used as standard curves of correlation between the signal and the concentration.

A
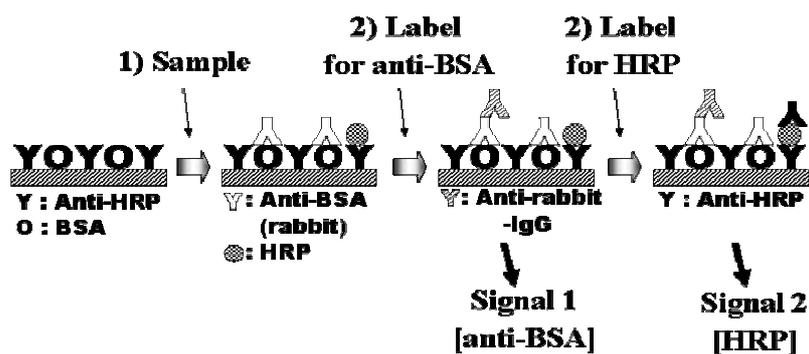
B
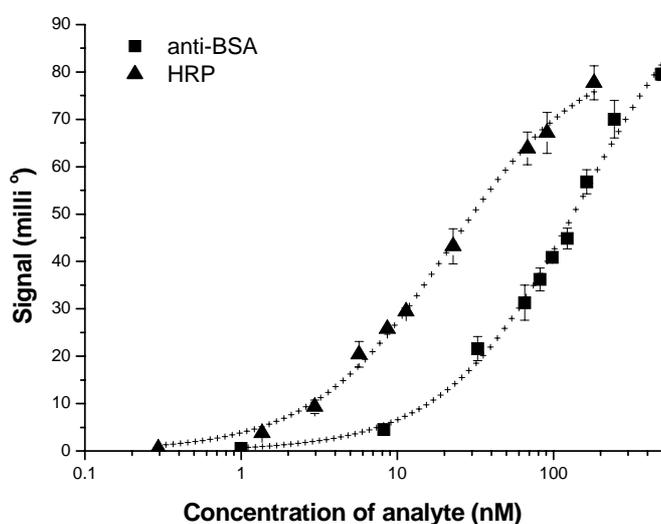
Figure 3-18: Standard curve for Model 2. (A) Schematic diagram of simultaneous detection Model 2. Each analyte was injected and the signal was measured after the injection of additional label. As the label for analytes (anti-BSA antibodies and HRP), anti-rabbit IgG and anti-HRP antibodies were respectively used. **(B)** Standard curve for Model 2. The standard curves for anti-BSA antibodies and HRP were separatetly made by the injection of single analyte. Each curve was made with several concentrations and the signal value for one concentarion was calculated from the mean value (n=3). As the curve fits were performed by using the Langmuir isotherm as a fitting model, the does-response curves of anti-BSA antibodies (r^2=0.993) and HRP (r^2=0.997) fit well to the fitting model. This result shows that two curves by Model 2 could be used as standard curves of correlation between the signal and the concentration.

The feasibility test using Model 1

The standard curve for each analyte was independently prepared by injection of only one kind of analyte. When two analytes are simultaneously injected into the same IA layer, the cross-reaction with another receptor in the IA layer can occurr and a false positive signal or interference can be made by the other proteins.

The samples were prepared by mixing anti-BSA antibodies and HRP at known concentrations and the signal was measured before and after injection of additional label (anti-HRP antibodies at the concentration of 320 nM). The concentrations of anti-BSA antibodies and HRP in test sample were prepared to be 81.7 – 490 nM, 9.5 – 38.1 nM, respectively. Additionally, samples at three random pairs of concentrations were measured. As shown in Table 3-6, Model 1 was feasible for the detection of both analytes at the described concentration ranges. The concentration of each analyte was calculated by using the standard curve and compared to actual concentration. Errors between the two values were calculated. As summarized in Table 3-6, the average error of simultaneous detection based on Model 1 was calculated to be 3.3 and 3.1 % for anti-BSA antibodies and HRP, respectively.

Table 3-6: The deviation of simultaneous detection method (Model 1. n=3).

Injected concentration (nM)		Calculated concentration (nM)		Error (%)	
Anti-BSA	HRP	Anti-BSA	HRP	Anti-BSA	HRP
490.0	9.5	486.6 ± 48.4	8.7 ± 1.7	-0.7	-8.4
490.0	38.1	501.2 ± 60.8	36.2 ± 3.3	2.3	-5.0
81.7	9.5	86.3 ± 8.1	9.8 ± 1.2	5.6	3.2
81.7	38.1	83.4 ± 13.4	39.1 ± 5.3	2.1	2.6
326.7	38.1	335.3 ± 42.6	38.1 ± 2.2	2.6	-0.1
108.9	19.0	110.6 ± 14.6	19.1 ± 3.1	1.6	0.3
81.7	14.3	75.3 ± 23.2	14.6 ± 1.8	-7.9	2.4
				3.3[*]	3.1[*]

[*] Mean of the absolute values of the error

The feasibility test using Model 2

The simultaneous detection Model 2 was also tested using a standard curve. The measurement was made for the sample containing anti-BSA antibodies and HRP by adjusting the concentrations of these analytes and their labels to the range which is used for the preparation of the standard curve. The concentrations of anti-BSA antibodies and HRP in test sample were prepared to be 8.2 – 490 nM, 3.1 – 71.4 nM, respectively. Additionally, samples at four random pairs of concentrations were measured. As shown in Table 3-7, Model 2 was feasible for the detection of both analytes at the described concentration ranges and the average error of analysis based on Model 2 was calculated to be 4.5 and 6.0 % for anti-BSA antibodies and HRP, respectively.

Table 3-7: The deviation of simultaneous detection method (Model 2. n=3).

Injected concentration (nM)		Calculated concentration (nM)		Error (%)	
Anti-BSA	HRP	Anti-BSA	HRP	Anti-BSA	HRP
490.0	3.1	456.5 ± 29.4	3.5 ± 0.5	-6.8	12.9
490.0	71.4	465.1 ± 33.3	71.9 ± 11.9	-5.1	0.7
8.2	3.1	7.6 ± 0.9	2.9 ± 0.4	-7.3	-6.5
8.2	71.4	8.3 ± 2.0	63.4 ± 8.0	1.2	-11.2
32.7	6.0	34.6 ± 5.7	5.9 ± 1.2	6.0	-1.3
82.0	71.4	83.7 ± 7.2	76.1 ± 14.5	2.1	6.5
98.0	23.8	96.4 ± 2.9	24.8 ± 3.8	-1.7	4.1
490.0	9.0	463.5 ± 27.8	9.2 ± 0.1	-5.4	1.3
				4.5[*]	6.0[*]

[*] Mean of the absolute values of the error

3.2.2 Optimization of the IA layer for simultaneous detection

3.2.2.1 Minimization of cross-reactions

As the simultaneous detections of Model 1 and Model 2 use several antigens and antibodies on the same IA layer, a cross-reaction among the participating antigens and antibodies can result in a false positive signal.

The cross reaction in Model 1 should be tested as shown in Figure 3-19. The concentrations of target analytes (anti-BSA antibodies and HRP) were adjusted to be high enough to

achieve saturated signals (1633 and 909 nM, respectively). The cross-reactions of anti-BSA antibodies (analyte) with HRP (co-injected analyte) and anti-HRP antibodies (IA layer for HRP) were measured as shown in Figure 3-19A. The IA layer was prepared by immobilizing anti-HRP antibodies. When HRP was injected, a signal of 11.9 milli° was observed. Then, the anti-BSA antibodies were injected and the signal was found to be less than zero. This result shows that the anti-BSA antibodies (analyte 1) for Signal 1 do not cross-react with HRP (analyte 2) and anti-HRP antibodies (IA layer for analyte 2). In a separated test, the IA layer was prepared by immobilizing BSA and anti-HRP antibodies as shown in Figure 3-19B. Then, anti-BSA antibodies (analyte 1) were injected and signal was found to be 49.1 milli°. When anti-HRP antibodies (label for analyte 2) were injected, the signal was estimated to be as small as 0.8 milli°. This result shows that anti-HRP antibodies (the label for analyte 2) for Signal 2 do not cross-react with anti-BSA antibodies (analyte 1) and the IA layer (IA layer for analyte 1 and analyte 2). From these results, the participating antigens and antibodies were determined to make no significant cross-reaction and no false positive signal was measured for the simultaneous detection based on Model 1.

The simultaneous detection based on Model 2 uses labels for each analyte. The test for the cross-reactivity of each label was made as follows. The IA layer was prepared by immobilizing the BSA (receptor 1 of analyte 1) and anti-HRP antibodies (receptor 2 of analyte 2) together. As shown in Figure 3-20A, HRP (analyte 2) was injected and the signal was found to be 5.1 milli°. Then, the anti-rabbit IgG (label 1 for analyte 1) for Signal 1 was injected and no significant signal (0.1 milli°) was measured. This result shows that anti-rabbit IgG (label 1 for analyte 1) does not cross-react with the other analyte (analyte 2) and the IA layer. When anti-HRP antibodies (label 2 for analyte 2) were injected, a signal of 59 milli° was measured. This result shows that the HRP injected first was still bound to the IA layer. In a separated test, anti-BSA antibodies (analyte 1) were injected and the signal was found to be 48.7 milli° as shown in Figure 3-20B. Then, the anti-rabbit IgG (label 1 for analyte 1) was injected and a signal of 118 m° was measured. When anti-HRP antibodies (label 2 for analyte 2) for Signal 2 were injected, no significant signal (1.6 milli°) was measured. This result indicates that anti-HRP antibodies (label 2 for analyte 2) also do not cross-react with the other analyte (analyte 1), the other label (label 1 for analyte 1) and the IA layer. From these results, the participating antigens and antibodies were determined to make no significant cross-reaction and no false positive signal was measured for the simultaneous detection based on Model 2.
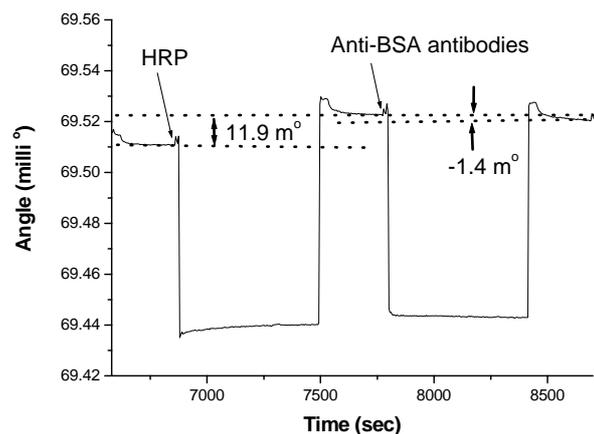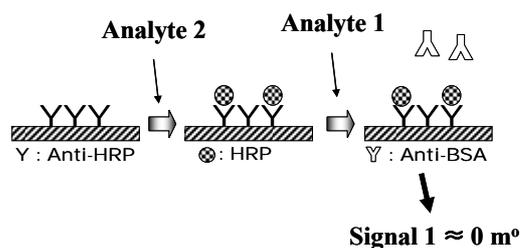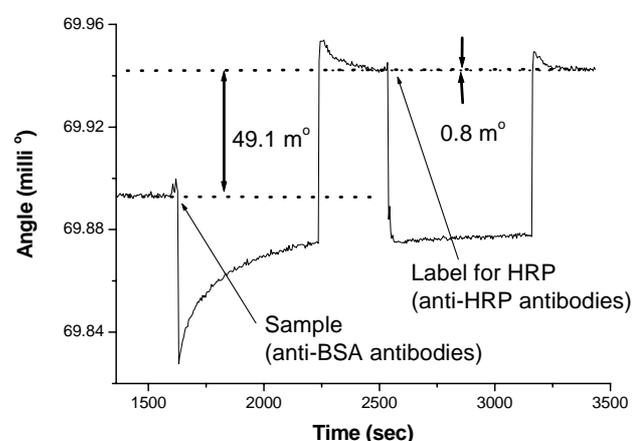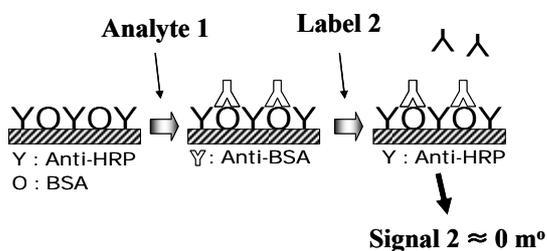
Figure 3-19: Test of cross-reaction in the Model 1. (A) The reaction scheme for the cross reaction of anti-BSA antibodies (analyte 1) and the SPR sensorgram of the reaction**.** The IA layer was prepared by immobilizing anti-HRP antibodies (IA layer for HRP). The cross-reactions of anti-BSA antibodies (analyte 1) with HRP (analyte 2) and anti-HRP antibodies (IA layer for analyte 2) were measured. When HRP was injected, a signal of 11.9 milli° was observed. Then, the anti-BSA antibodies were injected and the signal was found to be less than zero. This result shows that the anti-BSA antibodies (analyte 1) for Signal 1 do not cross-react with HRP (analyte 2) and anti-HRP antibodies (IA layer for the analyte 2) **(B)** The reaction scheme for the cross reaction of HRP antibodies (label for HRP) and the SPR sensorgram of the reaction. The IA layer was prepared by immobilizing BSA and anti-HRP antibodies. Then, anti-BSA antibodies (analyte 1) were injected and signal was found to be 49.1 milli°. When anti-HRP antibodies (label for HRP) for Signal 2 were injected, the signal was estimated to be as small as 0.8 milli°. This result shows that the anti-HRP antibodies (label for analyte 2) do not cross-react with anti-BSA antibodies (analyte 1) and the IA layer (IA layer for the analyte 1 and analyte 2). From the results of (A) and (B), the participating antigens and antibodies were determined to make no significant cross-reaction and no false positive signal was measured for the simultaneous detection based on Model 1.

A
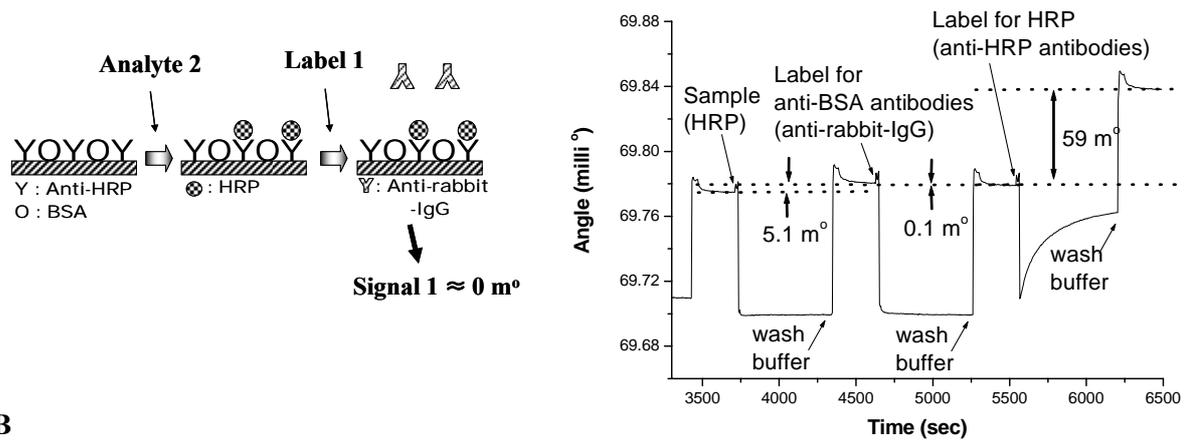
B
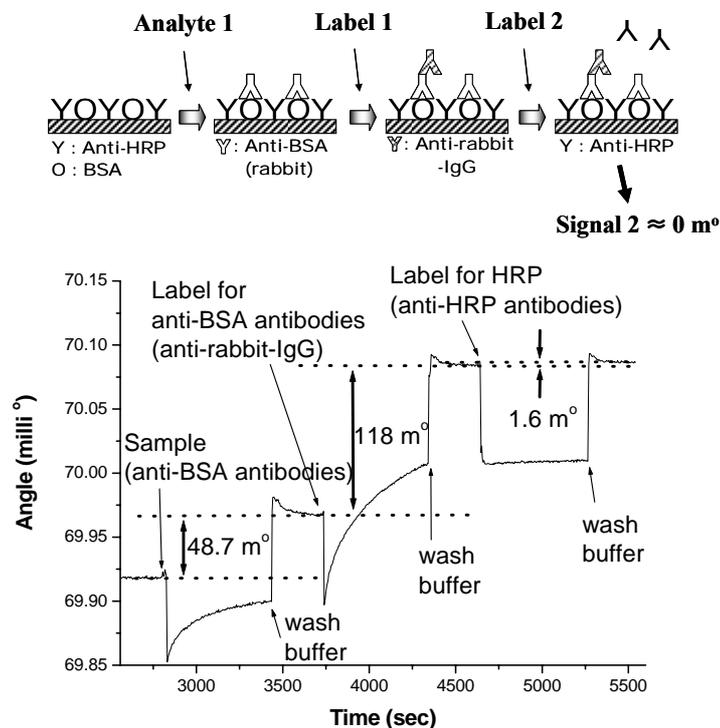
Figure 3-20: Test of cross-reaction in the Model 2. (A) The reaction scheme for the cross reaction of label 1 and the SPR sensorgram of the reaction. The analyte 2 was injected and the signal was found to be 5.1 milli°, and the label 1 generated no significant signal (0.1 milli°). This result shows that label 1 does not cross-react with the analyte 2 and the IA layer. When label 2 was injected, a signal of 59 milli° was measured, which shows that the analyte 2 injected first was still bound to the IA layer. **(B)** The reaction scheme for the cross reaction of label 2 and the SPR sensorgram of the reaction. Analyte 1 was injected and the signal was found to be 48.7 milli°. Then, the label 1 generated a signal of 118 milli°. When label 2 was injected, no significant signal (1.6 milli°) was measured. This result indicates that label 2 also do not cross-react with the analyte 1, the label 1 and the IA layer. From these results, the participating antigens and antibodies made no significant cross-reaction and no false positive signal was measured for the simultaneous detection based on Model 2.

3.2.2.2 Optimal division of the IA layer

The simultaneous detection based on Model 1 and Model 2 was performed by two molecular recognition elements on the same IA layer. In order to make each molecular recognition part to produce a detectable signal, the restricted area of IA layer should be effectively divided for the binding of each analyte. In this work, the surface area of IA layer was divided by controlling the concentration ratio of the molecular recognition elements (BSA and anti-HRP antibodies) at the immobilization step. The correlation between the concentration ratio and the analyte binding capacity was estimated by the comparison of maximum response (R_{max}) of the IA layer. As shown in Figure 3-21, the concentration ratio ([anti-HRP antibodies] / [BSA]) was changed from 0.002 to 10000 (0.002, 0.24, 0.48, 2.40, 20, 200 and 10000), and each maximum response (R_{max}) was calculated from the standard curves. This result shows that the optimal IA layer should be prepared by controlling the concentration ratio of analyte binding molecules according to certain detection ranges of the analytes in a specific test.
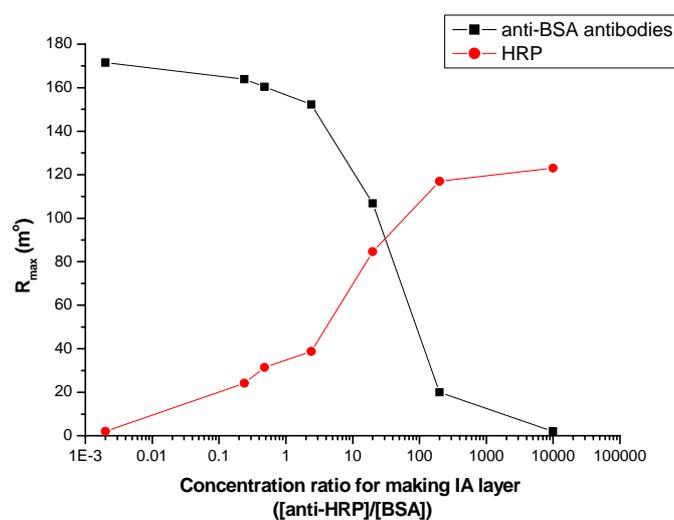
Figure 3-21: Correaltion between analyte binding capacity and the concentration ratio of molecular recognition elements at the immobilization step. The surface area of IA layer was divided by controlling the concentration ratio of the molecular recognition elements ([anti-HRP antibodies]/[BSA]) at the immobilization step. The correlation between the concentration ratio and the analyte binding capacity was estimated by the comparison of maximum response (R_{max}) of the IA layer. Each R_{max} was calculated from the standard curves. This result shows that the optimal IA layer should be prepared by controlling the concentration ratio of analyte binding molecules according to certain detection ranges of the analytes in a specific test.

3.2.3 Simultaneous detection of human chorionic gonadotropin (hCG) and human albumin (hA) in urine

The level of human chorionic gonadotropin (hCG) and human albumin (hA) in urine was determined by using the simultaneous detection method. These two proteins can be used for preliminary diagnosis for the abortion and the preterm delivery during early pregnancy (see section 1.4).

With the concentration ranges for medical application, signal differences were not distinct to use Model 1. Accordingly, Model 2 was applied for the analysis of hCG and hA. The IA layer was prepared by immobilizing polyclonal anti-hCG antibodies (500 μg/ml) and polyclonal anti-hA antibodies (100 μg/ml) together, which was controlled to make each detection limit to be similar with the cut-off value for diagnosis. The known concentrations of both analytes were dissolved in 10-fold diluted urine which was from healthy male volunteers without diabetes (random capillary blood glucose level ≤ 200 mg/dL (Clark, 2001)). When the urine sample without analyte was injected, no significant signal was detected. The concentration range of hCG for the standard curve was adjusted according to the concentration level of hCG at the 4-12 weeks of pregnancy (415 – 46,100 mIU/ml) (Chard, 2001). The concentration range of hA for standard curve was adjusted according to the concentration level of microalbuminuria (20 – 200 μg/ml) (Clark, 2001). Polyclonal anti-hCG antibodies (100 μg/ml) and polyclonal anti-hA antibodies (100 μg/ml) were used as labels for hCG and hA, respectively.

After adjusting optimal sharing of the IA layer by controlling concentrations of both antibodies at the immobilization step, standard curves of the two analytes were obtained for the detectable concentration ranges of each analyte (see Figure 3-22). The fitting parameters of standard curves for hCG and hA were calculated to be $r^2 = 0.964$ and $r^2 = 0.954$, respectively. For the estimation of non-specific binding of labels, label 1 (anti-hCG antibodies for signal 1) was injected after injection of analyte 2 (hA) to the IA layer, and label 2 (anti-hA antibodies for signal 2) was injected after injection of analyte 1 (hCG) and label 1 to the IA layer. The non-specific binding of labels (anti-hCG antibodies and anti-hA antibodies) were measured to be 3.0 ± 0.2 milli^o and 1.6 ± 0.9 milli^o (n=3), respectively. From these data, the non-specific bindings of labels were determined to be insignificant. By using respective standard curves and baseline drift, the detection limits for hCG and hA of 10-fold diluted samples were determined to be 46.4 mIU/ml (464 mIU/ml in undiluted

sample) and 2.5 µg/ml (25 µg/ml in undiluted sample), respectively. In comparison with the cut-off levels of 4th weeks of pregnancy and microalbuminuria, the simultaneous detection seemed to be feasible to determine pregnancy and to alarm preterm delivery for pregnant woman with type I diabetes.
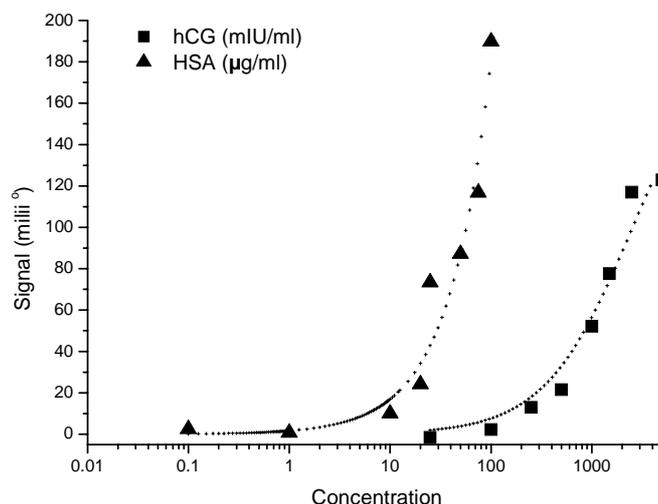
Figure 3-22: Simultaneous detection of hCG (■) and hA (▲) using Model 2. Two curves were made by using 10-fold diluted samples and the fitting parameters of standard curves for hCG and hA were calculated to be $r^2 = 0.964$ and $r^2 = 0.954$, respectively. By using respective standard curves and baseline drift, the detection limits for hCG and hA of 10-fold diluted samples were determined to be 46.4 mIU/ml (464 mIU/ml in undiluted sample) and 2.5 µg/ml (25 µg/ml in undiluted sample), respectively. These values correspond to the cut-off levels of 4th weeks of pregnancy and microalbuminuria, respectively. From this result, the simultaneous detection seemed to be feasible to determine early pregnancy and to alarm preterm delivery for pregnant woman with type I diabetes.

The concentrations of hCG and hA in the test sample were prepared to be 500 – 5000 mIU/ml, 20 – 100 µg/ml, respectively. Additionally, samples at three random pairs of concentrations were measured. As shown in Table 3-8, Model 2 was feasible for the detection of both analytes at the described concentration ranges and the average error of analysis based on Model 2 was calculated to be 6.5 and 5.9 % for hCG and hA, respectively.

Table 3-8: Results of simultaneous detection of hCG and hA based on Model 2 (n=3).

Injected concentration		Calculated concentration		Error (%)	
hCG (mIU/ml)	hA (µg/ml)	hCG (mIU/ml)	hA (µg/ml)	hCG	hA
5000	20	4635.5 ± 399.2	17.1 ± 3.5	-7.3	-14.5
5000	100	4711.4 ± 416.4	103.1 ± 3.9	-5.8	3.1
500	20	463.2 ± 45.3	18.6 ± 1.6	-7.4	-7
500	100	478.4 ± 35.7	97.2 ± 7.4	-4.3	-2.8
500	50	438.2 ± 50.8	49.9 ± 3.6	-12.4	-0.3
1000	100	966.3 ± 94.5	104.3 ± 4.0	-3.4	4.0
1500	75	1575.1 ± 17.7	67.6 ± 8.1	5.0	-9.9
				6.5^*	5.9^*

*Mean of the absolute values of the error.

3.3 Signal amplification of SPR biosensor

The mass change caused by the binding of analyte to the sensor surface affects the amount of plasmons to change the SPR angle, which is converted to the binding amount of analyte in the SPR-immunosensor. Generally, the sensitivity of immunosensors can be improved by the mass label and the control of the IA layer (orientation & density). Because the sensitivity of the SPR biosensor is usually not high enough for medical diagnosis, signal amplification is required. In this work, two amplification methods were tested.

As described in introduction (section 1.2.3), the first method is to increase the signal by using label proteins. Various label proteins have been added to the already bound analyte on the sensor surface to increase the sensitivity of the biosensor (Mullett et al., 2000). When labels are attached to target analytes, the mass on the surface of the SPR biosensor is increased and the SPR signal relative to the amount of target analytes is also increased. Especially for the SPR biosensor, several methods using various kinds of label proteins have been reported, such as secondary antibody (Goh et al., 2003), latex particle (Severs and Schasfoort, 1993) and avidin-biotinylated liposome (Wink et al.,1998).

The second method is to control the orientation of the IA layer composed of antibodies. The antibody is well known to have a 'Y' shaped structure with two binding sites at two variable regions called F(ab')s. For the effective detection of analyte by using immunosensors, the variable region (F(ab')) of the antibody should be exposed to the analyte (Liddell, 2001). For the control of orientation, avidin, LB film, self-assembly and protein A have been

widely used and the surface density and orientation of antibodies could be improved.

3.3.1 Signal amplification by using mass label

The signal amplification by using mass label proteins was tested and the improvement of the sensitivity of the IA biosensor was measured. In order to select the most efficient signal amplification method, the efficiencies of several amplification methods were compared with a direct assay by using secondary antibodies, avidin-biotynylated antibodies and peroxidase-anti-peroxidase (PAP) complex. By applying the selected amplification method, the medical diagnosis of human hepatitis B virus (hHBV) requiring of very high detection limit was demonstrated to approach closely the cut-off value for the diagnosis of hHBV from a commercial ELISA kit.

3.3.1.1 Comparison of the standard curves for the hHBV antibodies using ELISA and SPR biosensor

For the application of the signal amplification method, the SPR biosensor was applied to detect the anti-hHBV antibody which is used to confirm recovery and immunity in patients with acute hepatitis or to check the effectiveness of vaccination (see section 1.4). By using the SPR biosensor, a standard curve as shown in Figure 3-23 was obtained by injection of samples at known concentrations of hHBV antibodies in 5 % calf serum (in 10 mM PBS). The detection range of the standard curve was determined by comparing with the cut-off line of the commercial medical diagnosis. Each point in the Figure 3-23 indicates a mean value of SPR signals from the repeated measurements (n=3) of a sample at the specified concentration. The parabolic curve in Figure 3-23 was obtained by non-linear fit function of a statistical software, Origin^{TM} (USA) and Langmuir isotherm was used as a fitting model: $R = R_{max} \times [Ab] / (K_D + [Ab])$ (Faegerstam et al., 1992), where R represents the response by analyte, R_{max} represents the maximum response, [Ab] represents the concentration of hHBV antibodies, and K_D means the dissociation constant of hHBV antibodies from the IA layer. From this fitting, the maximum SPR response was estimated to be 387.6 milli° with a standard deviation of 55.0 milli° where the SPR biosensor signal is saturated and the K_D value was calculated as 2614.6 nM. This standard curve of anti-hHBV antibodies showed high correlation coefficient ($r^2 = 0.974$). Based on this result, the detection range of hHBV

antibodies was estimated to be from 10 nM to 2 µM hHBV antibodies. This detection range was determined to be similar to the result for hIgG antibodies (Huber et al., 1992).
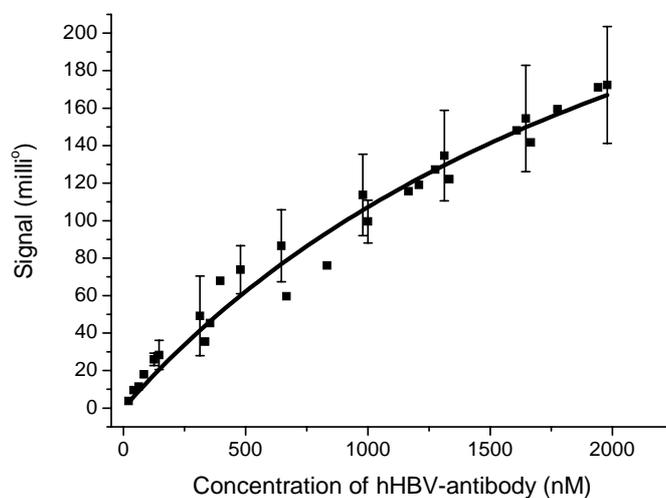
Figure 3-23: SPR sensor response to the concentration of the hHBV antibodies. A standard curve between SPR signal and concentration was obtained by injection of samples at known concentrations of hHBV antibodies in 5 % calf serum (in 10mM PBS) ($r^2 = 0.974$).

For the medical application, the detection range of the SPR biosensor was compared with that of a commercial ELISA kit as shown in Figure 3-24. The ELISA method determines the positiveness of hHBV antibodies using a cut-off value. With the commercial ELISA kit, the optical density (OD) of mean negative control value was detected as 0.03 (OD) and the cut-off value was determined to be around 0.10 (OD) corresponding to the 0.24 nM of hHBV antibodies. By using the standard curve of Figure 3-23, the SPR signal of hHBV antibodies at the concentration of 0.24 nM was estimated to be 0.03 milli°, which was far less than the detection limit of SPR IA biosensor and the cut-off value can not be detected by SPR signal by this direct detection method. From this result, signal amplification method should be used for detection limit of SPR signal to be improved as the cut-off value.
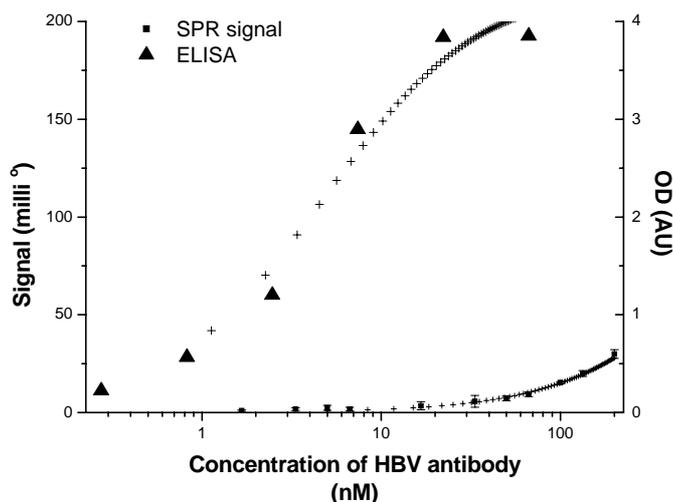
Figure 3-24: Comparison of the detection range of hHBV antibodies by SPR measurement with ELISA (n=3). The ELISA method determines the positiveness of hHBV antibodies using a cut-off value. With the commercial ELISA kit, the optical density (OD) of mean negative control value was detected as 0.03 (OD) and the cut-off value was determined to be around 0.10 (OD) corresponding to the 0.24 nM of hHBV antibodies. By using the standard curve of the SPR signal, hHBV antibodies at the concentration of 0.24 nM was estimated to be 0.03 milli°, which was far less than the detection limit of SPR IA biosensor. This result shows that signal amplification method is required to reach the cut-off value.

3.3.1.2 Selection of optimal label

In this work, three kinds of amplification methods were tested to improve the sensitivity of the SPR biosensor. The direct assay without label is shown in Figure 3-25A. The standard curve between SPR signal and the concentration of hHBV antibodies was explained in the previous section. Because the signal amplification was achieved by increasing the effective mass of the already bound analyte using label proteins, the amplified signal is expected by using heavy label proteins.

The amplification method based on a sandwich assay is shown in Figure 3-25B. In the sandwich assay, additional antibodies (secondary antibodies) as labels are attached to the target analyte after attachment of the target analyte to the IA layer and the signal is increased in proportion to the mass of labels. This sandwich assay has been reported to improve the sensitivity of the diffraction-based immunoassay as much as 3.5-fold (Goh et

al., 2003).

To further improve the efficiency of the signal amplification, the avidin-biotin interaction (Jordan et al., 1997) was applied as shown in Figure 3-25C. This method aims to bind more than one secondary antibody to each bound analyte by using the avidin protein.

Conventionally, the peroxidase-anti-peroxidase (PAP) complex has been used in ELISA to increase the sensitivity by using several peroxidases against one target analyte. The PAP complex was prepared by the method of Sternberger et al. (Sternberger et al., 1970). Theoretically, the PAP complex consists predominantly of two anti-horseradish peroxidase antibodies with three molecules of horseradish peroxidase with a heavy molecular weight (> 430 kDa). After attachment of secondary antibodies (anti-Rabbit IgG) to the target analyte (rabbit anti-hHBV antibodies), the PAP complex composed of antibodies from rabbit could be attached to the secondary antibodies and then additional secondary antibodies were injected to maximize the effect of amplification as shown in Figure 3-25D.
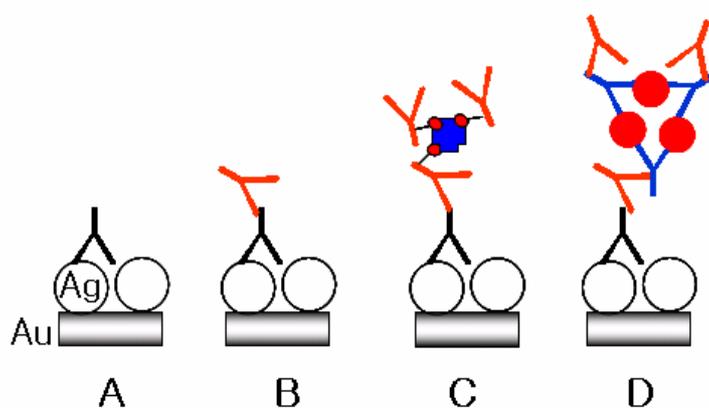
Figure 3-25: Schematic view of three amplification methods: (A) Direct assay. **(B)** Amplification using sandwich assay. **(C)** Avidin- biotinylated antibodies. **(D)** Peroxidase-anti-peroxidase (PAP) complex.

To compare the efficiency of the amplification methods (see Figure 3-26), a sample at a concentration of 30 nM of hHBV antibodies was injected and it resulted in a SPR signal of 4.9 milli° (n=3) by direct assay. The label proteins were also prepared in 5 % calf serum (in 10 mM PBS). The negative signal by non-specific binding of label proteins was determined by the treatment of blank buffer as an analyte and it was subtracted from the positive signal (Signal of sample − Signal of blank) and this value was compared with the result of the

direct assay. From the calculation, the sandwich assay by the application of secondary antibodies was determined to achieve a signal amplification of 7-fold compared with the direct assay. The amplification ratio using the avidin-biotin-label was estimated to be as much as 14-fold and the effective amplification ratio using the PAP complex was calculated to be 17-fold higher than the direct assay by considering the non-specific binding of label proteins. From these results, the amplification using the PAP complex was selected as the most efficient method among the three described amplification methods.
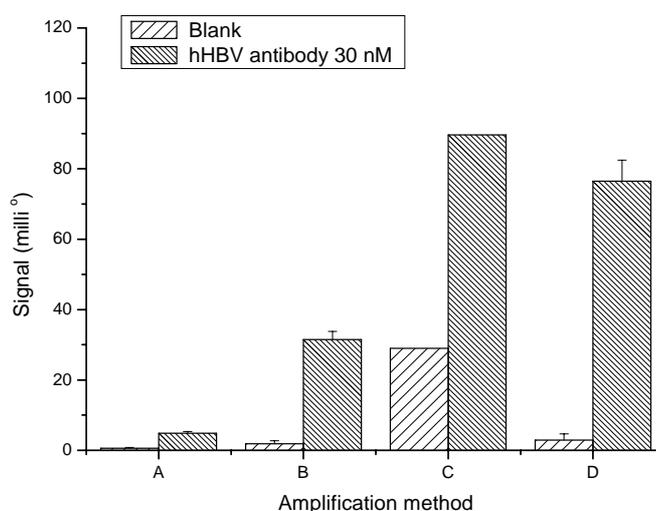
Figure 3-26: Comparison of the efficiencies of three amplification methods: **(A)** Direct assay. **(B)** Amplification using sandwich assay. **(C)** Avidin-biotinylated antibodies. **(D)** Peroxidase-anti-peroxidase (PAP) complex.

The typical sensorgram of the signal amplification by the PAP complex is shown in Figure 3-27 and this method consists of four steps: (1) injection of sample, (2) injection of secondary antibodies, (3) injection of PAP complex and (4) injection of secondary antibodies against PAP complex. The non-specific binding of the label proteins in each amplification method was estimated by injection of a blank sample (a sample without hHBV antibodies) followed by an injection of the corresponding label proteins. As shown in Figure 3-27A, the non-specific bindings at the injection step of sample and label proteins were represented as 'NS 1' and 'NS 2', respectively. The signal of the blank sample was first measured (NS 1), and then the signals by the label proteins were measured (NS 2). The 'NS 1' and 'NS 2' were regarded as the background of the signal before and after signal amplification step, respectively. The signals before and after the signal amplification were

indicated as 'Signal 1' and 'Signal 2', respectively (see Figure 3-27B). The signal of the 30 nM hHBV antibodies was first measured (Signal 1), and then the signals by the label proteins were measured (Signal 2).

A   **B**
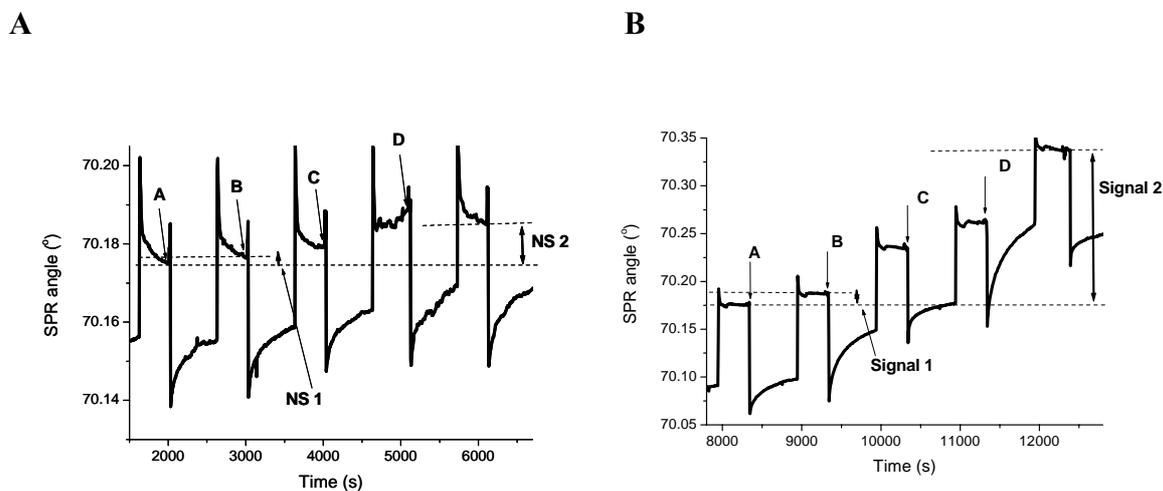
Figure 3-27: The sensorgram of the signal amplification using the PAP complex: (A) Signal amplification after blank sample injection. **(B)** Signal amplification after a sample (with 30 nM hHBV antibodies) injection. 'A' indicated the sample injection, 'B' indicates the injection of secondary antibodies, 'C' indicates the injection of the PAP complex, 'D' indicates the injection of secondary antibodies against the PAP complex. 'NS 1' and 'NS 2' indicate the non-specific bindings at the injection step of sample and label proteins, respectively. 'Signal 1' represents the signal without amplification, and the 'Signal 2' represents the signal after amplification.

In the real application, the signal was calculated by the difference between the signal by the sample treatment and negative signal by the blank treatment (Signal of sample – Signal of blank). The efficiency of the PAP method for the signal amplification was calculated at several analyte concentrations by comparing the net signals of the direct assay and the PAP method and it was defined to be the ratio of amplification. Net signal (Signal – NSB) was determined by the difference between signal of sample (positive signal) and signal of non-specific binding (NSB) (negative signal). Net signals of direct assay and PAP method were calculated as $(\text{Signal}^{\text{Direct assay}} - \text{NSB}^{\text{Direct assay}})$ and $(\text{Signal}^{\text{PAP}} - \text{NSB}^{\text{PAP}})$ by considering the non-specific binding (NSB) of the direct assay and the PAP method as 0.6 and 4.4 milli°, respectively. The ratio of amplification was calculated as comparing these net signals $(\text{Signal}^{\text{PAP}} - \text{NSB}^{\text{PAP}}) / (\text{Signal}^{\text{Direct assay}} - \text{NSB}^{\text{Direct assay}})$.

As shown in Table 3-9, the signal from injection of hHBV antibodies at the concentration of 3.3 nM was 2.6 milli° and the signal after amplification was 29.3 milli°. By considering non-specific binding, the net signals (signal – noise) were calculated to be 2 and 24.9 milli°, respectively. The ratio of amplification was calculated to be 12.5 by using these two values. For the other concentrations of 6.7, 30 and 66.7 nM, the ratio of amplification was calculated as 28.1, 23.4 and 17.1. This result shows that the PAP method is feasible for signal amplification.

Table 3-9: Signal amplification by the PAP method.

Concentration (nM)	Direct assay		PAP method		** Ratio of amplification
	Signal (milli°)	* (Signal - NSB) (milli°)	Signal (milli°)	* (Signal - NSB) (milli°)	
3.3	2.6	2	29.3	24.9	12.5
6.7	2.3	1.7	51.9	47.5	28.1
30.0	4.9	4.3	104.9	100.5	23.4
66.7	9.8	9.2	161.5	157.5	17.1

* Net signal was the difference between signal of sample and signal of nonspecific binding (Signal - NSB). Net signal of direct assay and PAP method were calculated as ($Signal^{Direct\ assay}$ - $NSB^{Direct\ assay}$) and ($Signal^{PAP}$ - NSB^{PAP}) by considering the non-specific binding (NSB) of direct assay and PAP method as 0.6 and 4.4 milli°, respectively.

** Ratio of amplification = ($Signal^{PAP}$ - NSB^{PAP}) / ($Signal^{Direct\ assay}$ - $NSB^{Direct\ assay}$).

3.3.1.3 Application of signal amplification by the PAP complex for medical diagnostics of hHBV antibodies.

For the practical application of the SPR biosensor to the medical diagnosis of hHBV antibodies, the sensitivity of the SPR biosensor should be considerably improved as discussed in the previous section. Here, the selected amplification methods (PAP complex method) were applied for the detection of hHBV antibodies. As shown in Figure 3-28, the sensitivity of the SPR biosensor was increased by using the PAP complex method in comparison to the sandwich assay and the direct assay method. Especially, the sensitivity of the SPR measurement with PAP complex approached closely to the commercial ELISA kit.
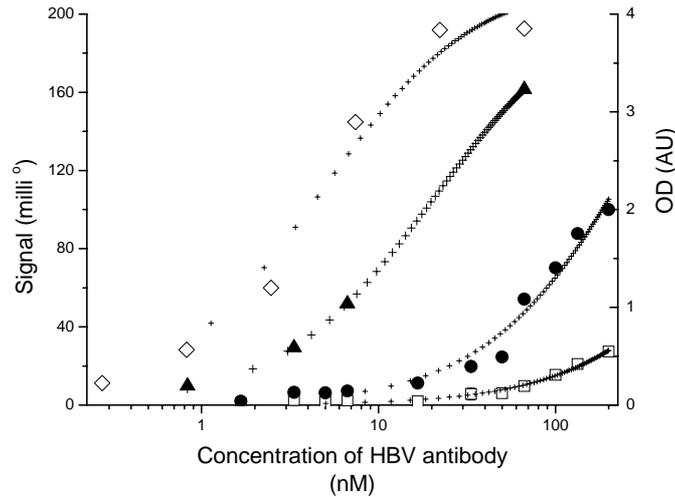
Figure 3-28: Comparison of the detection range for the detection of HBV antibodies. The sensitivity of the SPR biosensor was increased by using the PAP complex method (▲) in comparison to the sandwich assay (▲) and the direct assay method (□). Especially, the sensitivity of the SPR measurement with PAP complex approached closely to the commercial ELISA kit (◇). The (+) dots represent the fitting result using Langmuir isotherm model.

As shown in Table 3-10, the detection limit of the SPR biosensor was also significantly improved in comparison to the direct assay. The detection limits of SPR measurements by direct assay, sandwich assay and PAP complex method were calculated to be 9.20, 4.39 and 0.64 nM, respectively. In comparison to the detection limit of the direct assay, those of the sandwich assay and PAP method were determined to be improved by 2- and 14-fold, respectively. The result from the PAP method shows that the detection limit of the SPR biosensor (0.64 nM) approached closely the cut-off value for medical diagnosis (0.24 nM) by using the commercial ELISA kit.

Table 3-10. The comparison of the detection limits by the signal amplification methods.

Method	Detection limit (nM)
Direct assay	9.20
Sandwich assay	4.39
PAP method	0.64
Cut-off value (ELISA) = 0.24 nM	

3.3.2 Signal amplification by orientation control of the IA layer

3.3.2.1 Introduction

The sensitivities of immunosensors are known to be improved by the control of the IA layer (orientation & density). As more target analytes can be attached to this controlled IA layer, the signal at the same concentration of target analyte can be increased. For the selection of most effective orientation control and the density control of antibodies, several methods were compared by using avidin, NeutrAvidin, protein A, NeutrAvidin-protein A complex layer and the biotin-labelled SAM. For the feasibility test of orientation control by using selected layer, the SPR biosensor was applied for the detection of a cancer marker called carcinoembryonic antigen (CEA).

3.3.2.2 Orientation control of the IA layer on gold surface of SPR biosensor

In order to compare the effect of orientation, several kinds of IA layers such as NeutrAvidin layer, Protein A layer and NeutrAvidn-protein A complex layer were prepared on the differently modified gold surface (see Figure 3-29A). First, receptor (anti-hIgG) was added to the differently modified gold surface to compare the surface density of receptors and then, the ligand (hIgG) was added to the receptor (anti-hIgG) bound gold surface in order to compare the effect of orientation control of IA layer (see Figure 3-29B).

The amount of bound IgG was estimated by the corresponding SPR signal. The higher the SPR signal means the larger amount of the bound receptor IgG to the surface. Then, the ligand IgG was added to the receptor IgG bound surface which could selectively bind the ligand IgG and then the SPR signal was additionally measured. As two binding sites at two variable regions called F(ab')s are localized, the binding sites should be oriented to bind the ligand IgG.. This means that the bound amount of the ligand IgG is related to the amount of well-oriented receptor IgG and not to the total amount of the receptor IgG. And the ratio of two signal (Signal $^{ligand\ IgG}$ / Signal $^{receptor\ IgG}$) can be used to compare the binding ratio of ligand IgG per receptor IgG indicating the effect of orientation control of receptor layer (IA layer).

A   B
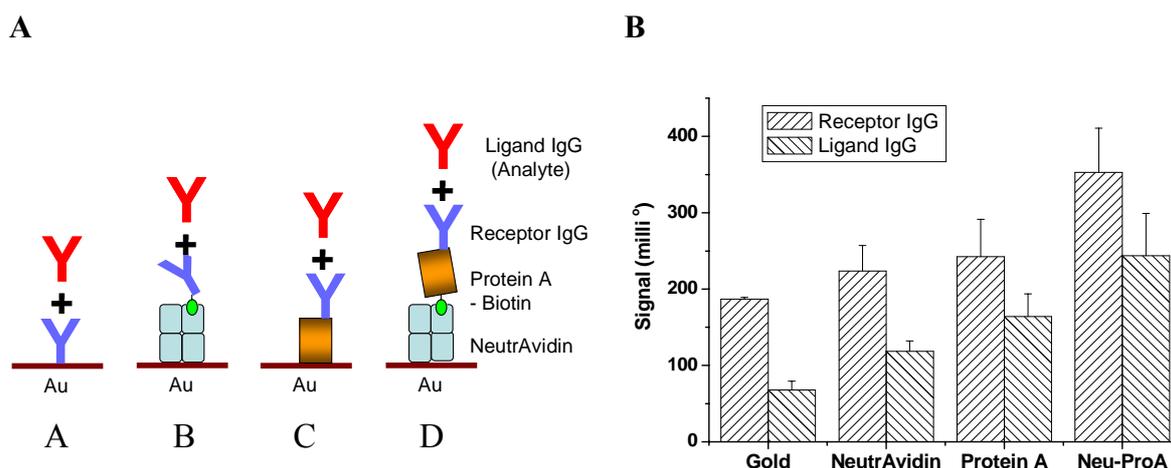
Figure 3-29: Comparison of three differently modified gold surface. The receptor IgG (anti-hIgG) was added to the differently modified gold surface to make IA layer and then, the ligand IgG (hIgG) was added to the receptor (anti-hIgG) as an analyte. **(A)** Schematic view of three differently modified gold surface. **(B)** Comparison of the binding amount of the receptor and ligand on the differently modified gold surface. 'A and Gold' represents the bare gold surface. 'B and NeutrAvidin', 'C and Protein A' and 'D and Neu-ProA' represent NeutrAvidin layer, Protein A layer and NeutrAvidin-protein A complex layer on the gold surface, respectively. The ratio of two signal (Signal $^{\text{ligand IgG}}$ / Signal $^{\text{receptor IgG}}$) can be used to compare the binding ratio of ligand IgG per receptor IgG indicating the effect of orientation control of receptor layer (IA layer).

The NeutrAvidin layer (see Figure 3-29A(B))

The NeutrAvidin layer was prepared on the gold surface of the SPR biochip by physical adsorption. In comparison with the sensor responses at the bare gold surface (receptor IgG: 186.9 milli$^{\circ}$, ligand IgG: 68.0 milli$^{\circ}$), the sensor responses at the NeutrAvidin layer by the attachment of the receptor (223.6 milli$^{\circ}$) and the ligand IgG (118.7 milli$^{\circ}$) were increased to 120 % (186.9 $\rightarrow$ 223.6 milli$^{\circ}$) and 175 % (68.0 $\rightarrow$ 118.7 milli$^{\circ}$), respectively (see Figure 3-29A(B)). The binding ratio of ligand antibody per receptor antibody was calculated by the ratio of the two signals (Signal $^{\text{ligand IgG}}$ / Signal $^{\text{receptor IgG}}$) to be 1.5-fold higher than that of the bare gold surface. This result shows that the density of the receptor in the IA layer as well as the binding capacity per unit receptor was slightly increased.

The Protein A layer (see Figure 3-29A(C))

Protein A is the surface protein of *Staphylococcus aureus* and it is well known to bind the

Fc region of antibodies (Hjelm et al., 1972). Such a property of protein A has been used for the orientation control of antibodies in immunoassays (Goding, 1978). In order to estimate the orientation of antibodies by protein A, the receptor and the ligand antibodies were added sequentially to the protein A bound SPR biosensor. In comparison to the bare gold surface of SPR biosensor, the binding of the receptor and the ligand antibodies were increased to be 130 % (186.9 $\rightarrow$ 242.6 milli^o) and 241 % (68 $\rightarrow$ 164.2 milli^o), respectively. The binding ratio of ligand antibody per receptor antibody is thus improved to be 1.9-fold compared with bare gold surface. This result shows that the binding capacity per unit receptor was significantly increased.

The NeutrAvidin-protein A complex layer (see Figure 3-29A(D))

NeutrAvidin-protein A complex layer was prepared as follows: After the preparation of NeutrAvidin layer on gold surface, the protein A layer was prepared above the layer of NeutrAvidin by treatment of biotin-labelled protein A molecules. The typical SPR sensorgram of Figure 3-30 shows the binding of receptor antibodies to the layer of protein A attached to the immobilized NeutrAvidin molecules on the bare gold surface.
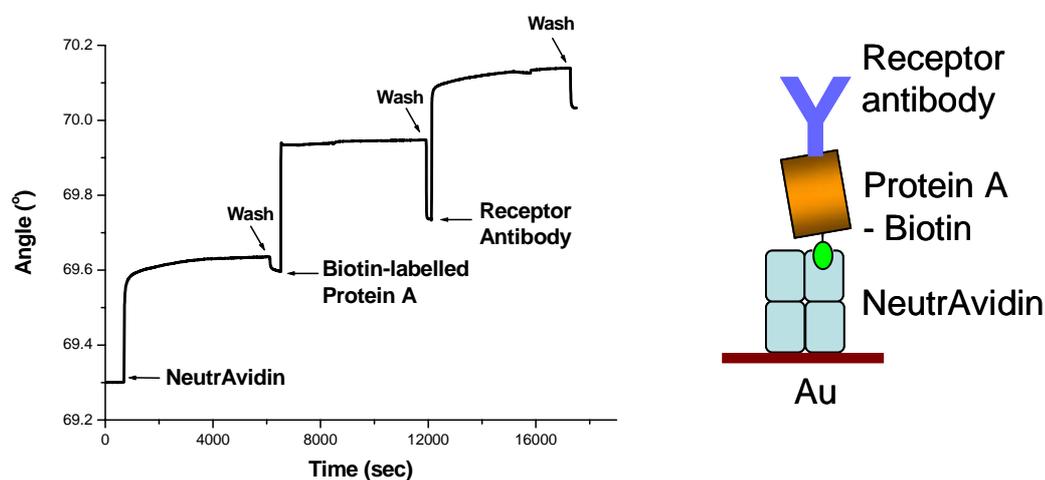
Figure 3-30: SPR responses during the preparation of NeutrAvidn-protein A complex layer. The NeutrAvidin layer was made on gold surface by treatment of NeutrAvidin molecules (1 mg/ml for 90 min), and then the protein A layer was prepared above the layer of NeutrAvidin by treatment of biotin-labelled protein A molecules (1 mg/ml for 90 min). Receptor antibodies (anti-hIgG antibodies; 1 mg/ml for 90 min) were attached to the NeutrAvidin-protein A complex layer.

By using the known correlation between the SPR signal and the absolute amount of protein (120 milli° = protein binding of 1 ng/mm^2) (Stenberg et al., 1991), the saturating amount of NeutrAvidin molecules (60kDa), biotin-labelled protein A molecules (50kDa) and receptor antibodies (150kDa) was calculated as shown in Table 3-11. The ratio of biotin-labelled protein A per NeutrAvidin and the ratio of receptor antibodies per biotin-labelled protein A were estimated to be 0.4 and 1.1, respectively.

Table 3-11: Surface density of the between-layers of Neutravidin-protein A complex layer.

	Surface density		Ratio
	(ng/mm^2)	(moles/mm^2)	
NeutrAvidin	2.7	$4.6 * 10^{-14}$	
Biotin-labelled Protein A	0.9	$1.8 * 10^{-14}$	0.4*
Receptor antibodies	2.9	$2.0 * 10^{-14}$	1.1**

*Ratio of biotin-labelled protein A per NeutrAvidin

**Ratio of receptor antibodies per biotin-labelled protein A

The receptor and ligand antibodies were sequentially added to the NeutrAvidin-protein A complex. As shown in Figure 3-29B ('Neu-ProA'), the absolute binding amount as well as the binding capacity per unit receptor molecule was significantly increased in comparison to the other layers. In comparison to the bare gold surface of the SPR biosensor, the amount of the receptor and the ligand antibodies were increased to be 189 % (186.9 → 352.9 milli°) and 359 % (68 → 243.8 milli°), respectively. The signal ratio by the binding of ligand antibody per receptor antibody is improved to be 1.9-fold compared with bare gold surface.

For the binding capacity per unit receptor (orientation control effect of receptor), the NeutrAvidin-protein A complex layer (1.9-fold higher than the bare gold surface) showed similar result with the protein A layer (1.9-fold higher than the bare gold surface). In the both of the protein A layer and the NeutrAvidin-protein A complex layer, the receptor antibody was immobilized on the same factor of orientation control for protein A. This means that both layers had similar orientation control effect for antibodies, which has higher value of orientation control effect than the NeutrAvidin layer (1.5-fold higher than the bare gold surface) or bare gold surface.

However, the orientation of protein A could be also controlled by interaction of biotin-

labelled protein A and NeutrAvidin in the NeutrAvidin-protein A layer, and NeutrAvidin could always show similar orientation of binding sites for biotin because of four same domains for binding sites. From this result, binding sites of protein A in the NeutrAvidin-protein A layer could be uniform for the receptor antibody to bind. On the contrary, protein A in the protein A layer bound to the gold surface without any orientation control. In this case, some binding sites of protein A could not be bind with the receptor antibody. As the protein A of NeutrAvidin-protein A layer seemed to have more controlled binding sites for receptor IgG than the protein A-only layer, the binding amount of receptor IgG (352.9 milli^o) or ligand IgG (243.8 milli^o) on the NeutrAvidin-protein A complex layer were significantly increased in comparison to the protein A layer (receptor IgG: 242.6 milli^o, ligand IgG: 164.2 milli^o). Compared with the protein A layer, the NeutrAvidin-protein A complex improved the surface density of the receptor antibody.

3.3.2.3 Orientation control of the IA layer on SAM surface of SPR biosensor

The orientation control effect of NeutrAvidin-protein A complex was also tested by using the self-assembled monolayer (SAM) of the SPR biosensor. Because of the easy preparation and the high quality of the monolayered structure as well as low non-specific binding of biomolecules (Silin et al., 1997), SAM based on the thiolated carbohydrate molecules have been widely used for the surface functionalization of the SPR biosensor.

In order to compare the signal amplification by orientation control on the SAM layer, NeutrAvidin-protein A layer on the biotinylated SAM layer and Chimeric complex layer were prepared on the biotinylated SAM layer (see Figure 3-31A) and the binding amount of the receptor (anti-hIgG) and ligand (hIgG) antibody on the differently modified SAM surfaces were measured (see Figure3-31B). And the ratio of two signal (Signal $^{\text{ligand IgG}}$ / Signal $^{\text{receptor IgG}}$) were calculated to compare the binding ratio of ligand IgG per receptor IgG indicating the effect of orientation control of receptor layer (IA layer).

A

B
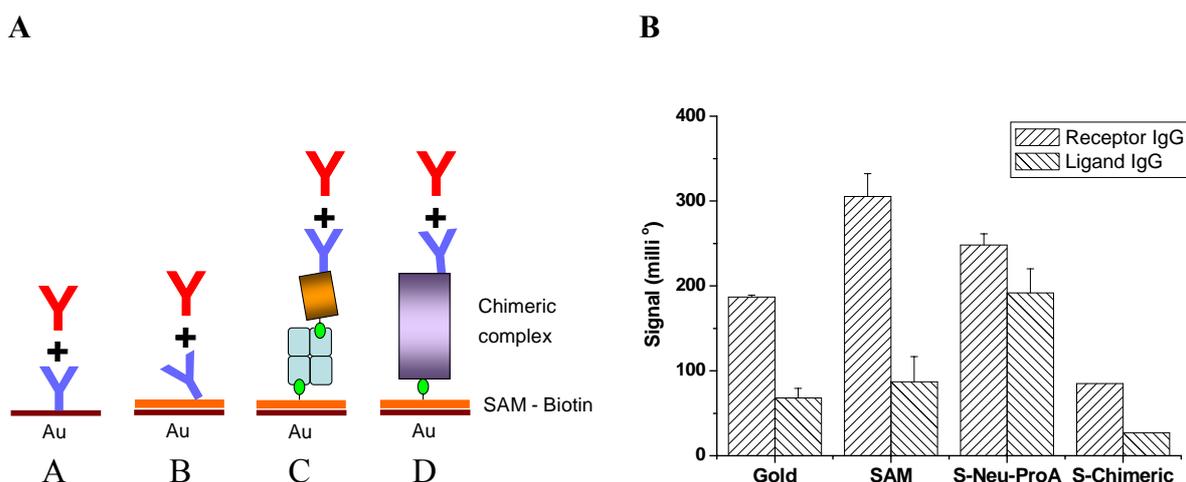
Figure 3-31: Comparison of three differently modified SAM layers. The receptor IgG (anti-hIgG) was added to the differently modified gold surface to make IA layer and then, the ligand IgG (hIgG) was added to the receptor (anti-hIgG) as an analyte. **(A)** Schematic view of three differently modified SAM layers. **(B)** Comparison of the receptor and ligand antibody binding on the differently prepared SAM surface. 'A and Gold' means the bare gold surface of SPR biochip. 'B and SAM' and 'C and S-Neu-ProA' represent the SAM layer on the bare gold surface and NeutrAvidin-protein A complex layer on the biotinylated SAM layer, respectively. 'D and S-Chimeric' means the purified NeutrAvidin-protein A chimeric complex immobilized on the biotin labelled SAM layer. The binding ratio of ligand IgG per receptor IgG can be used to indicate the effect of orientation control of receptor layer (IA layer).

The SAM layer (see Figure 3-31A(B))

The SAM layer was prepared on the gold surface of the SPR biosensor by using 11-mercaptoundecanoic acid. The receptor IgG was immobilized to the SAM by using coupling reagents (EDAC/NHS). As shown in Figure 3-31B ('SAM'), the amount of the receptor and the ligand binding was increased to be 163 % (186.9 → 305.3 milli°) and 128 % (68 → 87 milli°), respectively in comparison to that of bare gold surface ('Gold'). The binding ratio per unit receptor was estimated to be as low as 0.8-fold of bare gold surface. This low binding ratio per unit receptor (0.8-fold) means that the orientation of the receptor layer should be controlled for the suitable binding of ligand IgG. If the receptor layer is well-oriented, the amount of the ligand binding can be increased even if the amount of the receptor does not increase significantly.

The NeutrAvidin-protein A complex on the biotinylated SAM layer (see Figure 3-31A(C))

The NeutrAvidin-protein A complex was prepared on the biotinylated SAM layer by sequential treatment of NeutrAvidin and biotin-labelled protein A ('S-Neu-ProA' in Figure 3-31B). When the receptor and the ligand antibodies were reacted to the layer, the amounts of binding were estimated to be increased as much as 133 % (186.9 $\rightarrow$ 248.3 milli^o) and 282 % (68 $\rightarrow$ 191.9 milli^o), respectively in comparison to that of bare gold surface. Especially, the binding ratio of ligand per unit receptor was increased 2.1-fold compared with the bare gold layer. In comparison to the SAM layer, the binding ratio was improved as much as 2.7-fold, which clearly shows the effect of orientation control by Neutravidin-protein A complex.

The chimeric protein of NeutrAvidin-protein A complex on the biotin-labelled SAM surface (see Figure 3-31A(D))

The chimeric protein of NeutrAvidin-protein A complex was prepared by mixing equimolar biotin-labelled protein A and NeutrAvidin, and then the chimeric complex was purified by centrifugal filtration. When the chimeric protein was added to the biotin-labelled SAM surface ('S-Chimeric' in Figure 3-31B), the binding amount of the receptor and the ligand was estimated to be 45 % (186.9 $\rightarrow$ 85 milli^o) and 40 % (68 $\rightarrow$ 27 milli^o), respectively in comparison to the bare gold surface. The binding ratio per receptor was calculated to be 90 % in comparison to the bare gold surface. This result shows that the orientation of the receptor was randomly controlled as in the case of the immobilization of receptor IgG to SAM layer or bare gold surface.

As summarized in Table 3-12, NeutrAvidin-protein A layer on gold surface showed the highest binding amount of ligand antibodies. In the case of NeutrAvidin-protein A complex on the biotin-labelled SAM layer, the binding ratio per receptor antibody was estimated to be the highest among other layers.

Table 3-12: Comparison of binding amount of receptor and ligand antibodies to the differently modified SPR biosensor surface.

Surface	Amount of binding*		Ratio of Orientation**
	Receptor Ab	Lignad Ab	
Bare gold	1	1	1
NeutrAvidin	1.2	1.8	1.5
Protein A	1.3	2.4	1.9
NeutrAvidin-protein A	1.9	3.6	1.9
SAM	1.6	1.3	0.8
SAM-Biotin-NeutrAvidin-Protien A	1.3	2.8	2.1
SAM-Biotin-Chimeric complex	0.5	0.4	0.9

* Amount of binding was calculated in comparison to bare gold surface, which was (SPR Signal$^{\text{at each surface}}$ / SPR Signal$^{\text{at bare gold surface}}$).

**The ratio of orientation means the relative number of lignand Ab bound to unit receptor Ab in comparison to bare gold surface, which is calculated to be (Amount of binding$^{\text{ligand Ab}}$ / Amount of binding$^{\text{receptor Ab}}$).

3.3.2.4 Signal amplification for carcinoembryonic antigen (CEA) detection by using NeutrAvidin-protein A layer

The NeutrAvidin-protein A complex was applied for the detection of a cancer marker called carcinoembryonic antigen (CEA) by using the SPR biosensor. CEA is considered one of the broad spectrum cancer markers (see section 1.4). The cut-off level of CEA is reported to be 5 ~ 10 ng/ml and the detection range for diagnosis of CEA is reported to be between 0 and 100 ng/ml (Nishizono et al., 1991; Suresh, 2001).

For the detection of CEA, the IA layer of monoclonal anti-CEA antibodies was prepared on (1) bare gold surface of SPR biosensor and (2) the Neutravidin-protein A layer on bare gold surface. The injection of samples at the target concentration range for the diagnosis of CEA did not induce the sensor response higher than the level of baseline drift (0.8 milli°) by using both IA layers. In this work, the polyclonal anti-CEA antibodies were additionally injected for the formation of sandwich complex to the already bound CEA. For the improvement of sensitivity in the detection of CEA, NeutrAvidin-protein A layer was used and it was compared with the bare gold surface to measure the degree of "signal

amplification" (see Figure 3-32). The standard curves were fit by using the simple binding model: $R = [C \cdot R_{max} / (C + K_D)]$. Here, 'R' and 'C' represent the sensor response and concentration of CEA, respectively. K_D is dissociation constant and R_{max} is the maximal sensor response (O'Shannessy et al., 1993). As shown in Figure 3-32, the experimental results seem to fit well ($r^2 > 0.99$). By using the curve fit, the IA layer on the NeutrAvidin-protein A complex layer showed higher sensitivity than the bare gold surface. The R_{max} value was evaluated for NeutrAvidin-protein A layer and bare gold surface to be 85.8 milli° and 52.8 milli°, respectively. From the comparison of signals, the sensitivity with NeutrAvidin-protein A layer was determined to be improved 1.5-fold higher compared with the bare gold surface. The detection limit was also estimated for NeutrAvidin-protein A layer and bare gold surface to be 30 ng/ml and 36 ng/ml, respectively. This result shows that the NeurtAvidin-protein A complex can improve the sensitivity for the detection of CEA through the orientation control of antibodies in IA layer.
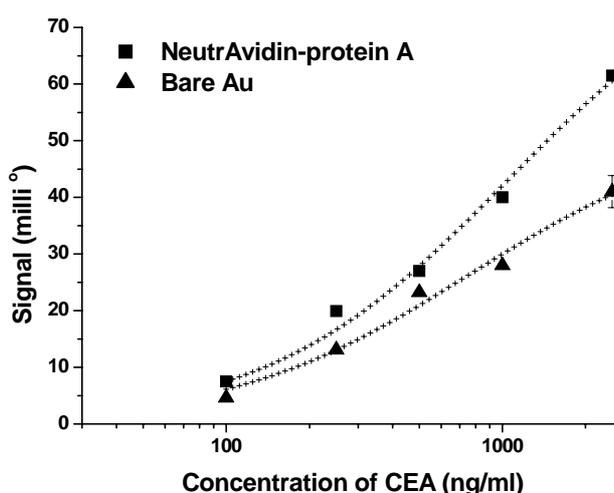
Figure 3-32. Standard curve for the detection of CEA in 10 mM PBS (pH 7.4). For the improvement of sensitivity in the detection of CEA, NeutrAvidin-protein A layer (■) was used and it was compared with the bare gold surface (▲) to measure the degree of "signal amplification". Each signal was obtained by additional injection of anti-CEA antibodies (label proteins) to the already bound CEA for the formation of the sandwich complex. The standard curves were fit by using the simple binding model: $R = [C \cdot R_{max} / (C + K_D)]$. The R_{max} value was evaluated for NeutrAvidin-protein A layer and bare gold surface to be 85.8 milli° and 52.8 milli°, respectively. This result shows that the sensitivity with NeutrAvidin-protein A layer was improved 1.5-fold higher compared with the bare gold surface for the detection of CEA through the orientation control of antibodies in IA layer.

4. Discussion

4.1 Application of biosensor in medical diagnosis

4.1.1 Introduction

The biosensor has been proposed as a tool to improve the "sensitivity", "selectivity" and "analysis time" by using biological materials, and this is composed of "biomaterial" and "transducer" (see introduction). According to the biomaterials for the molecular recognition, biosensor is classified into catalytic biosensors and affinity biosensors (Scheller and Schubert, 1992; Ramanavieius et al., 2005). In the catalytic biosensors, the recognition element (enzyme, cell and tissue) converts substrate molecules into product molecules, thereby making amplification of the signal possible. In the affinity biosensors, the recognition molecule (antibody, nucleic acid, peptide, cell receptor and protein) binds the analyte molecule. These two kinds of biosensors can be used with several transducers such as electrode, transistor, thermistor and optical device.

Body fluids (humors) such as blood, urine, sweat, saliva, etc. includes various kinds of bio-chemical materials and these bio-chemical materials related to any specific diseases are called biomarkers (see section 1.4). The biosensors have been used to detect the biomarkers in the body fluids for the medical diagnosis. Rapid and accurate detection of the biomarkers is one of the most important topics of modern medicine because it has a definite influence on the successful treatment of the patient.

The representative catalytic biosensors using the electro-chemical sensors have been generally used for the medical diagnosis, detecting biomolecules such as insulin, glucose, hCG, theophylline, α1-glycoprotein, apolipoprotein E, FSH and LH in serum or urine (Morgan et al., 1996). Such electro-chemical sensors have several advantages such as simplicity and high sensitivity. The electro-chemical sensors have been reported to have several problems under the existence of the interferences in the body fluids, such as proteins in serum (low selectivity). However, the most successful type of biosensors until now is the enzyme-based amperometric type and they are commercially used for the detection of glucose, lactate, urea *etc.* as disposable sensors (Scheller and Schubert, 1992).

Conventional IA-based bioassays such as radioimmunoassay (RIA), enzyme-linked immunosorbent assay (ELISA), immunoagglutination assays (IAA) and fluorescent immunoassays (FIA) have been generally used for the medical diagnosis and this bioassay has several advantages such as high sensitivity, low detection limit and broad detection range (Ngo, 2000). For example, ELISA showed the detection limit of 2 nM for the detection anti-AChR antibody **(**Franciotta et al., 1999**).** Although the development of immunoassays during the last three decades revolutionized medical diagnosis, these classical affinity assays such as ELISA takes more than one hour to achieve, and modern alternative tests are being examined as rapid screens. Moreover, assay system can not be used as continuous monitoring mode. The modern biosensor technology enables the label-free detection, quantification and continuously working immunoassay system. The most representative affinity biosensor is the immunosensor where antibodies or antibody fragments are applied as biological element and this sensor can be categorized based on the detection principle applied (see section 4.1.3). The immunosensor has been used for the detection of high-molecular weight compound such as protein, antigen and hormone, which is necessary for the medical diagnosis. In this work, major parts of the immunosensor (molecular recognition part and transducer) will be discussed for the practical application to medical diagnostics.

4.1.2. Molecular recognition part

4.1.2.1 Antibodies as molecular recognition tool

In the immunosensor, the biological component such as antibody or antigen is used as molecular recognition part and this part conveys selectivity and sensitivity to the sensor by the formation of complex between antigen-antibody.

Two kinds of antibodies can be used for the immnosensor: polyclonal antibodies and monoclonal antibodies (Kane and Banks, 2000; Liddell, 2001). Polyclonal antibodies are still widely used as primary antibodies, particularly in competitive immunoassays, and the great majority of polyclonal antibodies are used as label antibodies. Its great advantage is the relative simplicity and low cost of the procedures used for raising them. Double-antibody sandwich immunoassays can be set up with one kind of polyclonal antibodies and this is more simple system compared with the system with two kinds of monoclonal antibodies or a combination of polyclonal and monoclonal antibody. They are often

sufficiently specific for the purposes of their users and the long-term continuity of supply is possible by immunizing a large animal. However, polyclonal antibodies are a heterogeneous mixture of antibodies arising from a variety of constantly evolving B-lymphocytes, which have a varying binding affinities, isotype, and different specificities. As a consequence, even successive bleeds from one animal are always unique. In this case, uniform ratio of signal to concentration can be made by antibodies from only one bleed and mixture of polyclonal antibodies from several bleeds seems to change the ratio of signal in the immunoassay. This set limits to the quantity of antibodies to be used for uniform experiment by immunosensor. Moreover, polyclonal antibodies recognize epitopes both on the immunogen and any impurities injected with it. This can make a nonspecific binding to increase the detection limit of the immunosensor in the medical diagnosis.

Although early immunoassay used polyclonal antibodies prepared from the sera of animals, the monoclonal antibodies produced by fusion technology (Kohler and Milstien, 1975) are preferred for the immunoassay industry. The hybridoma cell lines can secrete only one particular type of antibody (monoclonal antibodies).

The production of new antibodies, whether polyclonal or monoclonal, always depends on new immunizations, which are lengthy and tedious procedures and do not always guarantee success. The genetic approach to antibody production has gained momentum due to the failure of the hybridoma method to produce human monoclonal antibodies reliably for therapeutic purposes. The production of recombinant antibodies (rAbs) will provide significant changes for antibody generation and diversification, which will provide a vast repertoire of new antibody types. New antibodies can be generated by selection from suitable antibody libraries, which can be constructed within shorter time. The main bottleneck is the handling and screening of large libraries for antibody genes (Hock, 1997). Antibodies in the immunosensors have been often used as conjugates with a variety of labels such as colorimetric enzymes, fluorescent and luminescent molecules and radiolabels. Genetically, recombinant antibody technology can be used to form antibody fusion proteins and this has potential to improve homogeneous production of conjugates in which antigen-binding site should be unaffected. Several useful fusion proteins for immunoassay have been described as shown in the Table 4-1 (Liddell, 2001).

Table 4-1. Recombinant antibody fusion proteins of use in diagnostics

Fusion partner	Antibody fragment	Use
Alkaline phosphatase	ScFv, F(ab')$_2$	Produces colorimetric product
Avidin	Fab, F(ab')$_2$, IgG	Binds biotin conjugated proteins
Biotin-carboxyl carrier protein	Fab	Biotin attached during secretion
Protein A fragment	ScFv	Fc binding
Metallothionein	F(ab')$_2$	Allows subsequent binding of ^{99M}Tc
Peptide	ScFv	Peptide chelates metal then binds to ^{99M}Tc
Peptide	ScFv	Peptide can be enzymetically labeled with ^{32}P
Amino terminal of *E.coli* major lipoprotein	ScFv	Attaches lipid during expression
Streptavidin	ScFv	Binds biotin conjugated proteins. Also useful for producing tetramers.

However, no fusion proteins are yet widely available. It has sometimes been difficult to express fully functional fusion proteins, and the capacity to vary the stability of the linkage as with chemical conjugation is lost.

4.1.2.2 Alternative analyte-binding compounds for immunosensor

Although immunosensors have generally used polyclonal or monoclonal antibodies, there are several limitations of these proteins for immuno-reaction as follows: (1) If working condition is different from body property, the structure of molecule can be changed to be unstable for immuno-reaction. (2) The treatment of regeneration can damage the immobilized antibodies or detach the immobilized antibodies from IA layer. An adequate analytical sensitivity can only be achieved if antibodies with increased affinity ($>10^{10}$ M^{-1}) (Hock, 1997). Therefore, a high-affinity constant and a labile immobilized antibody make regeneration of the surface difficult to realize in practice, limiting practical application of immunosensors to single-use devices (Morgan et al., 1996). (3) The reaction time between antibody and antigen is slower than the detection time by transducer, and all analysis time is extended. The following new tools as the molecular recognition part have been successively developed to solve above problems.

(1) Aptamers

Aptamers are synthetic single-stranded DNA or RNA oligonucleotide sequences with the ability to recognize various target molecules such as nucleotides, drugs, proteins with high affinity and specificity (Luppa et al., 2001). Aptamers are identified by an in vitro selection process known as systematic evolution of ligands by exponential enrichment (SELEX), which allows the simultaneous screening of more than 10^{15} individual nucleic acid molecules for different functionalities (Tuerk and Gold, 1990). Aptamers may have advantages over antibodies in the ease of depositing them on sensing surface of immunosensor and the highly reproducible synthetic approach in any quantities. In the detection of thrombin, a fiber-optic microarray biosensor using aptamers as receptors was reusable and did not show any sensitivity change during the experiment (Lee and Walt, 2000). However, the disadvantage of aptamer such as high cost and unstableness should be solved for the application of this in the IA biosensor.

(2) Molecularly imprinted polymers (MIPs)

Molecularly imprinted polymers (MIPs) is produced by polymerization of functional and cross-linking monomers in the presence of a molecular template (Boonpangrak et al., 2006). After polymerization and template removal, specific binding sites are left in the polymer material. Although natural receptors, enzymes and antibody have limitation of chemical and thermal instabilities limit, MIPs can withstand environments that would destroy natural antibodies, are easy to prepare at low cost, and can be prepared for compounds (e.g., immunosuppressive agents) against which it is difficult to produce natural antibodies (Li and Husson, 2006). In the detection of domoic acid (DA), MIP, comprising 2-(diethylamino) ethyl methacrylate as functional monomer and ethylene glycol dimethacrylate as cross-linker, outperform monoclonal antibody natural receptors with a wide detection range and long stability (Lotierzo et al., 2004). However, the high detection limit owing to low affinity between antigen and MIPs should be improved for the application of MIPs to the IA biosensor (Boonpangrak et al., 2006).

(3) Anticalin

As a promising alternative to recombinant antibody fragments, lipocalin scaffold can be

employed for the construction of "anticalins", which is made by subjecting various amino acid residues, distributed across the four loops, to targeted random mutagenesis. Lipocalins such as retinol-binding protein constitute a family of proteins for storage or transport of hydrophobic and/or chemically sensitive organic compounds (Luppa et al., 2001). These binding proteins share a conserved β–barrel, which is made of eight antiparallel β–strands, winding around a central core. For example, bilin-binding protein can be structurally reshaped in order to specifically complex potential antigens, such as digoxigenin (Schlehuber et al., 2000) However, there are several problems to be solved, such as the synthesis and stability of the anticalins, the magnitude of the affinity constants, and the versatility for being crafted against the large variety of ligands.

4.1.2.3 Immobilization technique

For the successful application of molecular recognition tools, immobilization technique for the connection of molecular recognition tools to the sensor surface should be developed. This technique is very important in the construction of molecular recognition part in order to avoid nonspecific binding and to improve sensitivity of IA biosensors. Immobilization can be achieved in several different ways: direct adsorption to the transducer surface, physical entrapment near the transducer surface (e.g. in a polymer layer or by use of a membrane), direct covalent coupling to the transducer surface, covalent coupling to a polymer layer on the transducer surface and use of 'capture system'.

In this work, we focused on the improvement of molecular recognition layer in order (1) to increase the density of IA molecules and (2) to optimize the orientation of IA molecules. For the orientation control of IA molecules, NeutrAvidin-protein A complex layer and biotin labeled SAM were used in this experiment (see section 3.3.2) and this orientation control showed the enhancement of the sensitivity. In this work, NeutrAvidin-protein A complex layer were made on the sensor surface by sequential injection of NeutrAvidin and protein A. By the sequential attachment, some NeutrAvidin on the sensor surface could not bind with protein A.

As described in section 1.3.1, self-assemble monolayer (SAM) was used in this work, as a linker layer between molecular recognition part and gold layer of SPR transducer. The application of mixed SAMs have been reported by co-adsorption of mixtures of two thiols with different chain lenghs, has been shown to prevent denaturation and thus improve the bioactivity of a protein immobilized on such layer in comparison with the protein

immobilized on a pure SAM (Briand et al., 2006). Mixed SAMs are generally constituted of one long thiolate with a functional headgroup (like a carboxylic acid) at a low mole fraction and of another short "diluting" thiolate at a high mole fraction to minimize steric hindrance, partial denaturation of the protein (Guiomar et al., 1999) and non-specific interactions (Ge and Lisdat, 2002; Frederix et al., 2003).

The prevention of nonspecific binding is also an important topic of immobilization method. In this work, various trials were performed and it will be separately discussed at section 4.3.

4.1.3 Transducer for immunosensors

Transducers of IA-biosensor can be divided as four types according to the principle of signal generation: electrochemical transducers (amperometric, potentiometric, conductometric, capacitative), optical transducers (fluorescence, luminescence, refractive index, ellipsometric, surface plasmon resonance, waveguide) or mass-sensitive transducers (piezoelectric, acoustic wave) or a thermal transducer (calorimetric). The IA-biosensor can be classified according to the detection method: (1) direct detection (2) indirect detection whether label is used for the detection of antigen-antibody reaction or not. (1) In the direct sensor, the binding event can change different physical properties such as the change of refractive index (SPR trasducer), mass change (QCM or SAW transducer) and change of a dielectric constant (electrochemical transducer). (2) The indirect sensor requires a signal-generating label on one of the biomolecules in the immune complex formation and this label needs a separate step to produce a change in the property. This sensor can use a great variety of different labels, which have been usually used in immunoassay (Morgan et al., 1996; Luppa et al. 2001; D'Orazio, 2003).

The direct sensors can save the analysis time and allow direct detection of analyte binding in real time. Without labels, these sensors can be more cost-effective. With the progress of MEMS technique, the development of direct sensors has been improved and recently, these sensors have been main type of immunosensors for medical application.

Optical immunosensors are most popular for bioanalysis thesedays, which has the advantage of rapid signal generation and reading. Among the several optical immunosensors, direct optical transducer such as SPR transducer is most popular one to monitor immunoreactions in clinical chemistry (Luppa et al., 2001). The major advantage of direct optical transducer is the lack of need of a label for the detection of analyte, avoiding a separation step to remove free from bound label. Further, there is no penetration of the sensing wave beyond

the immediate surface of the optical device being used, avoiding interference from substances present in the bulk sample (D'Orazio, 2003).

Among the direct biosensors such as SPR biosensor of this work, quartz crystal microbalance (QCM) sensor is also generally used for transducer and it has a high sensitivity. Although a QCM technique detects not the change of optical property but the mass change, both SPR and QCM are wave-propagation phenomena and show resonance structure. The QCM has been widely used as direct immunosensors. The SPR technique measures changes in the refractive index adjacent to the surface, whereas QCM technique detects changes in the frequency, corresponding to changes in the amount of mass coupled to the surface. In the QCM sensor, the relationship of the frequency change and the mass loading on the surface of the crystal can be described by the Sauerbrey equation (Sauerbrey, 1959):

$$\Delta F = -2F_0^2 \Delta m / A(\rho_q \mu_q)^{1/2}$$

Where ΔF is the measured frequency shift, F_0 is the fundamental frequency of the Pz crystal, A is the area coated, Δm is the mass change due to surface deposition, ρ_q is the density of the quartz crystal (2.684g cm^{-3}) and μ_q is the shear modulus (2.947 x 10^{11}g cm^{-1} s^{-2} for AT-cut quartz crystals).

When the SPR biosensor was compared with QCM biosensor for protein adsorption and antigen-antibody recognition, they were comparable with respect to sensitivity and the detection limit for monoclonal antibody (mAb) and sera was nearly the same for both methods (Koesslinger et al., 1995) (see Table 4-2).

Table 4-2 Overview of quantities that can be used for a comparison of the QCM and SPR

Quantity	QCM	SPR
Thickness sensitivity	184 Hz/nm	26.3 milli°/nm
Detection limit of mAb	20 nM	23 nM
Detection limit of sera	1:1000	1:1000
Immunological sensitivity for mAb	0.5 nM/Hz	3 nM/ milli°
Penetration depth	126 nm	150 nm
Sensitive area	5 mm^2	5 x 10^{-3} mm^2

Even if the QCM machine is less expensive and easier to handle, the SPR sensor has several advantages compared with QCM. SPR responses occur at a faster time than the QCM responses and the SPR technique was also cost effective (Laricchia-Robbio and Revoltella, 2004). Moreover, because the sensitive area of SPR is smaller than QCM sensor, fewer molecules are necessary for the same surface density and smaller flow-through cells with smaller sample volumes could be possible compared to the QCM (Koesslinger et al., 1995). Accordingly, SPR transducer can be more easily integrated with microfluidics to make total analysis system, so-called "lab on a chip", which includes sample preparation and handling, chemical analysis and signal acquisition capabilities.

There are two leading SPR systems on the market (Luppa et al., 2001); the BIAcore[TM] systems and the IAsys[TM]. Other systems (with small market positions) are the IBIS[TM], the BIOS-1[TM], the SPR-20[TM], the DPX[TM] and Spreeta[TM]. However, the BIAcore[TM] has the largest market share. Although first two commercial SPR systems are widespread in research laboratories due to the sophisticated apparatus and user friendly control software, they are composed of a disposable biochip and big SPR detection system and it is difficult to be remodeled as a point-of-care (field investigation) system. In the case of Spreeta[TM] system, which was used in this experiment, it is small enough to be used as a point-of-care system. However, even with the temperature control system of this experiment, there was a problem of unstable signal in this experiment and this problem makes a relatively big baseline drift (>0.5 milli°) for the detection limit to be increased (see section 2.2.2(3)). If this background noise can be reduced by using several methods such as the incorporation the Spreeta[TM] transducer into a well-designed sensor system, the detection limit will be decreased for the Spreeta[TM] system to be sufficient for medical application even in the field investigation (Chinowsky et al., 2003).

4.1.4 Future perspectives for clinical applications

The disposable enzyme electrode intended for home monitoring of blood glucose is the most representative world market for biosensor (Newman et al., 2001). However, the medical application of biosensors with "real" clinical samples is still rare. As shown in the application of the detection for hHBV antibody (see section 3.3.1), all immunosensors are still one magnitude less sensitive than commercial immunoassays for determining analytes in human serum, particularly those with low molecular weight (Kubitschko et al., 1997).

The improvement of sensitivity can be accomplished by the detection chemistry, such as the high molecular mass label or nanoparticle, or increasing the sensitivity of the transducer. And reducing background noise is also important and it can be done with well-established system. However, the analytical potential of immunosensor technique such as ease of use or short analysis time is evident and in particular, the applications of optical immunosensor systems will most likely be of clinical interest (Luppa et al., 2001).

4.2 Discussion on the limitations of biosensor for real application

For the real medical application, the techniques in this work have been developed and the feasibility was demonstrated. Here, the limitations of each technique as well as the alternative solutions will be discussed.

4.2.1 The number of repeated measurement by using in the additive assay

The applicability of the additive assay was demonstrated by using CA 19-9 in 10 mM PBS as a model biomarker (see section 3.1.4). The detection limit of CA 19-9 was determined to cover the general detection range (400 – 192,000 U/ml) of most patient samples with pancreatic cancer (Del Villano et al., 1983). In this experiment, the feasibility was tested by four concentrations such as 1.3, 2.5, 5.0 and 6.7 kU/ml. Although those concentrations were relatively low part of the detection range, the uncertainty of measurement increased steeply only after the measurement of several analytes and the number of use seemed to be very limited.

As the measured signal is saturated by repeated measurement, the uncertainty of concentration measurement increases steeply according to the increased accumulated concentration, even if the signal deviation (baseline uncertainty, ± 0.6 milli^o) is uniform (see Figure 3.7). In the saturated region of the correlation curve (the high accumulation concentration), only a small deviation in signal (baseline uncertainty) could result in the higher deviation of measured concentration in comparison to the low region of accumulation concentration. To maintain the accuracy of additive assay, the uncertainty of accumulated concentration by baseline uncertainty should be less than the detection limit (8.3 nM) (see section 3.1.3). In this case, the valid range of accumulated concentration should be within a limited range and it means that the applicable number of binding sites in the IA layer is strictly limited. When the number of additively attached analytes increases

the accumulated concentration, free binding sites of IA layer are also decreased.

If the signal of same size can be obtained by the less number of binding between analytes and IA layer, the number of use can be increased in the additive assay. If several methods such as the orientation control of IA layer (see section 3.3.2) can be used to improve the sensitivity, the less number of binding sites is required for the same sensitivity and number of use can be increased because there is a constant number of binding sites in the IA layer. For the decrease of attachment by the same concentration of analyte, the reaction time should be decreased and the valid range of reaction time is until the sensitivity is still enough for the diagnosis. According to the above methods, the number of use can be increased in the additive assay of CA 19-9.

4.2.2 Integration of simultaneous detection with additive assay

Because simultaneous detection in this experiment should use a label with the sandwich assay format, there was a problem to integrate simultaneous detection with the additive assay. As the labels made sandwich complex with a part of the analyte on the IA layer, the rest of the analytes remained on the IA layer. These rest analytes on the IA layer made a significant influence on the next measurement by participating as analytes in the next measurement. Even if no more target analyte was treated to the IA layer, the rest analytes on the IA layer without label made a false positive signal. And, it resulted in a difficulty to get a uniform correlation curve for additive assay, and the additive assay was not possible for the simultaneous detection. The simultaneous detection has been disposable method until now. If label treatment can saturate the all binding sites corresponding to the analytes on the IA layer, additive assay can be used for the simultaneous detection. It can be possible by the treatment of a large amount of labels or several treatments of labels until the signal by next treatment of labels is disappeared.

4.2.3 Signal amplification

For the detection of analytes in serum, label-free assays with SPR biosensor has been with one order of magnitude lower sensitivity than commercial enzyme immunoassays (Lundstroem, 1994; Mullett *et al*., 2000; Goh *et al*., 2003; Kubitschko *et al*., 1997). Even with the signal amplification of this experiment such as usage of mass label or control of IA layer, the sensitivity of SPR biosensor should be improved for the medical application.

4.2.3.1 The improvement of label effect for the signal amplification

In the detection of hHBV antibody (see section 3.3.1), several mass labels such as second antibody, avidin-biotin labeled antibody and PAP complex were compared and PAP complex was selected as efficient mass label. However, the detection limit of SPR detection with PAP complex label (0.64 nM) was still higher than the commercial ELISA kit (0.24 nM). Moreover, this experiment was done by 20-fold diluted serum sample (5 % serum) and the real detection limit by undiluted sample should be changed 20-times higher than 20-fold diluted sample from 0.64 nM to 12.8 nM. Accordingly, more effective label should be investigated. There are several factors such as mass, density and characteristic to influence the signal size of SPR biosensor as follows:

(1) Mass label

A large label with heavy mass such as liposome or latex particle could naturally make a higher signal than small label. By using liposome (100 ~ 1000 nm) as a label for the detection of interferon-γ, a liposome-enhanced sandwich SPR immunoassay improved the assay sensitivity 4×10^4 times and detection limit to a low picomolar level (Wink *et al.*, 1998). The sensor signal for hCG was also enhanced by using big latex particles (with a diameter of 238 nm) as a label (Severs and Schasfoort, 1993). Latex particles seemed to cause effect of signal amplification, compared to antibodies: at least twice at high concentration and 30 times at lower concentration of analyte.

(2) Density label

Label with a high density would be more efficient. High density means that mass is included in the smaller size. Because evanescent field for the SPR signal is inversely proportional to the distance from sensor surface (see Figure 4-1) (Ivarsson and Malmqvist, 2002), mass at the short distance can make high signal than mass at the long distance. Even if two different particles have same masses, label with high density will improve the effect of signal amplification.

Even if label with heavy mass was used, the effect of signal enhancement was lower than the expected value (Severs and Schasfoort, 1993). Though a mass of hCG-coated latex was about as much as 2×10^4 antibodies, the signal by hCG-coated latex was far less than 2×10^4-fold than antibodies because the size of hCG-coated latex was also as much as 400

antibodies. Evanescent field at a distance of 117 nM (the radius of the latex particle) should be less sensitive for refractive index changes than at a distance of about 10 nM (the dimension of an antibody). Considering the size and a mass between latex particle and antibody, theoretically expected signal of latex particle should be 50 times higher than antibodies. However, real efficiency for signal amplification was calculated to be less than 50 times. The fact that latex bound less efficiently than free anti-antibody might be the main reason for the lower signal increase.
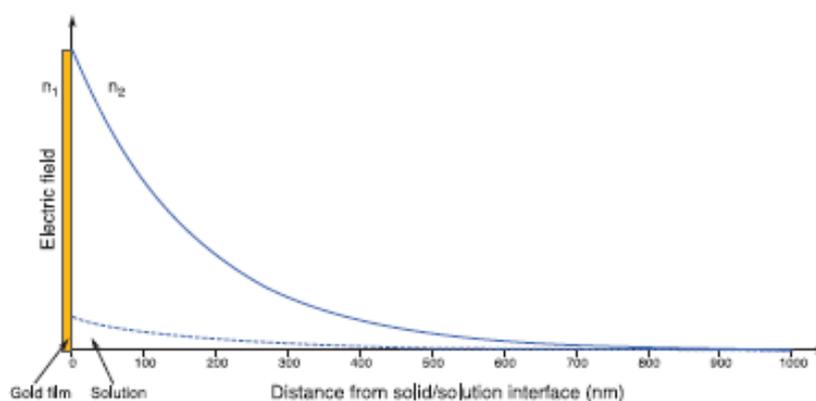
Figure 4-1: Relative evanescent electric field amplitude (E) versus distance from solid/solution interface into sample (BIACORE instrument). Continuous line for SPR-evanescent wave (gold film) and dashed line for non-absorbing TIR (no gold film).

(3) Characterisitic label for SPR signal

If label has good characteristic to make SPR signal, it would be better for signal amplification. Linkage with optically active particles has been proposed to enhance the sensitivity of SPR biosensor and among those particles, some particles such as colloidal gold with high optical refractive index lead to greater signal enhancement, while other particles such as polystyrene bead with smaller refractive index have less certain effect of the signal enhancement (Leung *et al.*, 1994). When the colloidal gold was incorporated in analyte or label in the SPR boisensor, the sensitivities of ligand-protein and DNA-DNA interactions were increased and the change in SPR angle magnitude was particle-size dependent up to 45 nm in diameter (Lyon et al., 1998; He et al., 2000).

In the future, the SPR signal amplification will be improved by developing efficient label, which simultaneously has several factors such as a heavy mass, high density and good characteristic to make SPR signal.

4.2.3.2 The optimal use of the NeutrAvidin-protein A complex

In the detection of CEA tumor marker in the 10 mM PBS, NeutrAvidin-protein A complex layer was used as efficient layer to control IA layer (see section 3.3.2). Although the sensitivity with NeutrAvidin-protein A layer was improved 1.5-fold higher compared with the bare gold surface, the detection limit (30 ng/ml) was still higher than the cut-off value for medical diagnosis (5~10 ng/ml). In the real medical application, the detection limit will be increased by the nonspecific binding of serum. Accordingly, more efficient method to use the NeutrAvidin-protein A complex should be investigated to improve the detection limit.

When NeutrAvidin-protein A complex was used in molecular recognition part, the orientation of receptor antibody in IA layer was controlled by protein A, which is a molecule for fixing receptor antibody. The degree of binding affinity between antibody and protein A is influenced by the species which makes antibody (Fulton, 1989). For the detection of CEA, anti-CEA antibody was used as receptor antibody of IA layer in this experiment and it was mouse IgG_1. Because immunoglobulin binding property of protein A is known to be weak for mouse IgG_1, the special ordering for the antibody from proper species such as rabbit, pig and human can improve the binding property between the receptor antibody and protein A to be strong (see Table 4-3). The improved binding property seems to have a potential to increase the amount of receptor antibody on the NeutrAvidin-protein A complex layer. In this case, more analytes can be also attached to the IA layer to increase the signal amplification.

If change of animal species is difficult, the change of protein A can be an alternative method. Protein G also has a binding property for the F_c binding domains of antibody similar to the protein A and biotin-labelled protein can be used instead of protein A to make NeutrAvidin-protein G layer. Although protein G has strong binding property for mouse IgG_1, binding ability was not distinctly improved in comparison with the NeutrAvidin-protein A and signal ratio of protein G to protein A was just 1.1-fold in our experiment. This phenomenon seemed to be due to the difference of number of binding sites between protein A (four F_c binding domains) and protein G (one F_c binding domains) (Dubrovsky *et al.*, 1996; Akerstrom *et al.*, 1985): Though the protein G has better binding property for mouse IgG_1 than protein A, protein A has more binding sites than protein G. From this result, most proper situation is when the protein A has good binding property.

Table 4-3: Immunoglobulin binding properties of protein A and protein G.

Antibody		Protein A	Protein G
Rabbit		++	++
Rat		−	+
Goat		+	++
Horse		−	++
Pig		++	++
Sheep		−	++
Cow		+	++
Dog		++	+
Cat		++	−
Guinea pig		+	++
Chicken		−	−
Mouse			
	IgG1	−	++
	Others	++	++
Human			
	IgG1	++	++
	IgG2	++	++
	IgG3	−	++
	IgG4	++	++
	IgM	++	−
	IgA	++	−
	IgE	++	−
	IgD	−	−

(Fulton, 1989)

Molecular biology can also play an important role for the control of IA layer. If orientation control part such as avidin is attached to the molecular recognition part of antibody in the construction of recombinant antibody, this recombinant antibody can be well-oriented immobilized on the biotin-labeled SAM surface.

4.3. The problems for the application to blood samples

The real samples of medical diagnosis include blood, hair, milk, saliva, semen, sweat and urine. These samples include not only target analytes, but also other components which can interrupt effective detection of the target analyte. Serum is prepared by separating blood cells from the whole blood and it has a high concentration of protein which includes albumin and other globulins and so on. As proteins in serum can bind to the IA layer on the sensor surface (Matson, 2000; Wilde, 2001), the proteins influence to make a false positive or negative signal as follows; (1) The binding substances in the serum may cause interference in some immunoassay systems by decreasing analyte binding and by suppressing the antigen-antibody reaction (Hedenborg et al., 1979; Vladutiu et al., 1982; Schmidt, 1984). (2) The protein in serum may increase an assay response in sandwich assay (Boscato and Stuart, 1988). For example, the presence of rheumatoid factors or autoantibodies is known to be a common source of non-specific binding in serum and it bridges between the first and the second antibody in the immunoassay. The presence of these substances in serum that are capable of binding antibodies multivalently can lead to erroneous analyte quantification in sandwich assay. As these substances can attach to the immobilized antibodies and they also bind with label antibodies, the substances can link two kinds of antibodies to make false positive signal. In the real application of assay, these interferences were caused from 15 % of serum samples (Boscato and Stuart, 1986).

Usually, the non-specific binding is one of the most serious problems for mass- or refractive index-sensitive detection systems such as SPR biosensor, especially when low-molecular-weight or low-concentration analytes are examined (Vikinge, et al., 1998). As the biosensor such as QCM or SPR biosensor generate a signal by the binding of analytes, the non-specific binding of other molecules can directly make a false positive signal. Various attempts to minimize the non-specific binding have been reported to detect target analytes in serum with SPR biosensors, and those methods were tried in our experiments. Several solutions to decrease the non-specific binding have been investigated, such as blocking of IA layer, dilution of blood sample and application of detergents.

(1) Blocking of IA layer

In solid-phase immunoassay, BSA and gelatin are commonly used as blocking agents after immobilization of antibody or antigen (Matson, 2000). For the polystyrene microtitre plates, many other proteins such as nonfat dry milk, casein, lipoprotein and BSA at high

concentration (120-3750 μg/ml) have been used (Vogt et al., 1987; Pratt and Roser, 1997). SAM was also used to block non-specific binding (Silin et al., 1997) and water-soluble-hydrophilic organic macromolecule such as dextran was used as a coating to prevent non-specific protein adsorption (Frazier et al., 2000). A number of polymers have been also used as blocking reagents such as polyvinyl alcohols, polyethylene glycols and polyvinyl pyrrolidone (Bangs laboratories, 1998).

In this work, the NeutrAvidin-protein A complex layer had three layers such as NeutrAvidin layer, protein A layer and receptor antibody layer on the gold surface, sequentially and these three layers seems to block the gold surface more well than the one receptor layer. With the treatment of BSA (10 mg/ml) similar to the concentration of 20 % serum, non-specific binding at the IA layer on the NeutrAvidin-protein A complex layer (< 0 milli$^{\circ}$) was far less than the IA layer on the bare gold surface (44 milli$^{\circ}$) (see Figure 4-2).

A   **B**
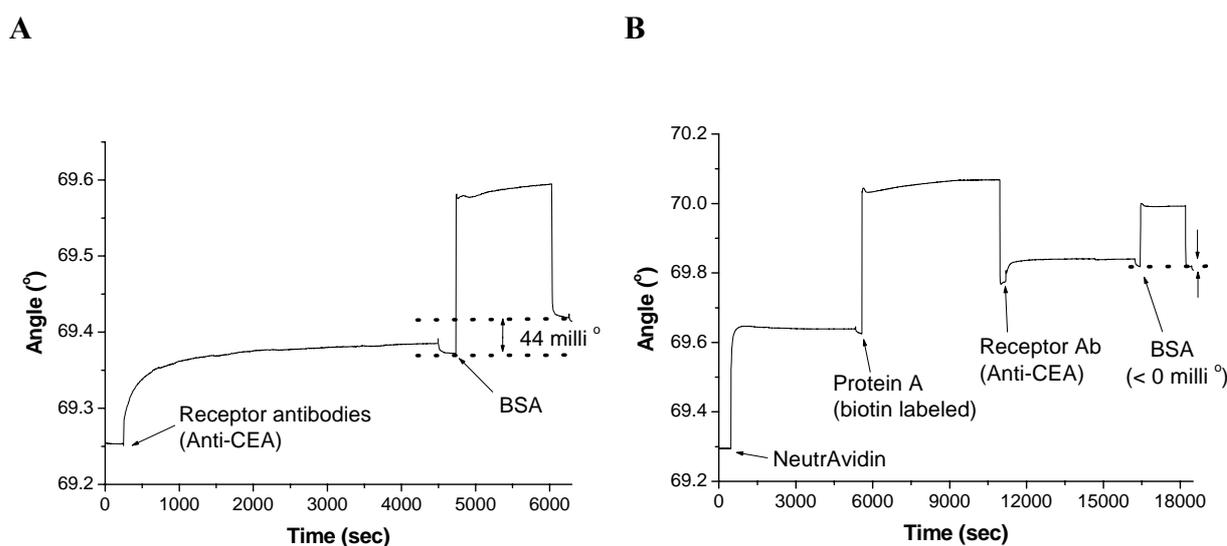
Figure 4-2: The comparison of non-specific binding between the IA layer on the NeutrAvidin-protein A layer and on the bare gold surface.

After the immobilization of the receptor antibody (anti-CEA) layer on (A) the bare gold surface and (B) the NeutrAvidin-protein A complex layer, non-specific bindings for each IA layer were measured by the treatment of BSA (10 mg/ml). Non-specific binding at the IA layer on the NeutrAvidin-protein A complex layer (< 0 milli$^{\circ}$) was far less than the IA layer on the bare gold surface (44 milli$^{\circ}$). The IA layer on the NeutrAvidin-protein A complex layer seemed to prevent the non-specific binding and real medical sample with high concentration of serum seems to be used with this layer.

(2) Dilution of serum sample

The non-specific binding with serum sample is proportional to the serum concentration and the dilution of serum sample has been used as a general solution against non-specific binding in the immunoassay. For example, serum samples for monitoring of tumor antigen were reported to be diluted as much as 15- folds (Campagnolo et al., 2004). In the detection of serum antibodies against *Salmonella enteritidis* and *Salmonella typhimurium*, the serum sample was diluted to be 40- folds (Jongerius-Gortemaker et al., 2002). If the signal by the non-specific binding in the diluted sample is similar with the signal of detection limit (2.1 milli$^{\circ}$), the interrupting effect by non-specific binding can be ignored. However, there is a limitation of dilution to minimize the non-specific binding. Even if serum samples were diluted upto 100- folds, the non-specific bindings by serum samples were still observed (Vikinge et al., 1998). Moreover, the diluted serum sample reduces the concentration of target analyte and it can be too low to obtain the required sensitivity. If high sensitivity is needed instead of accuracy and signal of target analyte can be distinguishable in the serum sample, low degree of dilution should be used. For the measurement of ferritin, the serum sample was only at a dilution of 1/2 (Cui et al., 2003). Generally, the serum is diluted to decrease erroneous signal in immunoassays and the dilution ratio should be around 1/500 ~ 1/2000 in the ELISA application (Crowther, 2001). However, if the sample is diluted too much, the sensitivity is also decreased under the required detection range. In the general ELISA, serum is diluted to be 10 % ~ 50 % according to the required sensitivity of the assay (http://www.m.ehime-u.ac.jp/~yasuhito/ElisaS.html). Therefore, an appropriate dilution factor should be selected for each application.

(3) Application of detergents

The application of detergent components in wash and assay buffers is also generally used to minimize nonspecific binding in immunoassay (Matson, 2000). Detergents can remove nonspecifically bound biomolecules from the surface by disruption of hydrophobic bonds formed between the biomolecule and surface groups. Generally, these are used at relatively low concentration (0.01 ~ 0.1 %) in order to avoid potential interference with the assay, such as the displacement of antibody or antigen coatings from the surface. There are nonionic detergents such as Tween 20, or ionic detergents such as SDS or DTAB. Though nonionic detergent of 0.5% Tween 20 had been used for our experiments, however, it seems to be valuable to try other strong detergents.

(4) Others

There were also other attempts to minimize nonspecific binding. For example, the proper selection of species which produces antibodies for IA layer can influence against the nonspecific binding (Vikinge *et al.*, 1998). When chicken IgY and mouse IgG were immobilized to a sensor chip CM5 dextran matrix and compared their background signals with serum (negative signal by nonspecific binding), chicken antibodies and mouse antibodies bound low quantities and large quantities of human serum, respectively. Chicken IgY is known to have a much lower reactivity to human serum proteins than any known murine antibody (Weber *et al.*, 1990; Larsson *et al.*, 1991; Larsson *et al.*, 1993). The immobilized chicken antibodies can improve the detection of serum antigens with surface plasmon resonance.

Moreover, addition of EDTA to serum can also reduce the background signal modestly for both IgG and IgY (Vikinge *et al.*, 1998). When diluted normal human serum samples (1% in HBS) were flown over IgG or IgY immobilized to the dextran matrices, serum protein binding was quantified. After addition of 3.4 nM EDTA, responses by non-specific binding were reduced from 924 to 347 RU (1 kRU = 1 ng/mm^2) for the IgG matrices and from 606 to 114 RU for the IgY matrices, respectively.

In the making of IA layer, the use of F_{ab} fragments instead of whole antibodies may also help to minimize non-specific binding (Matson, 2000). Moreover, since rheumatoid autoantibodies react mainly with the F_c region, the use of F_{ab} fragments can also reduce this problem. In our experiments, antibodies for IA layer were not F_{ab} fragments but whole antibodies. Accordingly, blocking property seems to be improved by using F_{ab} fragments.

The pH at which the assay operated was also evaluated to minimize interference by sera (Jongerius-Gortemaker *et al.*, 2002). A pH-dependent non-specific and specific response was found in the tested pH range from 5.0 to 7.6. A pH of 7.4 was selected as the working pH for minimal interference stemming from the serum matrix. Our experiment was already done with a condition of pH 7.4.

5. References

Ahluwalia A, De Rossi D, Ristori C, Schirone A and Serra G.
A comparative study of protein immobilization techniques for optical immunosensors, Biosens. Bioelectron., (7) 207-214; 1991

Akerstrom B, Brodin T, Reis K, and Bjorck L
Protein G: a powerful tool for binding and detection of monoclonal and polyclonal antibodies, J. Immunol., (135) 2589-2592; 1985

Allan IJ, Vrana B, Greenwood R, Mills GA, Roig B and Gonzalez C
A "toolbox" for biological and chemical monitoring requirements for the European Union's Water Framework Directive, Talanta, (69) 302-322; 2006

Allara DL
Critical issues in applications of self-assembled monolayers, Biosens. Bioelectron., (10) 771-783; 1995

Anderson GP, Jacoby MA, Ligler FS and King KD
Effectiveness of protein A for antibody immobilization for a fiber optic biosensor, Biosens. Bioelectron., (12) 329-336; 1997

Anderson K, Haemaelaeinen M and Malmqvist M
Identification and optimization of regeneration conditions for affinity-based biosensor assays. A multivariate cocktail approach, Anal. Chem., (71) 2475-2481; 1999

Askari MDF, Miller GH and Vo-Dinh T
Simultaneous detection of the tumor suppressor FHIT gene and protein using the multi-functional biochip, Cancer Detect. Prev., (26) 331-342; 2002

Bachmann TT and Schmid RD
A disposable multielectrode biosensor for rapid simultaneous detection of the insecticides paraoxon and carbofuran at high resolution, Anal. Chim. Acta, (401) 95-103; 1999

Bae YM, Oh BK, Lee W, Lee WH and Choi JW
Study on orientation of immunoglobulin G on protein G layer, Biosens. Bioelectron., (21) 103-110; 2005

Bangs laboratories
Technical note, No. 22: Carboxylate-modified mocrospheres; 1998

Betts TA, Catena GC, Huang J, Litwiler KS, Zhang J, Zagrobelny J and Bright FV
Fibre-optic-based immunosensors for haptens, Anal. Chim. Acta, (246) 55-63; 1991

Blake C, Al-Bassam MN, Gould BJ, Marks V, Bridges JW and Riley C
Simultaneous enzyme immunoassay of two thyroid Hormones, Clin. Chem., (28) 1469-1473; 1982

Bontidean I, Ahlqvist J, Mulchandani A, Chen W, Bae W, Mehra RK, Mortari A and Csöregi E
Novel synthetic phytochelatin-based capacitive biosensor for heavy metal ion detection, Biosens. Bioelectron., (28) 547-553; 2003

Boonpangrak S, Whitcombeb MJ, Prachayasittikul V, Mosbacha K and Ye L
Preparation of molecularly imprinted polymers using nitroxide-mediated living radical

polymerization, Biosens. Bioelectron., (22) 349–354; 2006

Boscato LM and Stuart MC
Heterophilic antibodies: a problem for all immunoassays, Clin. Chem., (34) 27-33; 1988

Boscato LM and Stuart MC
Incidence and specificity of interference in two-site immunoassays, Clin. Chem., (32) 1491-1495; 1986

Briand E, Salmain M, Herry JM, Perrot H, Compere C and Pradier CM
Building of an immunosensor: How can the composition and structure of the thiol attachment layer affect the immunosensor efficiency?, Biosens. Bioelectron., (22) 440-448; 2006

Bright FV, Betts TA and Litwiler KS
Regenerable fibre-optic-based immunosensor, Anal. Chem., (62) 1065-1069; 1990

Brogan KL, Wolfe KN, Jones PA and Schoenfisch MH
Direct oriented immobilization of F(ab') antibody fragments on gold, Anal. Chim. Acta, (496) 73-80; 2003

Campagnolo C, Meyers KJ, Ryan T, Atkinson RC, Chen YT, Scanlan MJ, Ritter G, Old LJ and Batt CA
Real-Time, label-free monitoring of tumor antigen and serum antibody interactions, J. biochem. Biophysic. Methods, (61) 283-298; 2004

Chard T
58 Pregnancy. In: Wild D (Ed.), The immunoassay handbook, Nature Publishing Group, London, UK, 578-580 ; 2001

Chen S, Liu L, Zhou J and Jiang S
Controlling Antibody Orientation on Charged Self-Assembled Monolayers, Langmuir, (19) 2859–2864; 2003

Chinowski TM, Quinn JG, Bartholomew DU, Kaiser R and Elkind JL
Performance of the spreeta 2000 integrated surface plasmon resonance affinity sensor, Sens. Actuators B Chem., (91) 266-274; 2003

Chung JW, Kim SD, Bernhardt R and Pyun JC
Application of SPR biosensor for medical diagnostics of human hepatitis B virus (hHBV), Sens. Actuators B Chem., (111-112) 416-422; 2005

Clark P
60 Diabetes mellitus. In: Wild D (Ed.), The immunoassay handbook, Nature Publishing Group, London, UK, 600-605; 2001

Crowther JR
6 Practical exercises. In: The ELISA Guidebook, Humana Press Inc., New Jersey, USA; 2001

Cui X, Yang F, Sha Y and Yang X
Real-time immunoassay of ferritin using surface plasmon resonance biosensor, Talanta (60) 53-61; 2003

Davis F and Higson SPJ
Structured thin films as functional components within biosensors, Biosens. Bioelectron., (21) 1-20; 2005

DeBruijn HE, Altenburg BSF, Kooyman RPH and Greve J
Choice of metal and wavelength for surface-plasmon resonance sensors: some considerations, Appl. Opt., (31) 440-442; 1992

Del Villano BC, Brennan S, Brock P, Bucher C, Liu V, McClure M, Rake B, Space S, Westrick B, Schoemaker H and Zurawski VR
Radioimmunometric assay for a monoclonal antibody-defined tumor marker, CA 19-9, Clin. Chem., (29) 549-552; 1983

DeMars DD, Katzmann JA, Kimlinger TK, Calore JD and Tracy RP
Simultaneous measurement of total and IgA-conjugated alpha 1-microglobulin by a combined immunoenzyme/immunoradiometric assay technique, Clin. Chem., (35) 766-772; 1989

Dillon PP, Daly SJ, Manning BM and O'Kennedy R
Immunoassay for the determination of morphine-3-glucuronide using a surface plasmon resonance-based biosensor, Biosens. Bioelectron., (18) 217-227; 2003

D'Orazio P
Biosensors in clinical chemistry, Clin. Chimica Acta, (334) 41-69; 2003

Du D, Yan F, Liu S and Ju H
Immunological assay for carbohydrate antigen 19-9 using an electrochemical immunosensor and antigen immobilization in titania sol-gel matrix, J. Immunol. Methods, (283) 67-75; 2003

Dubrovsky T, Tronin A, Dubrovskaia S, Guryev O and Nicolini C
Langmuir films of Fc binding receptors engineered from protein A and protein G as a sublayer for immunoglobulin orientation, Thin Solid Film, (284-285) 698-702; 1996

Edelstein RL, Tamanaha CR, Sheehan PE, Miller MM, Baselt DR, Whitman LJ and Colton RJ
The BARC biosensor applied to the detection of biological warfare agents, Biosens. Bioelectron., (14) 805-813; 2000

Ekbom P, Damm P, Feldt-Rasmussen B, Feldt-Rasmussen U, Molvig J and Mathiesen ER
Pregnancy outcome in type I diabetic women with microalbuminuria, Diabetes Care, (24) 1739-1744; 2001

Ekin R
Immunoassay and other ligand assays: from isotopes to luminescence, J. Clin. Ligand Assay, (22) 61-77; 1999

Erden A, Kerman K, Meric B, Akarca US and Ozsoz M
DNA electrochemical biosensor for the detection of short DNA sequences related to the Hepatitis B Virus, Electoanalysis, (11) 586-587; 1999

Eskola JU, Naentoe V, Meurling L and Loevgren NE
Direct solid-phase time-resolved immunofluorometric assay of cortisol in serum, Clin. Chem. (31) 1731-1734; 1985

Ezan E and Grassi J
7 Optimization. In: JP Gosling (Eds.) Immunoassays. Oxford University Press, Oxford, UK, 187-210; 2000

Faegerstam LG, Frostell-Karlsson A, Karlsson R, Persson B and Roennberg I
Biospecific interaction analysis using surface plasmon resonance detection applied to kinetic,

binding site and concentration analysis, J. Chrom., (597) 397-410; 1992

Franciotta D, Martino G, Brambilla E, Zardini E, Locatelli V, Bergami A, Tinelli C, Desina G and Cosi V
TE671 Cell-based ELISA for anti-acetylcholine receptor antibody determination in myasthenia gravis, Clin. Chem., (45) 400-405; 1999

Frazier RA, Matthijs G, Davis MC, Roberts CJ, Schacht E and Tendler SJB
Characterization of protein-resistant dextran monolayers, Biomaterials, (21) 957-966; 2000

Frengen J, Lindmo T, Paus E, Schmid R and Nustad K
Dual analyte assay based on particle types of different size measured by flow cytometry, J. Immunol. Methods, (178) 141-151; 1995

Frederix F, Bonroy K, Laureyn W, Reekmans G, Campitelli A, Dehean W and Maes G
Enhanced performance of an affinity biosensor interface based on mixed self-assembled monolayers of thiols on gold, Langmuir, (19) 4351-4357; 2003

Fulton SP
Antibody purification techniques, Grace WR & Co. Publ. No. 8685M589, 46-47; 1989

Ge B and Lisdat F
Superoxide sensor based on cytochrome c immobilized on mixed-thiol SAM with a new calibration method, Anal. Chim. Acta, (454) 53-64; 2002

Goding JW
Use of staphylococcal protein A as an immunological reagent, J. Immunol. Methods, (20) 241-253; 1978

Goh JB, Tam PL, Loo TW and Goh MC
A quantitative diffraction-based sandwich immunoassay, Anal. Biochem., (313) 262-266; 2003

Guiomar AJ, Guthrie JT and Evans Sd
Use of mixed self-assembled. monolayers in a study of the microenvironment on immobilized glucose oxidase, Langmuir, (15) 1198-1207; 1999

Gutcho S and Mansbach L
Simultaneous radioassay of serum vitamin B_{12} and folic acid, Clin. Chem., (23) 1609-1614; 1977

Hadfield SG, Lane A and McIllmurray MB
A novel coloured latex test for the detection and identification of more than one antigen, J. Immunol. Methods, (97) 153-158; 1987

Hayes FJ, Halsall HB and Heineman WR
Simultaneous immunoassay using electrochemical detection of metal ion labels, Anal. Chem., (66) 1860-1865; 1994

He L, Musick MD, Nicewarner SR, Salinas FG, Benkovic SJ, Natan MJ and Keating CD
Colloidal Au-enhanced surface plasmon resonance for ultrasensitive detection of DNA hybridization, J. Am. Chem. Soc., (122) 9071-9077; 2000

Hedenborg G, Pettersson T and Carlström A
Heterophilic antibodies causing falsely raised thyroid-stimulating-hormone results, The Lancet, (314) 755-758; 1979

Hemmilae I, Holttinen S, Pettersson K and Loevgren T
Double-label time-resolved immunofluorometry of lutropin and follitropin in serum, Clin. Chem., (33) 2281-2283; 1987

Hjelm H, Hjelm K and Sjoequist J
Protein A from Staphylococcus aureus. Its isolation by affinity chromatography and its use as an immunosorbent for isolation of immunoglobulin, FEBS Lett., (28) 73-76; 1972

Hock B
Antibodies for immunosensors a review, Anal.Chim.Acta., (347) 177-186; 1997

Homola J
7 Surface plasmon resonance biosensors for food safety. In: Narayanaswamy R and Wolfbeis OS (Ed.), Optical sensors, Springer-Verlag, Heidelberg, Germany, 145-172; 2004

Huber W, Barner R, Fattinger C, Huebscher J, Koller H, Mueller F, Schlatter D and Lukosz W
Direct optional immunosensing (sensitivity and selectivity), Sens. Actuators B Chem., (6) 122-126; 1992

Hurley JP, Haagensen DE Jr., Hansen HJ and Zamcheck N
Capture and detection of carcinoembryonic antigen on antibody coated beads used in enzyme immunoassay, J. Immunoassay, (7) 309-336; 1986

Ivanov I, Gnedenko OV, Nikolaeva LI, Konev AV, Kovalev OB, Govorun VM, Pokrovskii VI and Archakov AI
Detection of hepatitis B virus surface antigen with optical biosensor, Zh Mikrobio. Epidemiol. Immunobiol., (Mar-Apr) 58-62; 2003

Ivarsson B and Malmqvist M
9 Surface plasmon resonance. Development and use of BIACORE instruments for biomolecular interaction analysis. In: Gizeli E and Lowe CR (Ed.), Biomolecular sensors, Nature Taylor & Francis, London, UK, 241-268; 2002

Johnsson B, Lofas S and Lindquist G.
Immobilization of proteins to a carboxymethyldextran-modified gold surface for biospecific interaction analysis in surface plasmon resonance sensors, Anal. Biochem., (198) 268-277; 1991

Jones DA, Parkin MC, Langemann H, Landolt H, Hopwood SE, Strong AJ and Boutelle MG
On-line monitoring in neurointensive care enzyme-based electrochemical assay for simultaneous, continuous monitoring of glucose and lactate from critical care patients, J. Electroanal. Chem., (538-539) 243-252; 2002

Jongerius-Gortemaker BGM, Goverde RLJ, van Knapen F and Bergwerff AA
Surface plasmon resonance (BIACORE) detection of serum antibodies against *Salmonella enteritidis* and *Salmonella typhimurium*, J. Immunol. Methods, (266) 33-44; 2002

Jordan CE, Frutos AG, Thiel AJ and Corn RM
Surface plasmon resonance imaging measurements of DNA hybridization adsorption and streptavidin/DNA multilayer formation at chemically modified gold surfaces, Anal. Chem., (69) 4939-4947; 1997

Kane and Banks
2 Raising antibodies. In: JP Gosling (Eds.) Immunoassays. Oxford University Press, Oxford, UK, 19-58; 2000

Kanno S, Yanagida Y, Haruyama T, Kobatake E and Aizawa M
Assembling of engineered IgG-binding protein on gold surface for highly oriented antibody immobilization, J. Biotechnol., (76) 207-214; 2000

Karlsson R and Faelt A
Experimental design for kinetic analysis of protein-protein interactions with surface plasmon resonance biosensors, J. Immunol. Methods, (200) 121-133; 1997

Kim MG, Shin YB, Jung JM, Ro HS and Chung BH
Enhanced sensitivity of surface plasmon resonance (SPR) immunoassays using a peroxidase-catalyzed precipitation reaction and its application to a protein microarray, J. Immunol. Methods, (297) 125-132; 2005

Koesslinger C, Uttenthaler E, Drost S, Aberi F, Wolf H, Brink G, Stanglmaier A and Sackman E.
Comparison of the QCM and the SPR method for surface studies and immunological applications, Sens. Actuators B Chem., (24/25) 107-112; 1995

Kohler G and Milstien C
Continuous cultures of fused cells secreting antibody of predefined specificity, Naure, (256) 495-497; 1975

Kretschmann E and Raether H
Radiative decay of non-radiative surface plamons excited by light, Z. Naturforsch., (23A) 2135-2136; 1968

Kubitschko S, Spinke J, Brueckner T, Pohl S and Oranth N
Sensitivity enhancement of optical immunosensors with nanoparticles, Anal. Biochem., (253) 112-122; 1997

Laricchia-Robbio L and Revoltella RP
Comparison between the surface plasmon resonance (SPR) and the quartz crystal microbalance (QCM) method in a structural analysis of human endothelin-1, Biosens Bioelectron, (19) 1753-1758; 2004

Larsson A, Bålöw RM, Lindahl T and Forsberg PO
Chicken antibodies: taking advantage of evolution: a review, Poultry Science, (72) 1807–1812; 1993

Larsson A, Karlsson-Parra A and Sjöquist J
Use of chicken antibodies in enzyme immunoassays to avoid interference by rheumatoid factors, Clin. Chem., (37) 411-414; 1991

Lee JW, Sim SJ, Cho SM and Lee J
Characterization of a self-assembled monolayer of thiol on a gold surface and the fabrication of a biosensor chip based on surface plasmon resonance for detecting anti-GAD antibody, Biosens. Bioelecton., (20) 1422-1427; 2005

Lee M and Walt DR
A fiber optic microarray biosensor using aptamers as receptors, Anal. Biochem., (282) 142-146; 2000

Lee W, Oh BK, Lee WH and Choi JW
Immobilization of antibody fragment for immunosensor application based on surface plasmon resonance, Colloid. Surface B, (40) 143-148; 2005

Leung PT, Pollard-Knight D, Malan GP and Finlan MF
Modelling of particle-enhanced sensitivity of the surface-plasmon-resonance biosensor, Sens. Actuators B Chem., (22) 175-180; 1994

Liddell E
7 Antibodies. In: Wild D (Ed.), The immunoassay handbook, Nature Publishing Group, London, UK, 118-139; 2001

Liedberg B, Nylander C and Lundstroem I
Surface plasmon resonance for gas detection and biosensing, Sens. Actuators, (4) 299-304; 1983

Li X and Husson SM
Adsorption of dansylated amino acids on molecularly imprinted surfaces: A surface plasmon resonance study, Biosens. Bioelectron., (22) 336–348; 2006

Lin J, Yan F, Hu X and Ju H
Chemiluminescent immunosensor for CA 19-9 based on antigen immobilization on a cross-linked chitosan membrane, J. Immunol. Methods, (291) 165-174; 2004

Liu X, Sun Y, Song D, Zhang Q, Tian Y, Bi S and Zhang H
Sensitivity-enhancement of wavelength-modulation surface plasmon resonance biosensor for human complement factor 4, Anal. Biochem., (333) 99-104; 2004

Lotierzo M, Henry O.Y.F., Piletsky S, Tothill I, Cullen D, Kania M, Hock B and Turner APF
Surface plasmon resonance sensor for domoic acid based on grafted imprinted polymer, Biosens. Bioelectron., (20) 145–152; 2004

Lu B, Smyth MR and O'Kennedy R
Orientated immobilization of antibodies and its applications in immunoassays and immunosensors, The Analyst, (121) 29-32; 1996

Lu F, Wang KH and Lin Y
Rapid, quantitative and sensitive immunochromatographic assay based on strippin voltammetric detection of a metal ion label, The Analyst, (130) 1513-1517; 2005

Lundstroem I
Real-time biospecific interaction analysis, Biosens. Bioelectron., (9) 725-736; 1994

Luppa PB, Sokoll LJ and Chan DW
Immunosensors-principles and applications to clinical chemistry, Clin. Chim. Acta, (314) 1-26; 2001

Lyon LA, Musick MD and Natan MJ
Colloidal Au-Enhanced Surface Plasmon Resonance Immunosensing, Anal. Chem., (70) 5177-5183; 1998

Matson RS
5 Solid-phase reagents. In: JP Gosling (Eds.) Immunoassays. Oxford University Press, Oxford, UK, 129-164; 2000

Min RW, Rajendran V, Larsson N, Gorton L, Planas J and Hahn-Haegerdal B
Simultaneous monitoring of glucose and L-lactic acid during a fermentation process in an aqueous two-phase system by on-line FIA with microdialysis sampling and dual biosensor detection, Anal. Chim. Acta, (366) 127-135; 1998

Morgan CL, Newman DJ and Price CP
Immunosensors: technology and opportunities in laboratory medicine, Clin. Chem., (42) 193-209; 1996

Morgan CR
Immunoassay of human insulin and growth hormone simultaneously using ^{131}I and ^{125}I tracers, Proc. Soc. Exp. Biol. Med., (123) 230-233; 1966

Morton TA, Myszka DG and Chaiken IM
Interpreting complex binding kinetics from optical biosensors: A comparison of analysis by linearization, the integrated rate equation, and numerical integration, Anal. Biochem., (227) 176-185; 1995

Mullett WM, Lai EPC and Yeung JM
Surface plasmon resonance based immunoassays, Methods, (22) 77-91; 2000

Muramatsu H, Watanabe Y, Hikuma M, Ataka T, Kubo I, Tamiya E and Karube I
Piezoelectric crystal biosensor system for detection of E.coli, Anal. Lett., (22) 2155-2166; 1989

Mushahwar IK
68 Hepatitis. In: Wild D (Ed.), The immunoassay handbook, Nature Publishing Group, London, UK, 722-736; 2001

Naimushin AN, Soelberg SD, Nguyen DK, Dunlap L, Bartholomew D, Elkind J, Melendez J and Furlong CE
Detection of Staphylococcus aureus enterotoxin B at femtomolar levels with a miniature integrated two-channel surface plasmon resonance (SPR) sensor, Biosens. Bioelectron., (17) 573-584; 2002

Nakamura C, Hasegawa M, Nakamura N and Miyake J
Rapid and specific detection of herbicides using a self-assembled photosynthetic reaction center from purple bacterium on an SPR chip, Biosens. Bioelectron., (18) 599-603; 2003

Nakanishi K, Karube I, Hiroshi S, Uchida A and Ishida Y
Detection of the red tide-causing plankton Chattonella marina using a piezoelectric immunosensor, Anal. Chim. Acta, (325) 73-80; 1996

Narang U, Gauger PR, Kusterbeck AW and Ligler FS
Multianalyte detection using a capillary-based flow immunosensor, Anal. Biochem., (255) 13-19; 1998

Neto EV, Carvalho ECD and Fonseca A
Adaptation of alpha-fetoprotein and intact human chorionic gonadotropin fluoroimmunometric assays to dried blood spots, Clin. Chim. Acta, (360) 151-159; 2005

Newman JD, Tigwell LJ, Warner PJ and Turner APF.
Biosensors: boldly going into the new millennium, Sens. Rev., (21) 268-271; 2001

Nichols JH
50 Point-of-care Testing. In: Wild D (Ed.), The immunoassay handbook, Nature Publishing Group, London, UK, 448-457; 2001

Nishizono I, Iida S, Suzuki N, Kawada H, Murakami H, Ashihara Y and Okada M
Rapid and sensitive chemiluminescent enzyme immunoassay for measuring tumor markers, Clin. Chem., (37) 1639-1644; 1991

Ngo TT
Developments in immunoassay technology, Methods, (22) 1-3; 2000

Ohkura H, Sakawaki O and Ozaki H
Enzyme immunoassay of CA 19-9. Enzyme immunoassay and its clinical application, Kan. Tan. Sui. Japan, (11) 21-28; 1985

O'Shannessy DJ, Brigham-Bruke M, Soneson KK, Hensley P and Brooks I
Determination of rate and equilibrium binding constants for macromolecular interactions using surface plasmon resonance: use of nonlinear least squares analysis methods, Anal. Biochem., (212) 457-468; 1993

Otto A
Excitation of nonradiative surface plasma waves in silver by the method of frustrated total reflection, Z. Physik, (216) 398-410; 1968

Owaku K and Goto M
Protein A Langmuir-Blodgett film for antibody immobilization and its use in optical immunosensing, Anal. Chem., (67) 1613-1616; 1995

Pratt RP and Roser B
NUNC product bulletin, No. 7: Comparison of blocking agents for ELISA; 1997

Preininger C, Clausen-Schaumann H, Ahluwalia A and de Rossi D
Characterization of IgG Langmuir–Blodgett films immobilized on functionalized polymers, Talanta, (52) 921-930; 2000

Ramanavieius A, Herberf FW, Hutschenreiter S, Zimmermann B, Lapenaite I, Kausaite A, Finkelsteinas A and Ramanavieius A
Biomedical application of surface plasmon resonance biosensor (review), Acta Medica Lituanica, (12) 1-9; 2005

Roos H, Karlsson R, Nilshans H and Persson A
Thermodynamic analysis of protein interactions with biosensor technology, J. Mol. Recognit., (11) 204-210; 1998

Rowe-Taitt CA, Hazzard JW, Hoffman KE, Cras JJ, Golden JP and Ligler FS
Simultaneous detection of six biohazardous agents using a planar waveguide array biosensor, Biosens. Bioelectron., (15) 579-589; 2000

Sauerbrey GZ
Verwendung von Schwingquarzen zur Wagung dunner Schichten und zur Mikrowagung, Z. Phys., (155) 206-222; 1959

Scheller F and Schubert F
Biosensors, Elsevier Science Publishers B.V.: Amsterdam, 1992

Schlehuber S, Beste G and Skerra A
A novel type of receptor protein, based on the lipocalin scaffold, with specificity for digoxigenin, J. Mol. Biol., (297) 1105-1120; 2000

Schmidt NA
Catecholamine standards in radioenzymic assays, Clin. Chem., (30) 592; 1984

Severs AH and Schasfoort RBM

Enhancement surface plasmon resonance inhibition test (ESPRIT) using latex particles, Biosens. Bioelectron., (8) 365-370; 1993

Silin V, Weetall H and Vanderah DJ,
SPR studies of the nonspecific adsorption kinetics of human IgG and BSA on gold surfaces modified by self-assembled monolayers (SAMs), J. Colloid. Interf. Sci., (185) 94-103; 1997

Sjoelander S and Urbaniczky C
Integrated fluid handling system for biomolecular interaction analysis, Anal. Chem., (63) 2338–2345; 1991

Song SP, Li B, Hu J and Li MQ
Simultaneous multianalysis for tumor markers by antibody fragments microarray system, Anal. Chim. Acta, (510) 147-152; 2004

Soper SA, Brown K, Ellington A, Frazier B, Garcia-Manero G, Gau V, Gutman SI, Hayes DF, Korte B, Landers JL, Larson D, Ligler F, Majumdar A, Mascini M, Nolte D, Rosenzweig Z and Wang J, Wilson
Point-of-care biosensor systems for cancer diagnostics/prognostics, Biosens. Bioelectron., (21) 1932-1942; 2006

Stefan RI, Van Staden, J(Koos)F and Aboul-Enein HY
Amperometric biosensors/sequential injection analysis system for simultaneous determination of S- and R-captopril, Biosens. Bioelectron., (15) 1-5; 2000

Stenberg E, Persson B, Roos H and Urbaniczky C
Quantitative determination of surface concentration of protein with surface plasmon resonance using radio labeled proteins, J. Colloid. Interf. Sci., (143) 513-526; 1991

Sternberger LA, Hardy PH Jr, Cuculis JJ and Meyer HG.
The unlabeled antibody enzyme method of immunohistochemistry: preparation and properties of soluble antigen-antibody complex (horseradish peroxidase-antihorseradish peroxidase) and its use in identification of spirochetes, J. Histochem. Cytochem., (18) 315–333; 1970

Su X, Chew FT and Li SFY
Self-assembled monolayer-based piezoelectric crystal immunosensor for the quantification of total human immunoglobulin E, Anal. Biochem., (273) 66-72; 1999

Suresh MR
63 Cancer Markers. In: Wild D (Ed.), The immunoassay handbook, Nature Publishing Group, London, UK, 635-663; 2001

Svitel J, Dzgoev A, Ramanathan K and Danielsson B
Surface plasmon resonance based pesticide assay on a renewable biosensing surface using the reversible concanavalin A monosaccharide interaction, Biosens. Bioelectron., (15) 411-415; 2000

Tuerk C and Gold L
Systematic evolution of ligands by exponential enrichment: RNA ligands to bacteriophage T4 DNA polymerase, Science, (249) 505-510; 1990

Ulman A
Formation and structure of self-assembled monolayers, Chem..Rev., (96) 1533-1554; 1996

Vaitukaitis JL, Braunstein GD and Ross GT
A radioimmunoassay which specifically measures human chorionic gonadotropin in the presence of

human luteinizing hormone, Am. J. Obstet. Gynecol., (113) 751–758; 1972

van der Gaag B, Spath S, Dietrich H, Stigter D, Boonzaaijer G, van Osenbruggen T and Koopal K
Biosensors and multiple mycotoxin analysis, Food Control, (14) 251-253; 2003

Vikinge TP, Askendal A, Liedberg B, Lindahl T and Tengvall P
Immobilized chicken antibodies improve the detection of serum antigens with surface plasmon resonance (SPR), Biosens. Bioelectron., (13) 1257-1262; 1998

Vladutiu AO, Sulewski JM,Pudlak KA and Stull CG
Heterophilic antibodies interfering with radioimmunoassay. A false-positive pregnancy test, J. Am. Med. Assoc., (248) 2489–2490; 1982

Vo-Dinh T, Griffin G, Stokes DL, Stratis-Cullum DN, Askari M and Wintenberg A
6 Multi-functional biochip for medical diagnostics and pathogen detection. In: Narayanaswamy R and Wolfbeis OS (Ed.), Optical sensors, Springer-Verlag, Heidelberg, Germany, 135-136; 2004

Vogt RF, Phillips DL, Henderson LO, Whitfield W and Spierto FW
Quantitative differences among various proteins as blocking agents for ELISA microtiter plates, J. Immunol. Methods, (101) 43-50; 1987

Wadkins RM, Golden JP, Pritsiolas LM and Ligler FS
Detection of multiple toxic agents using a planar array immunosensor, Biosens. Bioelectron., (13) 407-415; 1998

Weber TH, Käpyaho KI and Tanner P
Endogenous interference in immunoassays in clinical chemistry, Scand. J. Clin. Lab. Invest., 50 Suppl., (201) 77–82; 1990

Wehmann RE, Harman SM, Birken S, Canfield RE and Nisula BC
Convenient radioimmunoassay for urinary human choriogonadotropin without interference by urinary human lutropin, Clin. Chem., (27) 1997-2001; 1981

Wheeler MJ
19 Over-the-counter pregnancy test kits. In: Wild D (Ed.), The immunoassay handbook, Nature Publishing Group, London, UK, 271-277 ; 2001

Wijesuriya D, Breslin K, Anderson G, Shriver-Lake L and Ligler FS
Regeneration of immobilized antibodies on fiber optic probes, Biosens. Bioelectron., (9) 585-592; 1994

Wilde C
47 Subject preparation, sample collection and handling. In: Wild D (Ed.), The immunoassay handbook, Nature Publishing Group, London, UK, 411-422; 2001

Wink T, van Zuilen SJ, Bult A and van Bennekom WP
Liposome-mediated enhancement of the sensitivity in immunoassays of proteins and peptides in surface plasmon resonance spectrometry, Anal. Chem., (70) 827-832; 1998

Wink T, van Zuilen SJ, Bult A and van Bennekom WP
Self-assembled Monolayers for Biosensors, The Analyst, (122) 43-50; 1997

Zhou X, Liu L, Hu M, Wang L and Hu J
Detection of hepatitis B virus by piezoelectric biosensor, J. Pharm. Biomed. Anal., (27) 341-345; 2002